EMEP/CCC-Report 5/2003

EMEP Co-operative Programme for Monitoring and Evaluation of the Long-Range Transmission of Air Pollutants in Europe

Measurements of Particulate Matter: Status Report 2003

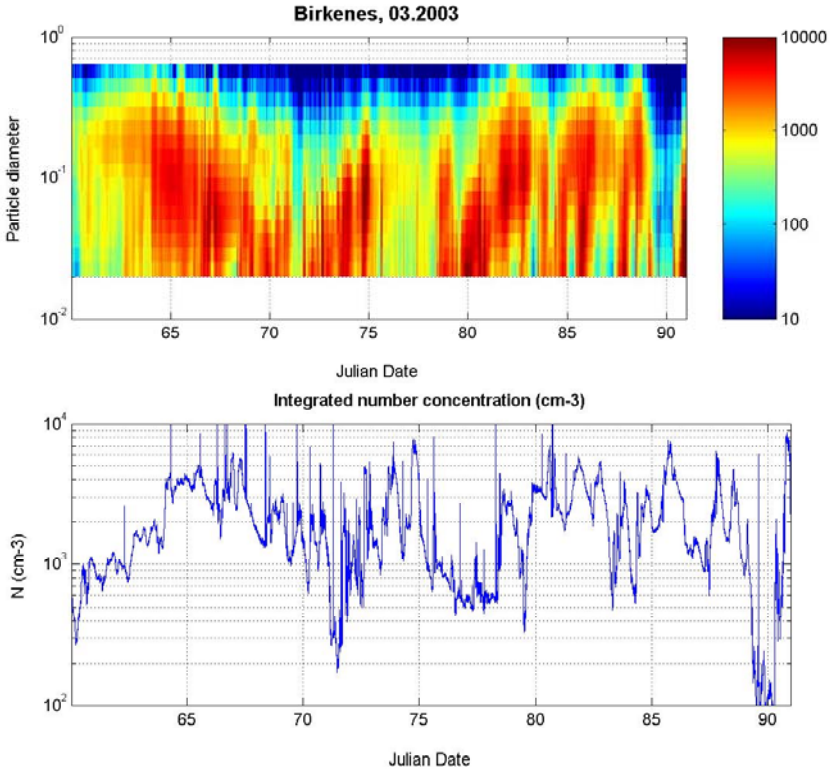

Norwegian Institute for Air Research
PO Box 100, NO-2027 Kjeller, Norway
Chemical Co-ordinating Centre of EMEP (CCC)

NILU : EMEP/CCC-Report 5/2003
REFERENCE : O-98134
DATE : AUGUST 2003

EMEP Co-operative Programme for Monitoring and Evaluation of the Long-range Transmission of Air Pollutants in Europe

Measurements of Particulate Matter: Status Report 2003

Edited by Michael Kahnert

Norwegian Institute for Air Research
P.O. Box 100, N-2027 Kjeller, Norway

Contents

Page

Measurements of Particulate Matter: Status Report 2003

1. Introduction

M. Kahnert
Norwegian Institute for Air Research, P.O. Box 100, 2027 Kjeller, Norway

Observations are fundamental for achieving a better understanding of the chemical and physical processes relevant for the long-range trans-boundary transport and deposition of particulate pollutants. They provide the basis for model validation and exposure studies. It is therefore important to develop the monitoring capacity for particulate matter and to sustain it with stable and reliable resources.

EMEP is the main framework for establishing a monitoring network on the regional scale for particulate pollutants in Europe. There exists a partial overlap between EMEP and Airbase monitoring stations for PM_{10}, and it is important that both networks make use of relevant data and exchange information. However, measurements of policy-relevant quantities (PM_{10}, $PM_{2.5}$) under the EC-requirements for PM monitoring are not sufficient to meet EMEP's objectives. More detailed information on chemical and physical properties of aerosols is needed in order to understand and correctly predict long-range trans-boundary transport of aerosols, their deposition, and their effects on human health. EMEP therefore needs to pursue a dual strategy of extending its own aerosol monitoring programme of particulate matter and of obtaining supplemental information from external data providers. In particular, for obtaining information from advanced and resource-intensive measurement techniques it is essential to intensify co-operation with the research community. EMEP is also intensifying its cooperation with GAW. Joint supersites are being established, and a harmonisation of the data flow in both networks is currently being implemented.

Monitoring of PM mass concentrations is a relatively recent addition to the EMEP monitoring programme. Measurement results obtained in 1998–2000 were presented in two previous reports (EMEP/CCC, 2001; EMEP/CCC, 2002). The EMEP monitoring strategy is currently reviewed, and possible improvements are discussed. One objective of this report is to provide relevant information for this discussion pertaining to monitoring of particulate matter. Fulfilling EMEP's objectives poses a significantly larger challenge for particulate matter than for many other single-component pollutants, due to the highly complex and variable nature of particles in air. A critical review of the current EMEP monitoring capacity for aerosols is therefore in order. EMEP's monitoring of PM mass concentrations is relatively young and still expanding. This offers the opportunity for designing the network such that it is well coordinated with existing EMEP observations on aerosol chemical composition. A good coordination is important for obtaining an as complete as possible characterisation of particulate pollutants. Thus a focus of this report will be to evaluate the information that can be obtained

from the current PM monitoring network, and to present some case studies to illustrate the information obtainable form comprehensive physical, chemical, and optical aerosol measurements.

Chapter 2 will give a status report of the current EMEP measurement activities concerning particulate matter. Current needs and possible extensions/improvements of the PM monitoring programme are discussed. Chapter 3 presents a case study of the EMEP site at Birkenes (Norway), which currently performs one of the most complete aerosol characterisation within the EMEP network. Chapter 4 presents results from a research campaign in the Eastern Mediterranean region. As an illustration of the information available from optical aerosol observations, Chapter 5 shows an analysis of sun photometer data obtained at the arctic EMEP site on Spitsbergen (Norway).

2. Measurements of particulate pollutants within EMEP

M. Kahnert
Norwegian Institute for Air Research, P. O. Box 100, 2027 Kjeller, Norway

2.1 Measurements of particle mass

Monitoring of particulate pollutants in air is expanding in Europe both on a regional and on a local scale. As current legislation is using the integrated mass of particulate matter up to 10 µm (PM_{10}) as the relevant metric, most available data are PM_{10} mass. Figure 1 shows annual averages of PM_{10} mass and total suspended particles (TSP) mass concentrations at the different EMEP stations in 2000 and 2001. The annual averages are based on daily averaged values, except those for Lista in Southern Norway, which are based on weekly mean values. Only those stations are shown in the figures that had a data coverage over 50%. Time series of all PM_{10}, $PM_{2.5}$ and TSP measurements at EMEP stations in 2000 and 2001 can be found in the appendix.

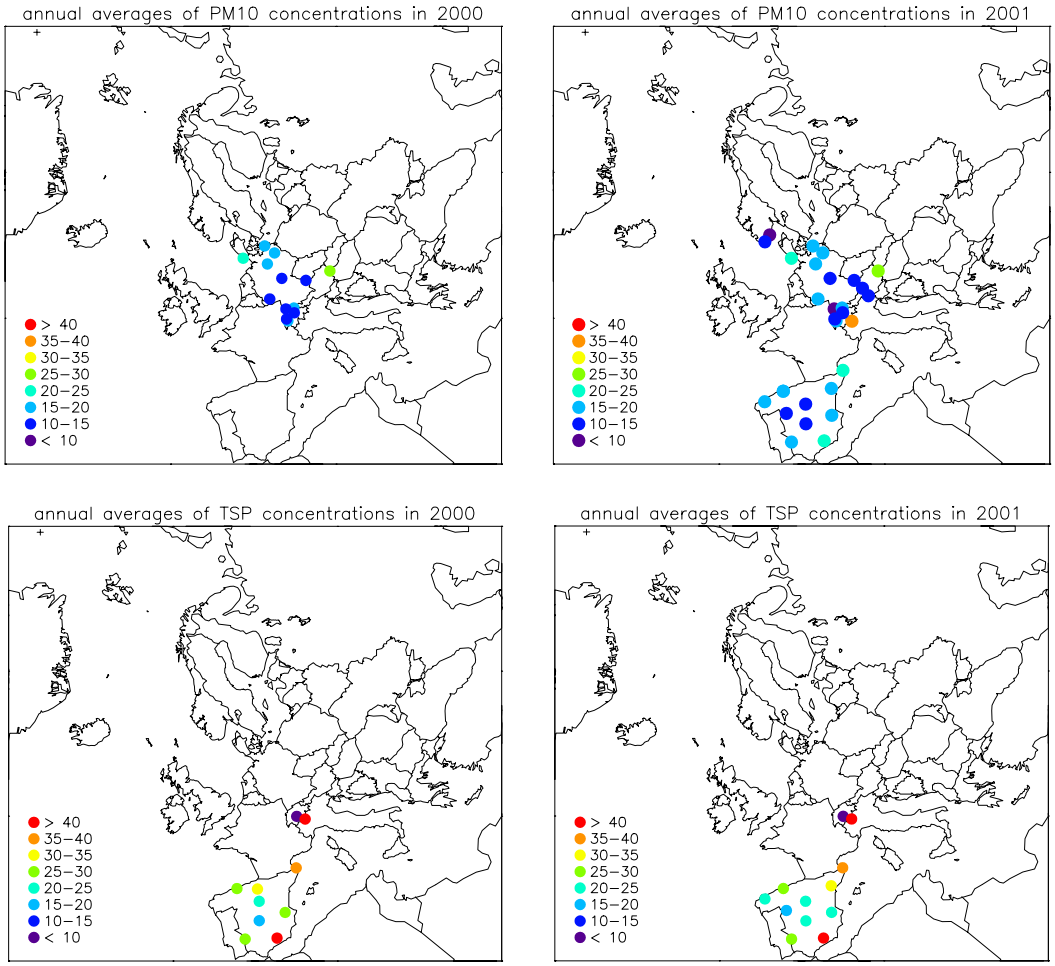

Figure 1: PM_{10} and TSP mass concentrations at EMEP stations for 2000 and for 2001.

As can be seen, none of the stations lie above the indicative limit value for 2005 of 40 μg/m^3. However, exceedances of the corresponding limit value for 2010 of 20 μg/m^3 are still not uncommon. Levels of both PM_{10} and TSP mass concentrations are comparable in 2000 and 2001. Particularly high PM_{10} concentrations occurred in 2001 in Northern Italy. The low TSP and PM_{10} values measured nearby at Jungfraujoch in Switzerland are due to the high altitude of the Jungfraujoch site above the boundary layer.

Figure 2 and Figure 3 show country averages simplistically calculated based on the annual averages of PM_{10} concentrations for 2000 and 2001, respectively. Numbers above the bars indicate the number of stations in each country. Again, only those EMEP stations with a minimum data coverage of 50% were taken into account. A comparison of Figure 2 and Figure 3 shows a lower average in the annual country average of PM_{10} concentrations in Austria. However, as can be seen in Figure 1-Figure 3, this is due to the fact that PM_{10} data were only reported from one Austrian EMEP station in 2000, whereas three Austrian stations reported PM_{10} data in 2001.

For comparison, Figure 2 and Figure 3 also show PM_{10} concentrations from rural, urban, and street sites that were reported into the AIRBASE database maintained by the European Topic Centre on Air and Climate Change (ETC/ACC) under contract of the European Environmental Agency (EEA). Many of the AIRBASE data from rural sites are actually joint EMEP stations. Many countries, such as Germany, Spain, Great Britain, Poland and Switzerland, show clearly lower rural values of PM_{10} than corresponding values at urban centres or hot spots, thus indicating a significant contribution of local sources on a local scale. In other countries, such as Belgium and The Netherlands, there are little differences between rural and urban values, mainly due to the relatively high rural values. This could indicate that high emissions from local sources (agricultural or traffic) in these countries can significantly contribute to the regional background values.

Figure 4, Figure 5 and Figure 6 show annual averages of AIRBASE rural, urban, and hotspot sites, respectively. In Figure 5 and Figure 6, PM_{10} concentrations are given in terms of policy-relevant measures, namely the limit value for 2005 LV=40 μg/m^3 (for the annual average of PM_{10}), the upper assessment threshold UAT=70 % of the LV, and the lower assessment threshold LAT=50 % of the LV.

It is evident that PM_{10} mass alone will not provide enough information to investigate adverse health effects of particulate matter, to study anthropogenic contributions to ambient aerosol concentrations, and to understand the significance of long-range transport. The coarse fraction in particle size distributions is often dominated by particles of natural origin, such as sea salt particles or mineral dust, although sulphate and nitrate can also contribute to the coarse particle mass. By contrast, fine particles usually contain a significant fraction of aged secondary aerosols formed from anthropogenic precursor gases. Also, fine particles are removed much less efficiently by dry or wet deposition processes than coarse particles and therefore play the most important role in long-range transport processes. For this reason, EMEP is establishing and extending monitoring of fine particles. The metric currently used is the integrated mass of particles up to 2.5 μm ($PM_{2.5}$). The reason for using this metric is that future EU

policies on particulate matter are expected to be based on $PM_{2.5}$. However, it should be noted that from a scientific standpoint PM_1 is likely to be a better metric, since in a typical aerosol size distribution the minimum between the fine and the coarse mode lies around 1 μm. There is no significant mass transfer between the fine and the coarse mode fraction. Thus the PM_1 metric in conjunction with PM_{10} measurements allows us to separate fine, aged, long-range transported aerosols with an often large portion of anthropogenic constituents from relatively short-lived coarse aerosols consisting of predominantly natural constituents.

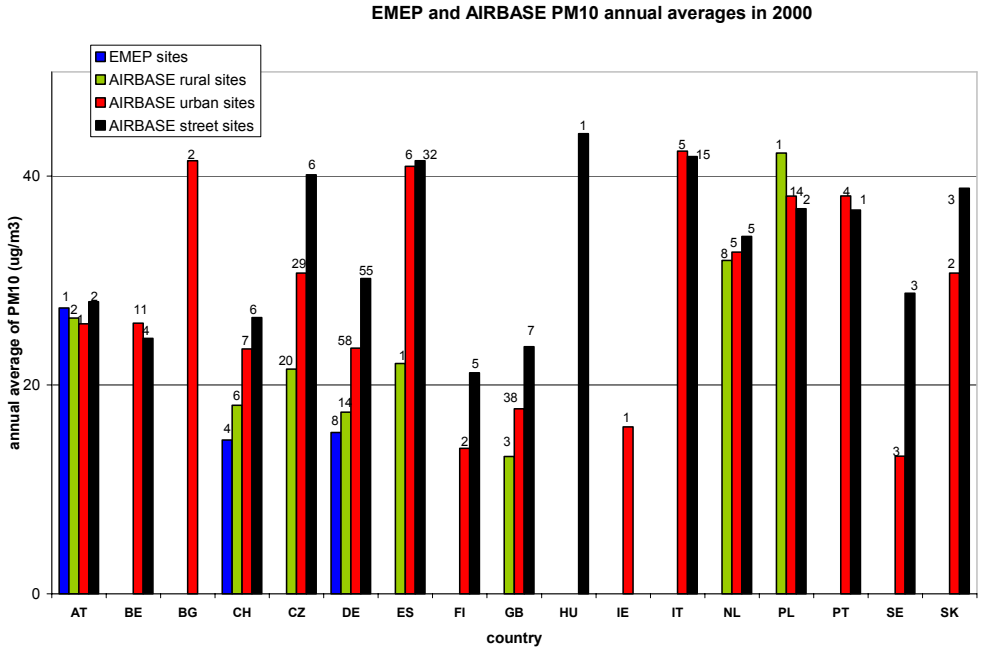

Figure 2: Annual country averages of PM_{10} at EMEP stations and at rural, urban, and AIRBASE street sites in 2000.

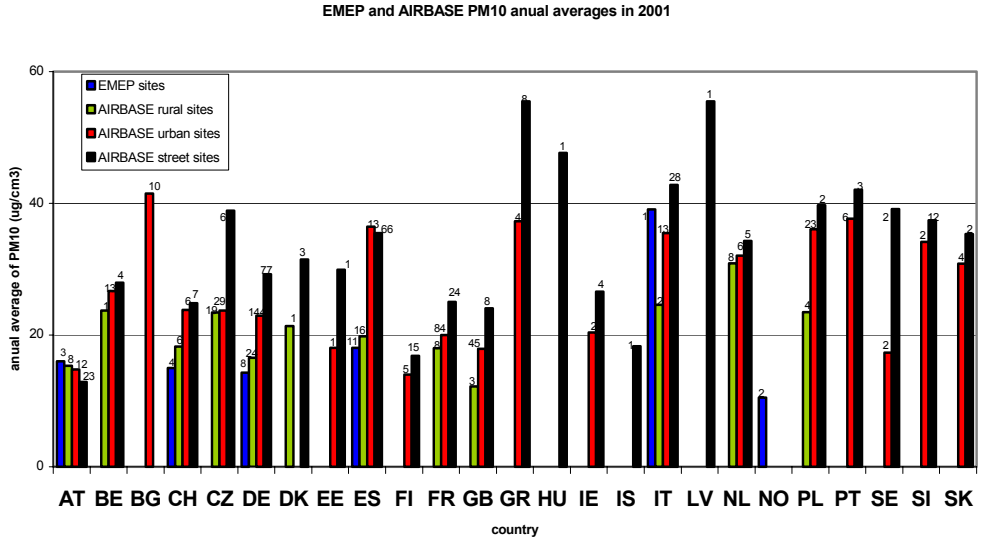

Figure 3: As Figure 2, but for 2001.

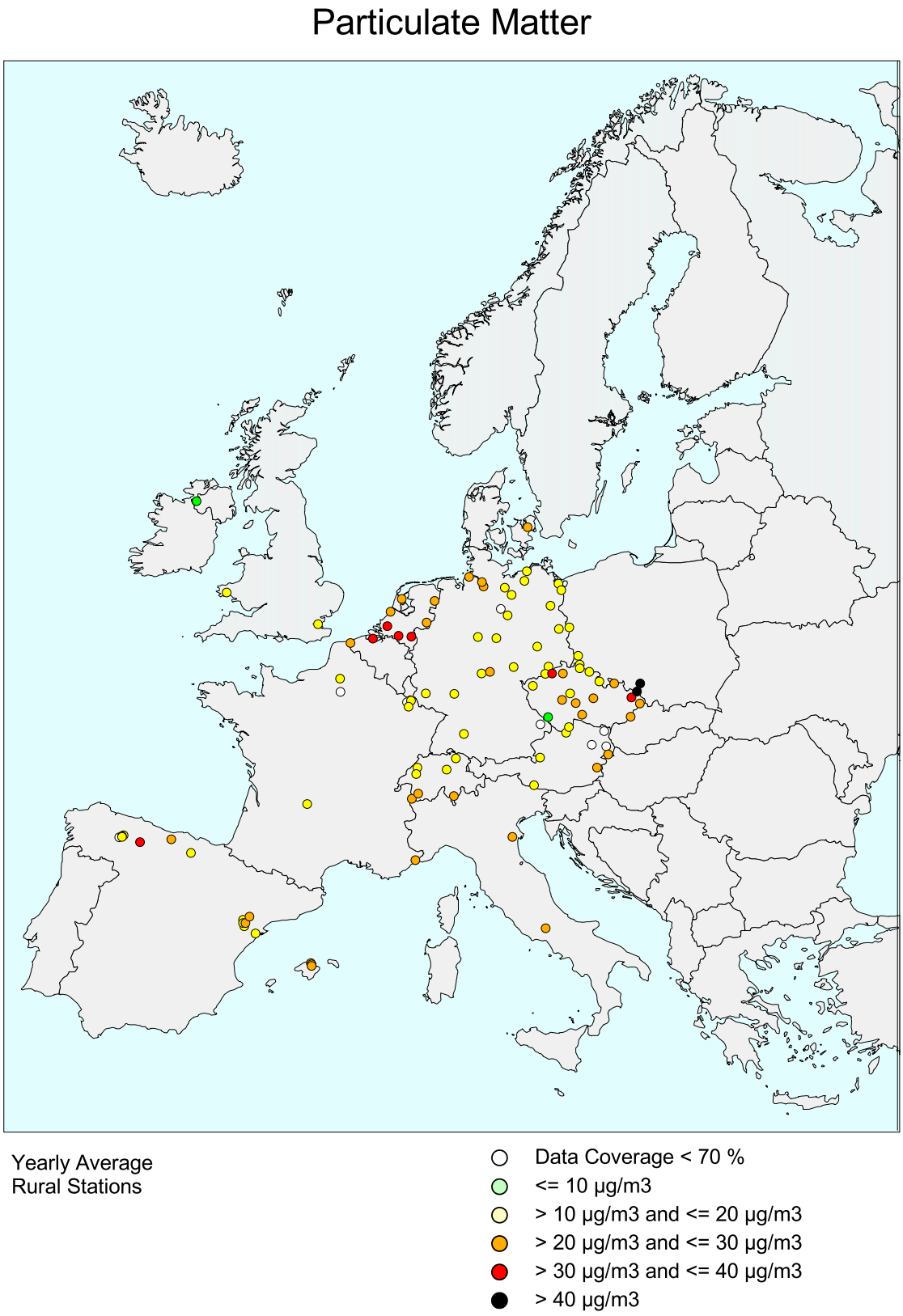

Figure 4: Annual averages of PM_{10} concentrations at AIRBASE rural sites in 2001.

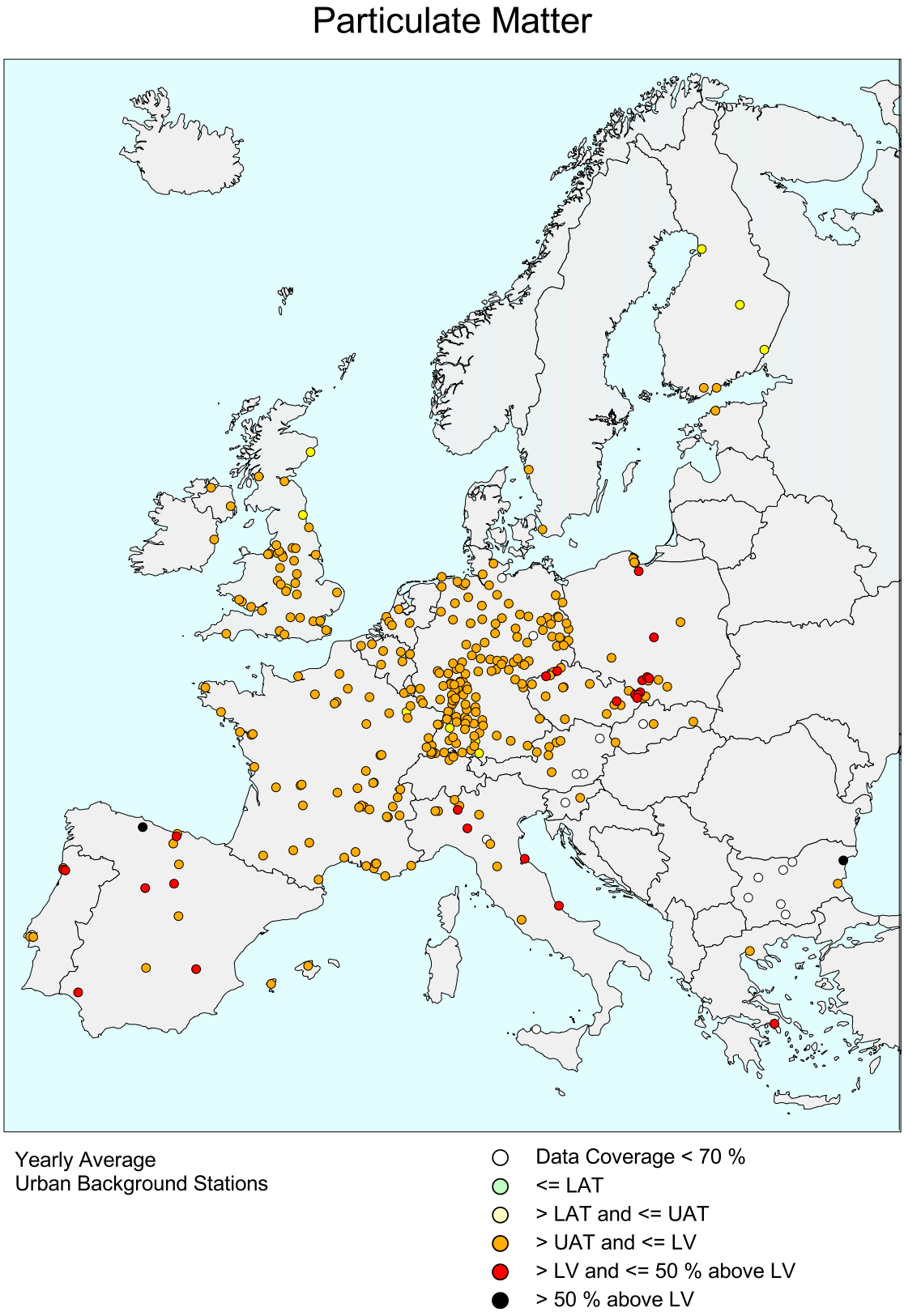

Figure 5: Annual averages of PM_{10} concentrations at AIRBASE urban sites in 2001. The measures LV, UAT, and LAT are explained in the text.

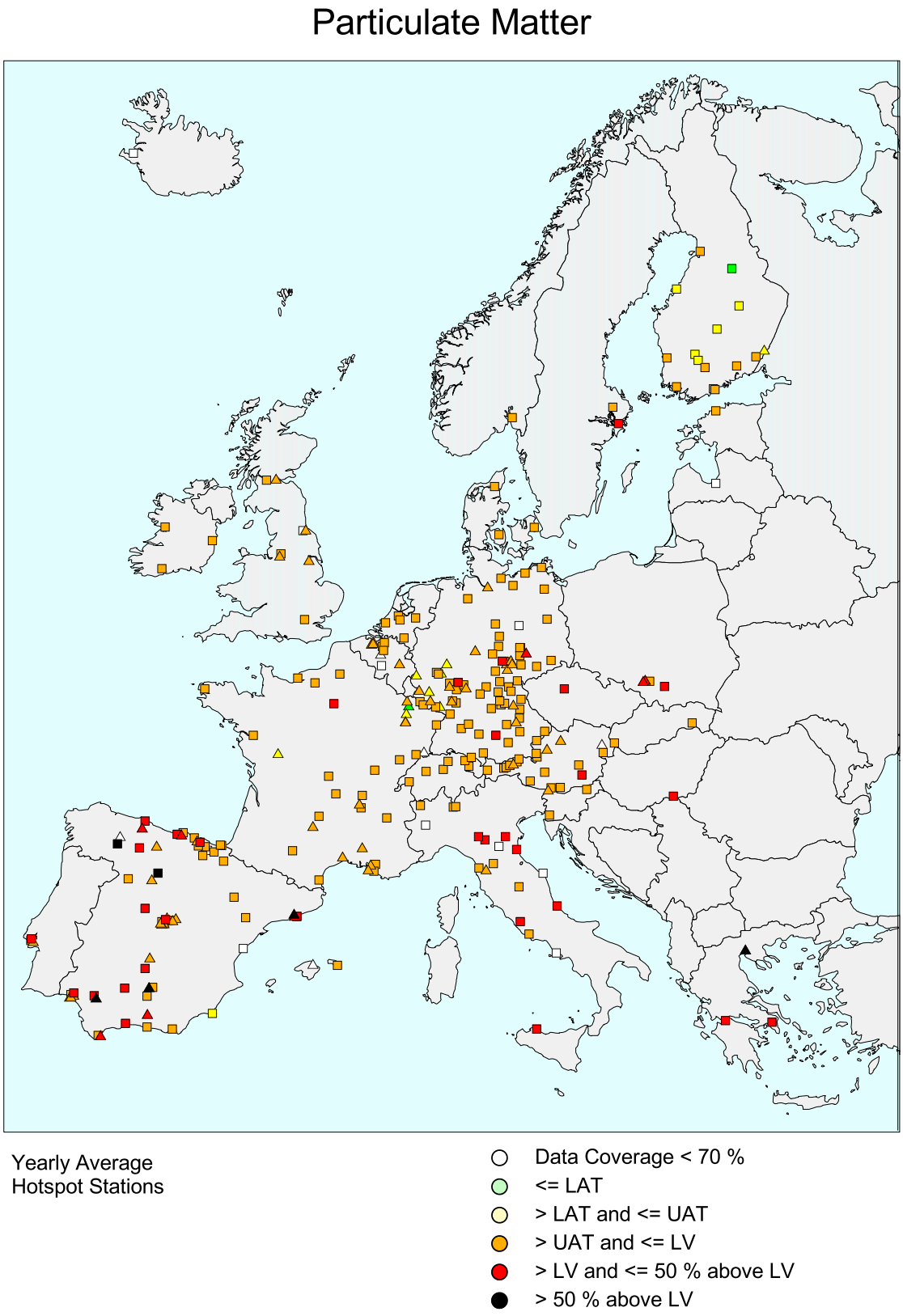

Figure 6: Annual averages of PM_{10} concentrations at AIRBASE hotspot sites in 2001. The measures LV, UAT, and LAT are explained in the text. Triangles denote industrial hotspots, squares represent traffic sites.

Figure 7 shows annual averages of $PM_{2.5}$ mass concentrations in 2001 at EMEP stations. This map should be compared with Figure 1. In many cases, notably in Northern Italy, we see that the fine fraction mass $PM_{2.5}$ contributes significantly to PM_{10}. This may indicate a high contribution of anthropogenic fine-mode aerosols. However, more detailed data on the chemical composition of the aerosols are required to substantiate this hypothesis. Also, PM_1 data would, as explained, provide us with a clearer separation of fine and coarse mode particles and would make it easier to obtain source information from physical data. The opposite effect can be observed comparing $PM_{2.5}$, PM_{10}, and TSP values measured at the Spanish stations (Figure 1 and Figure 7). PM_{10} values are significantly higher than $PM_{2.5}$ values, and TSP values, in turn, are clearly higher than PM_{10} mass concentrations. This indicates a significant contribution from coarse particles, most likely consisting to a high degree of mineral dust.

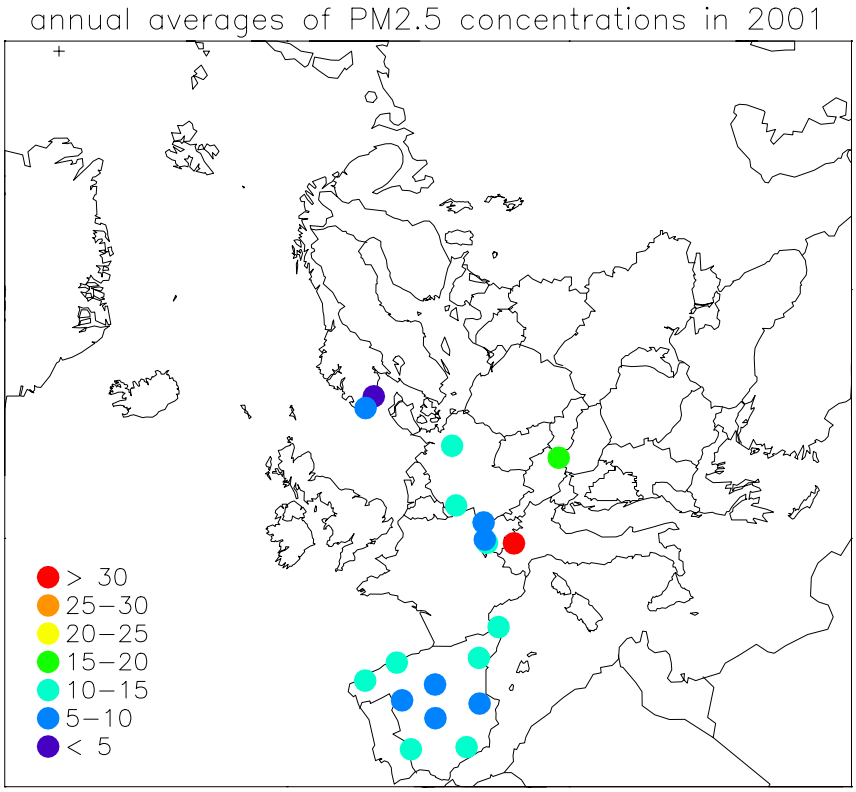

Figure 7: Annual averages of $PM_{2.5}$ mass concentrations in $\mu g/m^3$ in 2001 at EMEP stations. Only those stations are shown that had a data coverage over 50%.

2.2 Measurements of inorganic components in aerosols

The EMEP database contains a large number of inorganic chemical species in aerosols throughout Europe. Table 1 provides an overview over the number of stations in different countries that reported different chemical constituents and physical parameters to CCC in 2001.

Table 1: Number of EMEP stations in different countries reporting different chemical and physical aerosol parameters in 2001.

	AT	CH	CZ	DE	DK	ES	FI	FR	HU	IE	IS	IT	LT	LV	NL	NO	PL	RU	SE	SI	SK	TR	total
acidity												1											**1**
Al											1												**1**
NH4									1			2		2	2	7	3	3				1	**21**
NH3+NH4	1	1	2	5	3	10	4						1	2		7	4		3	1			**44**
As				4	2		1				1				1	1							**10**
Cd	3		2	8	3	2	1				1		1	2	1	1					5		**30**
Ca															1	7							**8**
Cl																7							**7**
Cr					3		1				1					1					5		**11**
Co																1							**1**
Cu				8	3	2	1				1		1	2		1					5		**24**
Fe				2	3		1				1												**7**
Pb	3		2	8	3	2	1				1		1	2	1	1					5		**30**
Mg																7							**7**
Mn				8	2		1				1					1					5		**18**
Hg											1					1							**2**
Ni				8	3		1				1			2		1					5		**21**
NO3									1			2		2	2	7	3	3			5	1	**26**
HNO3+NO3	1	1	2	6	4	10	4						1	2		10	4		3	1		1	**50**
K																7							**7**
Na					3											7							**10**
SO4	1	3	2	5	3	10	4	8	1	3	1	2		2	2	7	4	3	4	1	5	1	**72**
V							1				1					1							**3**
Zn					3		1				1		1	2	1	1					5		**15**
TSP		1				10						1							4				**16**
PM10	3	4		8		10						1				2							**28**
PM2.5	1	2		3		10						1				2							**19**
Total	**13**	**12**	**10**	**73**	**38**	**66**	**22**	**8**	**3**	**3**	**13**	**10**	**6**	**20**	**11**	**88**	**18**	**9**	**14**	**3**	**45**	**4**	**489**

A complete description of precursor gases and inorganics is required for gaining a better understanding of the chemical processes in the atmosphere leading to the formation of secondary inorganic aerosols from precursor gases. The main inorganic constituents are ammonium, nitrate, and sulphate. Figure 8–Figure 10 show concentrations of these three components at EMEP stations in 2000 and 2001. Also here, all stations with data coverage under 50% were excluded in these figures. At several observation sites mass of ammonia, nitrate, and sulphate in aerosols is comparable in 2000 and 2001. However, higher levels of all three species are observed in The Netherlands in 2001 as compared to 2000. Also, there are clearly more stations at which higher sulphate concentrations have been observed in 2001 than stations that have shown lower sulphate concentrations.

Relatively few sites perform denuder/filterpack measurements in order to correctly separate ammonia and ammonium as well as nitric acid and nitrate. Significantly more sites measure the sum of ammonia and ammonium, and the sum of nitric acid and nitrate. Corresponding results are shown in Figure 11 and Figure 12.

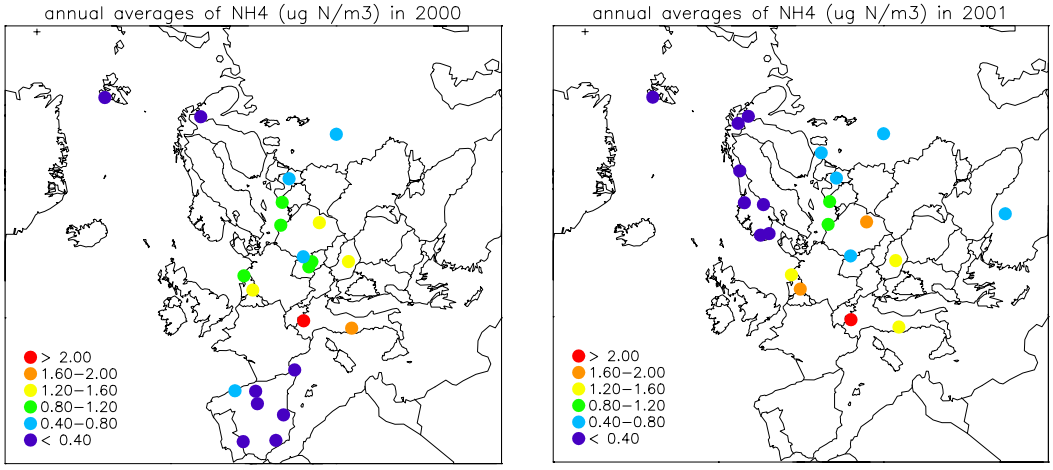

Figure 8: Annual averages of ammonium concentrations in aerosols in 2000 (left) and in 2001 (right).

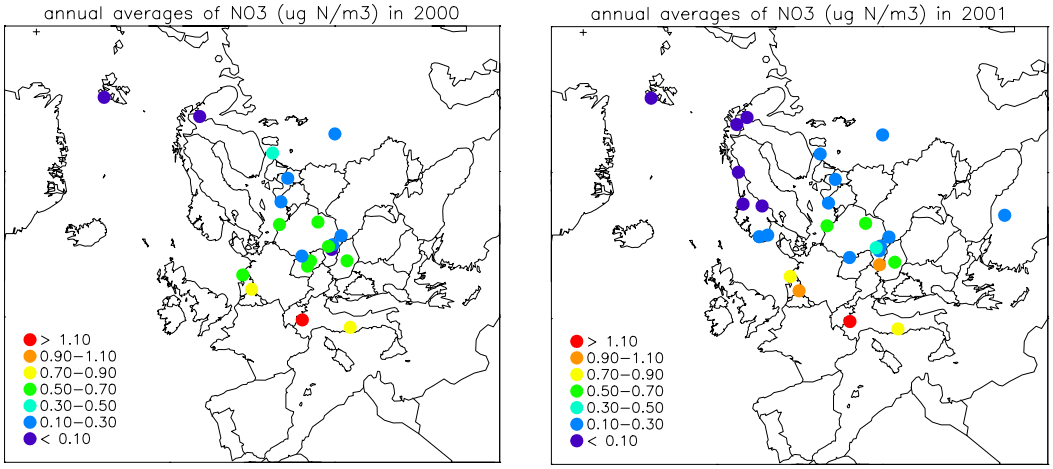

Figure 9: As Figure 8, but for nitrate.

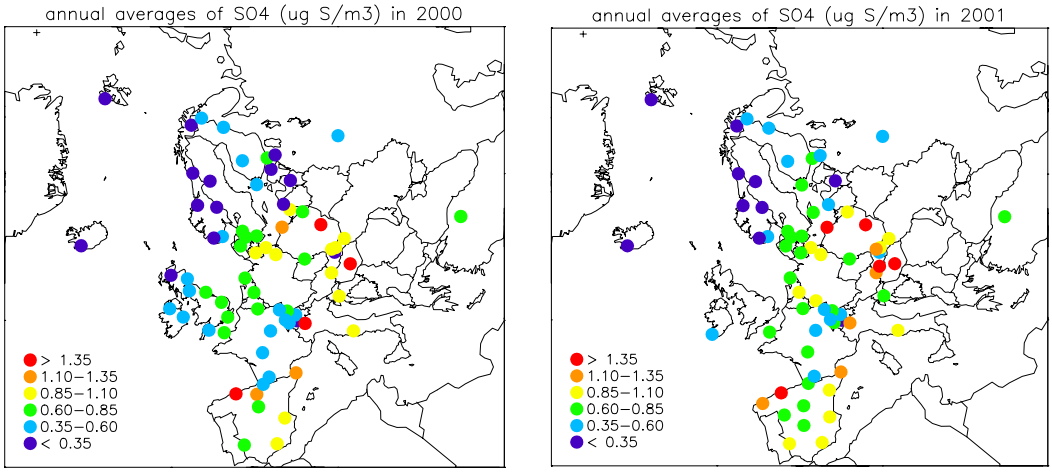

Figure 10: As Figure 8, but for sulphate.

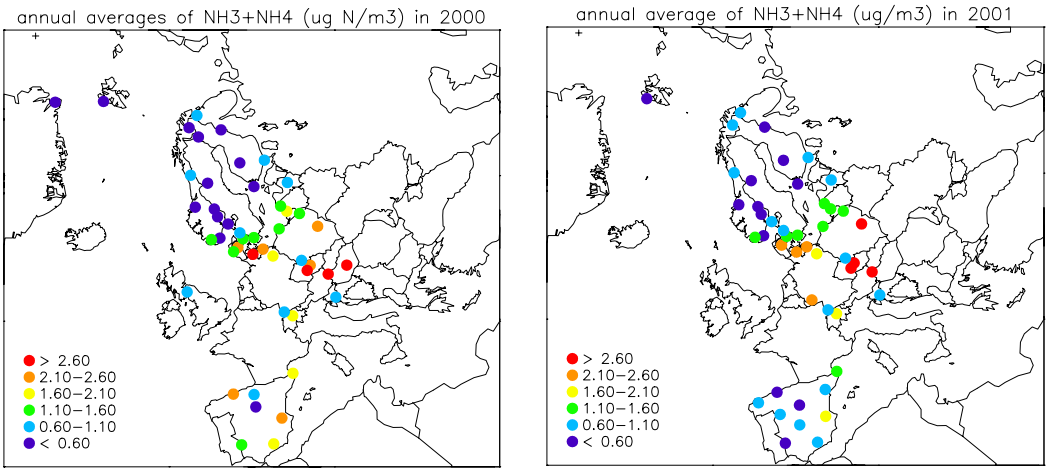

Figure 11: As Figure 8, but for the sum of ammonia and ammonium (μg N/m^3).

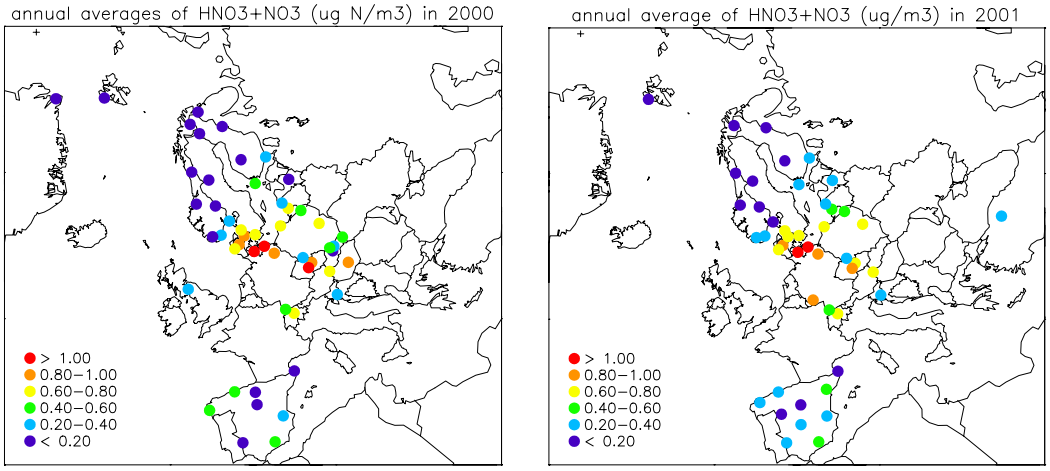

Figure 12: As Figure 8, but for the sum of nitric acid and nitrate (μg N/m^3).

The spatial data coverage for sulphate is quite good in Europe, although more data from Eastern Europe would be desirable. Sulphate measurements are reasonably well coordinated with particle mass monitoring. Thus almost all stations from which $PM_{2.5}$ data were available in 2001 also reported sulphate concentrations in aerosols (with the exception of Chaumont in Switzerland, Langenbrügge in Germany, and Lista in Norway). 20 out of 28 stations from which PM_{10} data were available in 2001 also reported sulphate concentrations in aerosols.

The spatial data coverage for denuder/filterpack measurements, which allow us to correctly separate NH_3 and NH_4^+ as well as HNO_3 and NO_3^+, is less satisfactory and not sufficiently coordinated with particle mass measurements. Only two stations (Birkenes in Norway and Ispra in Italy) from which $PM_{2.5}$ and PM_{10} data were available in 2001 also reported ammonium and nitrate concentrations in aerosols instead of the sums (NH_3+NH_4^+) and (HNO_3+NO_3^+). However, only filterpack measurements without denuder were performed at Birkenes. For all other stations that measured PM mass we have no such data. The number of sites measuring the sum of ammonia and ammonium and the sum of nitric acid and

nitrate is significantly higher than that of ammonium and nitrate, respectively. But even for these components more data from France, the UK, and from Southeastern Europe would be desirable.

Also, at many stations aerosols are still sampled for chemical analysis without using a size selection inlet. Thus for many of the mass concentrations obtained for different chemical species it is difficult to say what the actual size cut-off of the samples is.

Information on heavy metals in aerosols is available from several EMEP stations. Figure 13 and Figure 14 show as examples annual averages of cadmium and lead, respectively, in 2000 and 2001. All stations shown have a data coverage over 50%. Cadmium concentrations are noticeably lower in 2001 than in 2000, except in the Baltic countries. In 2001, lead concentrations are comparable to those observed in 2000 in Central Europe. However, in Slovakia lower lead concentrations have been measured in 2001 at all five EMEP stations. In Latvia, lead concentrations in 2001 are lower by almost 50% compared to 2000 values, whereas slightly higher values have been observed at one Lithuanian EMEP station.

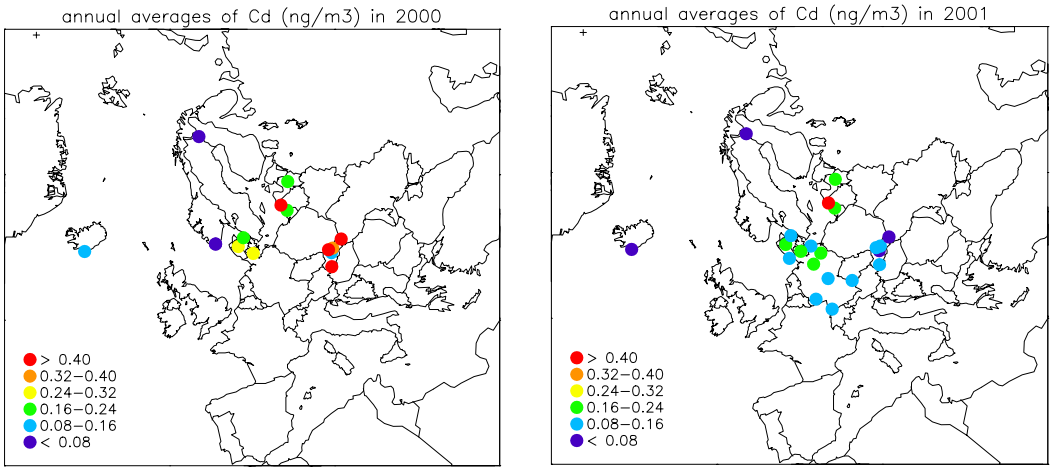

Figure 13: As Figure 8, but for cadmium.

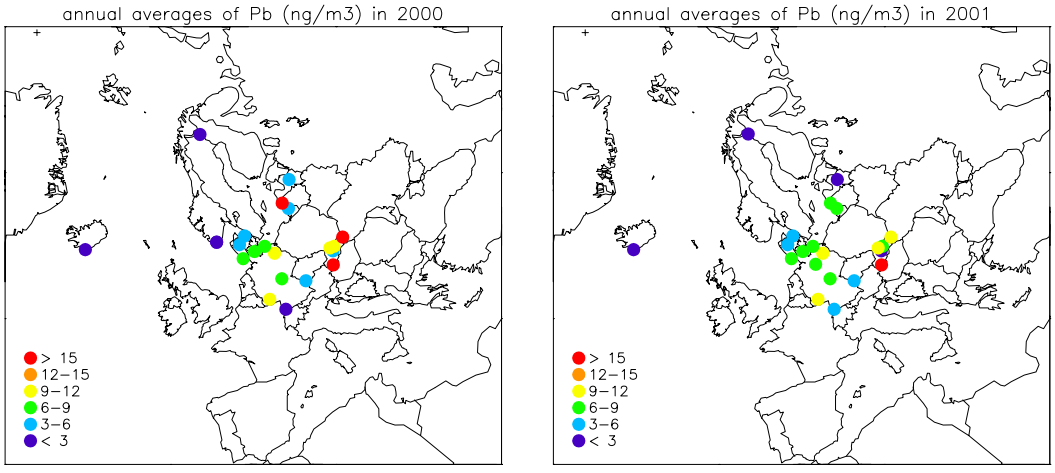

Figure 14: As Figure 8, but for lead.

Only one site has reported in 2001 a reasonably complete data set of all relevant inorganic components coordinated with monitoring of particle mass, namely Birkenes in Southern Norway[1]. Figure 15 shows a comparison of the chemical constituents measured at Birkenes in 2001 with corresponding data for particle mass. One can see that sulphate, nitrate, and ammonium only account for roughly 75% of the inorganic mass, and for only 1/3 of the total mass. Thus monitoring of at least sodium and chloride is important at Birkenes. A high contribution of sea salt is to be expected at monitoring sites in close proximity to the ocean. Even more strikingly, we see that the sum of all inorganic components accounts for only 50% of the total PM_{10} mass. Organic carbon (OC) and "elemental carbon" (EC, originating from combustion processes) contribute significantly to the total particle mass. CCC, in cooperation with 13 different countries, therefore undertook an EC/OC measurement campaign that lasted for one year. First results from this campaign are presented in the next section.

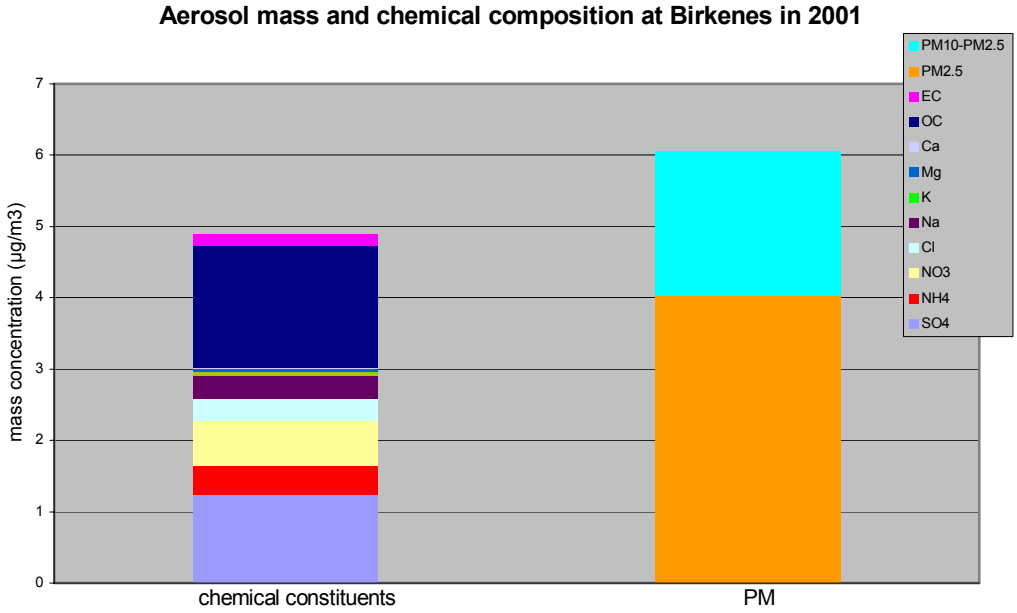

Figure 15: Annual averages of chemical composition and particle mass measured at Birkenes (Norway) in 2001.

Figure 15 also shows that we are missing about 20% to obtain a full mass closure from the chemical constituents. This reflects several uncertainties in the measurements. Water and volatile organic compounds (VOC) in the condensed aerosol and in the gaseous phase are in thermodynamic equilibrium with each other at the time of sampling. During transport and conditioning of the filter samples the conditions change, which can lead to the loss (or addition) of material. Likewise the partitioning between gaseous and condensed chemical species, such as nitric acid and ammonia on the one hand and ammonium nitrate on the other hand, can

[1] We note that in different geographical regions there are different inorganic components that, in addition to sulphate, nitrate, and ammonium, may be important. At Birkenes, for instance, sea salt is usually more important than mineral dust, whereas in Southern Europe mineral dust can be more important than sea salt.

change with shifting temperature, relative humidity, and pressure. Sampling of OC is subject to additional artefacts, as the quartz filters used in conjunction with OC determination have a relatively high affinity to adsorption of organic vapours. Finally, thermo-optical measurements of OC capture only the mass of the carbon atoms. Correction factors to account for other atoms vary between 1.2 (for species mainly containing hydrogen) to 1.8 (for water soluble organic species with a large portion of oxygen, nitrogen, and other heavier atoms) (Matta et al., 2003). Even higher correction factors have been suggested. In Figure 15 we used a factor of 1.5. Clearly, the relatively large range for the OC correction factor introduces a significant uncertainty in the OC mass.

2.3 EMEP measurement campaign of organic and elemental carbon in Europe – first results

The EC/OC campaign was initiated and coordinated by CCC/NILU. Sampling of PM_{10} (and in Birkenes also $PM_{2.5}$) started in summer 2002 and continued until summer 2003. 15 stations from 13 different European countries participated in the campaign (see Table 2). Samples were taken on one day per week. All filters were preconditioned at CCC and sent to the participants. After sampling the filters were sent back to CCC, where they were post-conditioned. The pre- and post-conditioning of the quartz filters was in accordance with the new EMEP quality assurance guidelines for PM_{10} sampling as defined in the EMEP manual for Sampling and Chemical Analysis. Subsequently, EC and OC masses are determined at CCC by thermo-optical analysis (EMEP/CCC, 2002). Analysis of the filters is still in progress. We will present some first results for the EC/OC data here. A thorough analysis of the data will be conducted soon.

Table 2: Stations that participated in the EC/OC campaign and their sampling equipment.

Stations		Instrument/Impactor	Filter size	Flow rate
AT02	Illmitz	Partisol	47 mm	16.7 l/min
CZ03	Košetice	FH 95 SEQ	47 mm	38 l/min
BE	Ghent	Gent	47 mm	17 l/min
FI17	Virolahti		47 mm	38 l/min
DE02	Langenbrügge	HiVol (Digitel)	150 mm	500 l/min
IE31	Mace Head	KFG	47 mm	38 l/min
IT04	Ispra	KFG	47 mm	38 l/min
IT	San Pietro Capofiume	Gent	47 mm	17 l/min
NL09	Kollumerwaard	KFG	47 mm	38 l/min
NO01	Birkenes	KFG	47 mm	38 l/min
NO42	Zeppelin	HiVol	8x10 inch	1133 l/min
PT01	Braganza	HiVol (Sierra)	8x10 inch	1133 l/min
SK04	Stara Lesna	Partisol	47 mm	16.7 l/min
SE12	Aspvreten	Gent	47 mm	15-18 l/min
GB	Penicuik	Partisol	47 mm	16.7 l/min

Figure 16–Figure 30 show time series of PM_{10}, EC, and OC mass concentrations (upper panels) and the mass concentration ratios OC/PM_{10} and EC/PM_{10} (lower panel) obtained at the different sites. No data are available yet for the Zeppelinfjell station on Spitsbergen (Norway). Note that the OC mass concentrations given in the Figures pertain to carbon atoms only. No correction factor has been applied yet to account for other atoms in the organic compounds. Thus the OC data shown most likely provide a lower bound for the true OC mass concentrations.

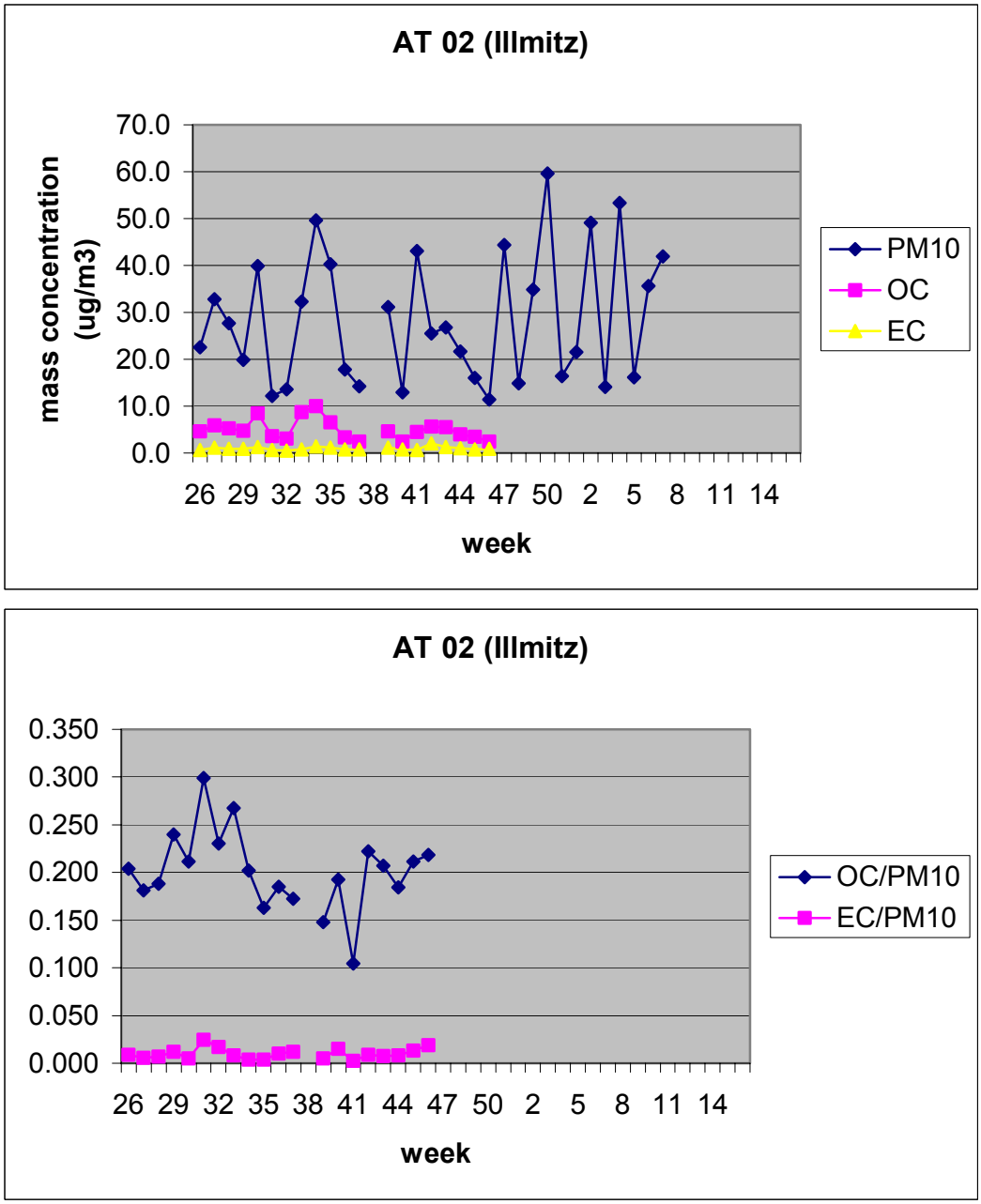

Figure 16: EC/OC results for Illmitz (Austria): mass concentrations in PM_{10} (upper panel); mass ratios OC/PM_{10} and EC/PM_{10} (lower panel).

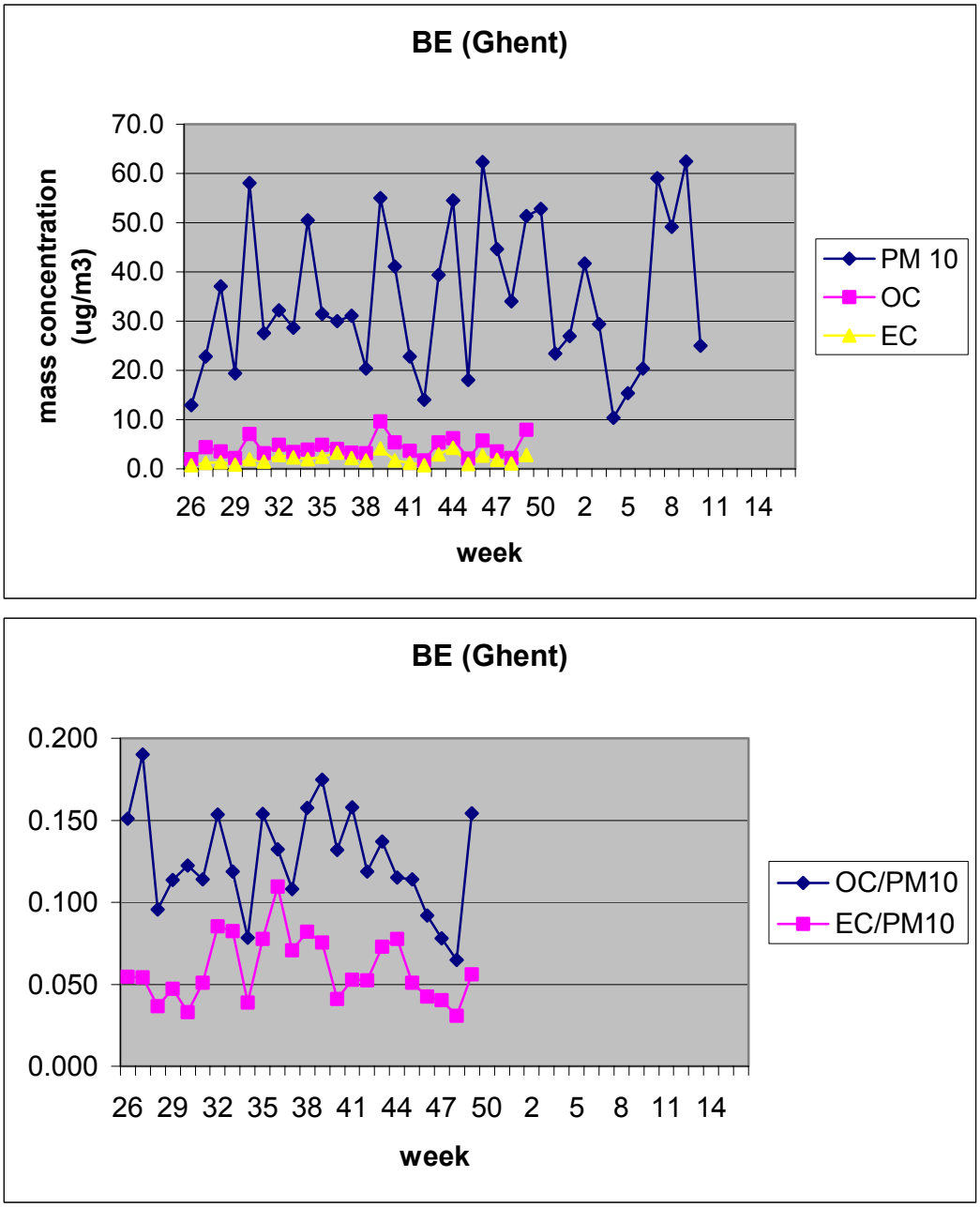

Figure 17: As Figure 16, but for Ghent (Belgium).

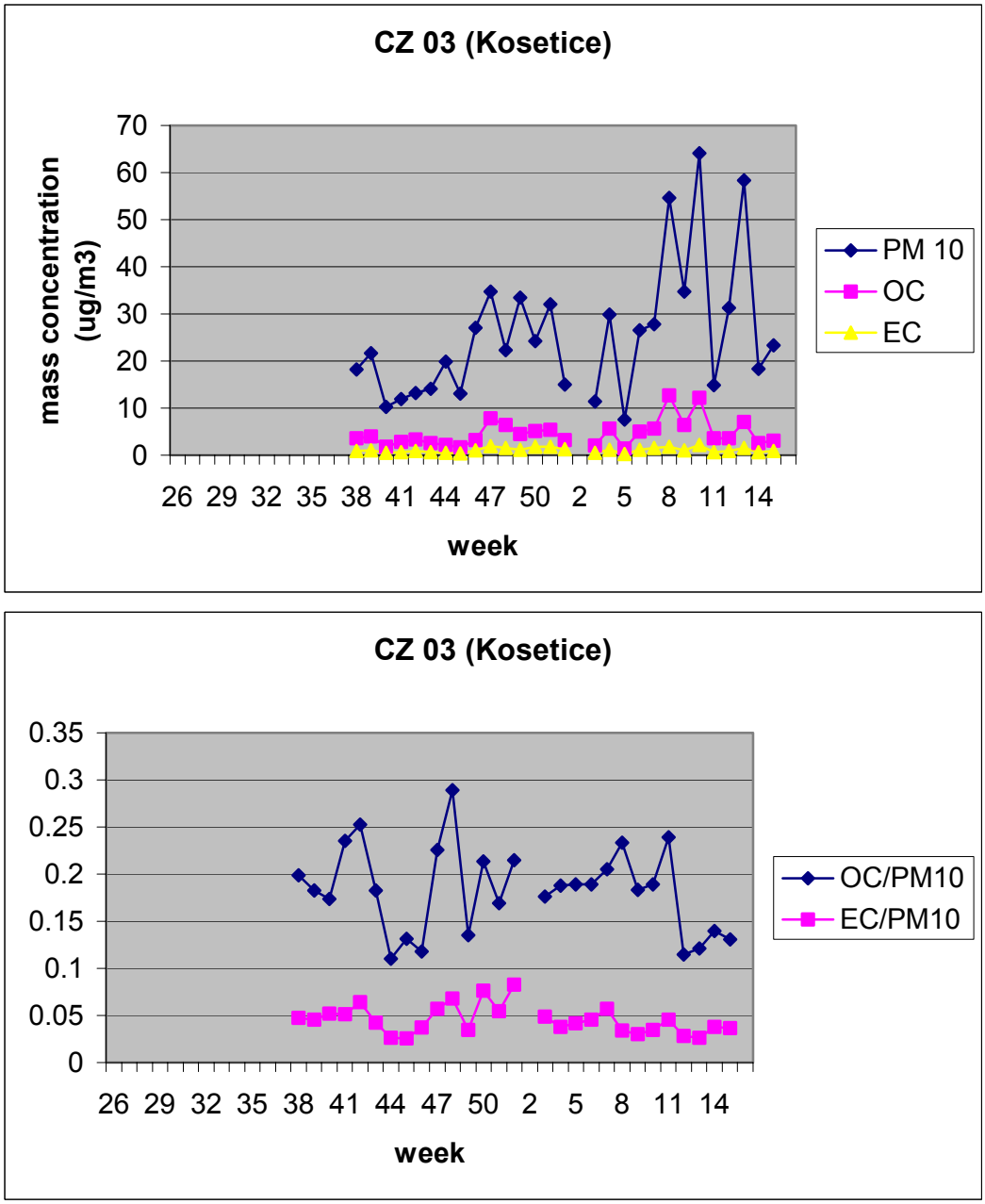

Figure 18: As Figure 16, but for Košetice (Czech Republic).

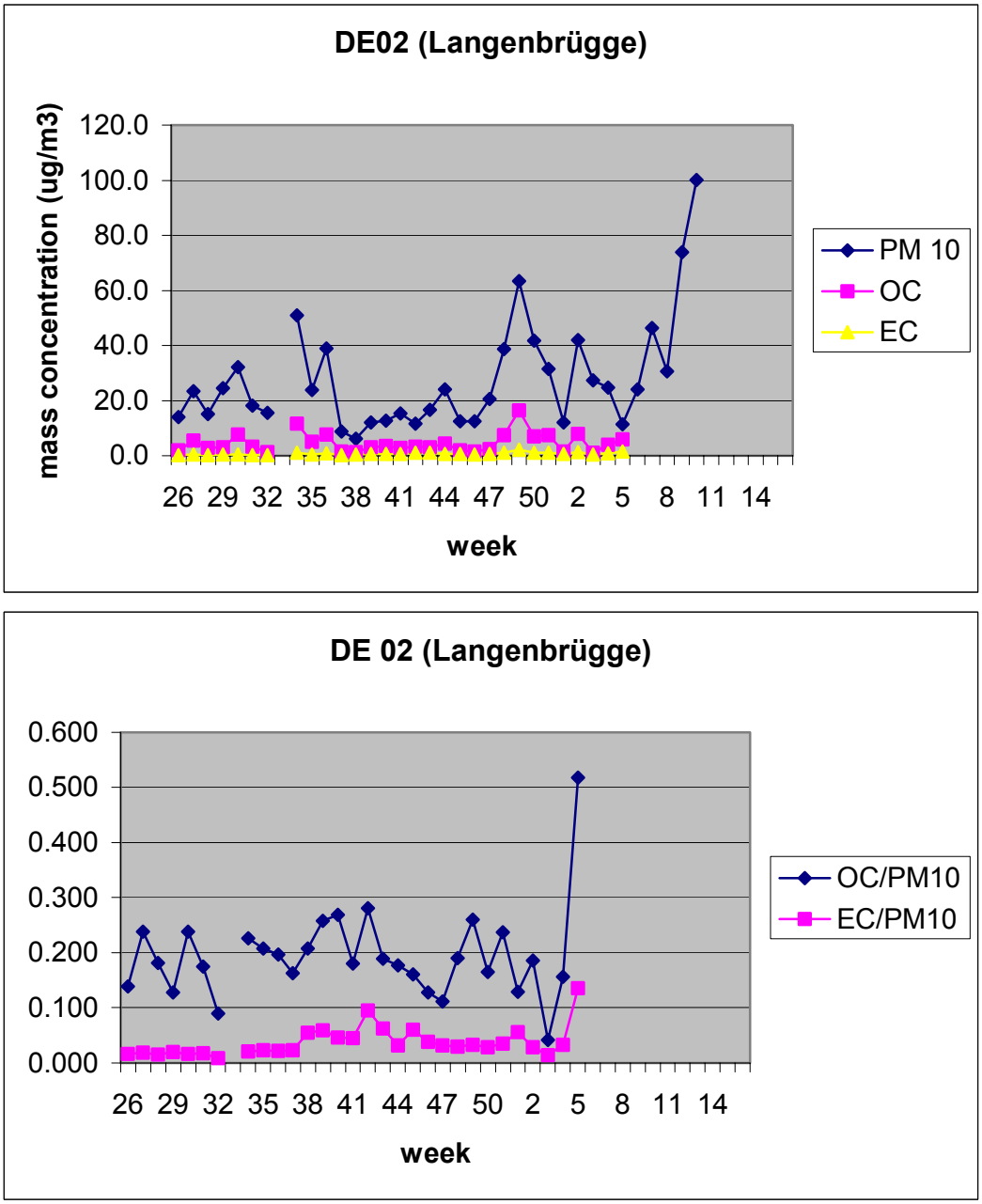

Figure 19: As Figure 16, but for Langenbrügge (Germany).

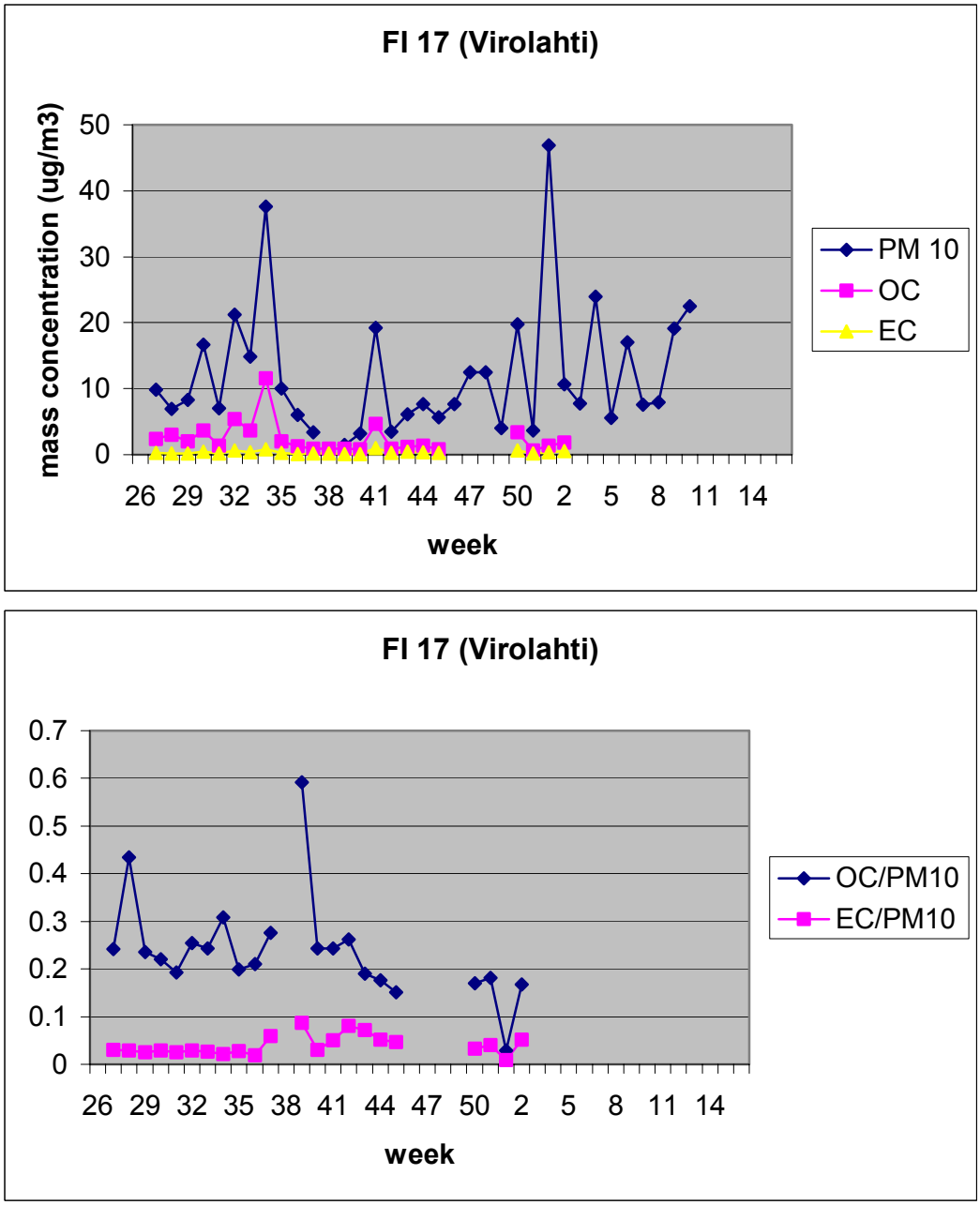

Figure 20: As Figure 16, but for Virolahti (Finland).

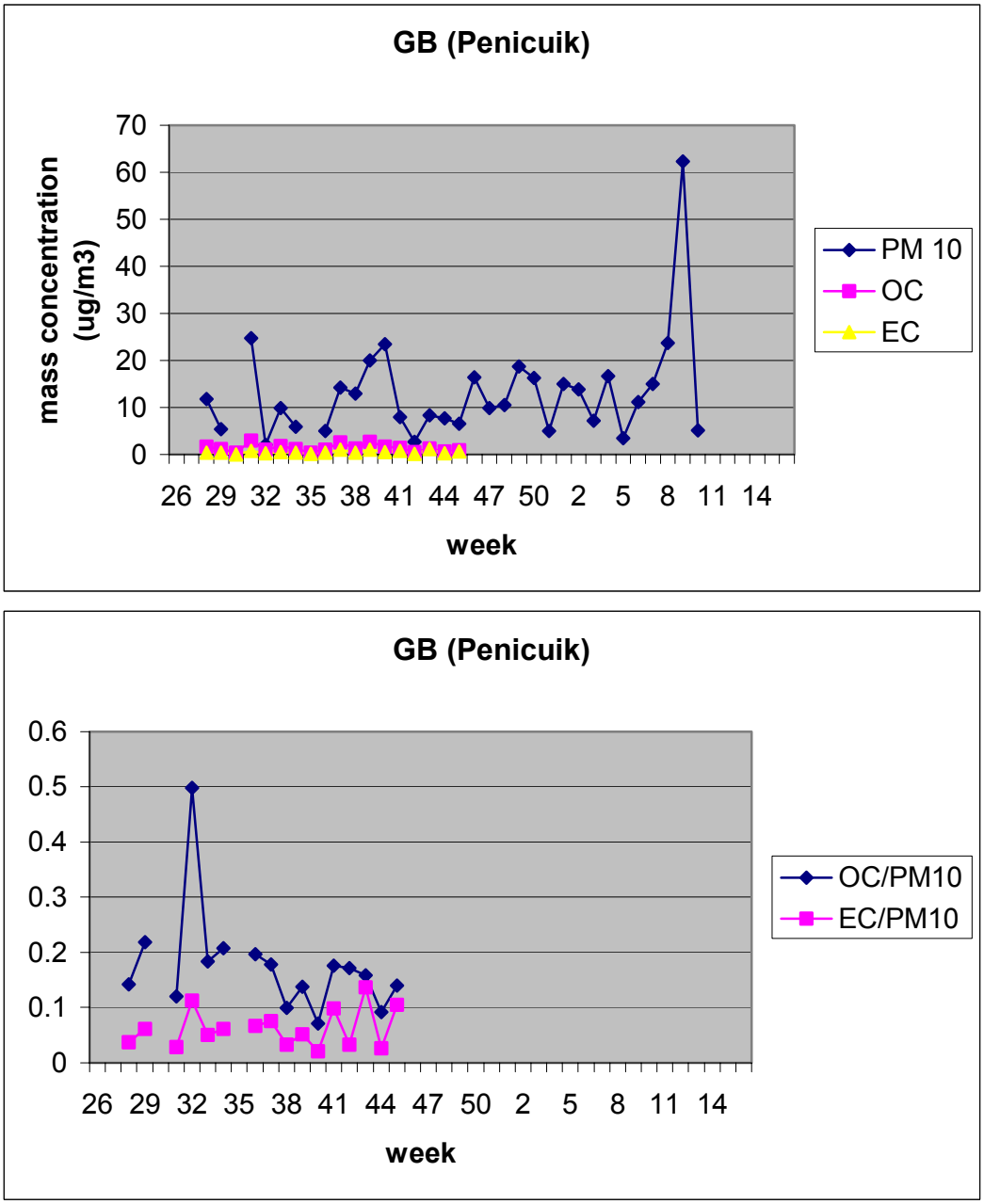

Figure 21: As Figure 16, but for Penicuik (Great Britain).

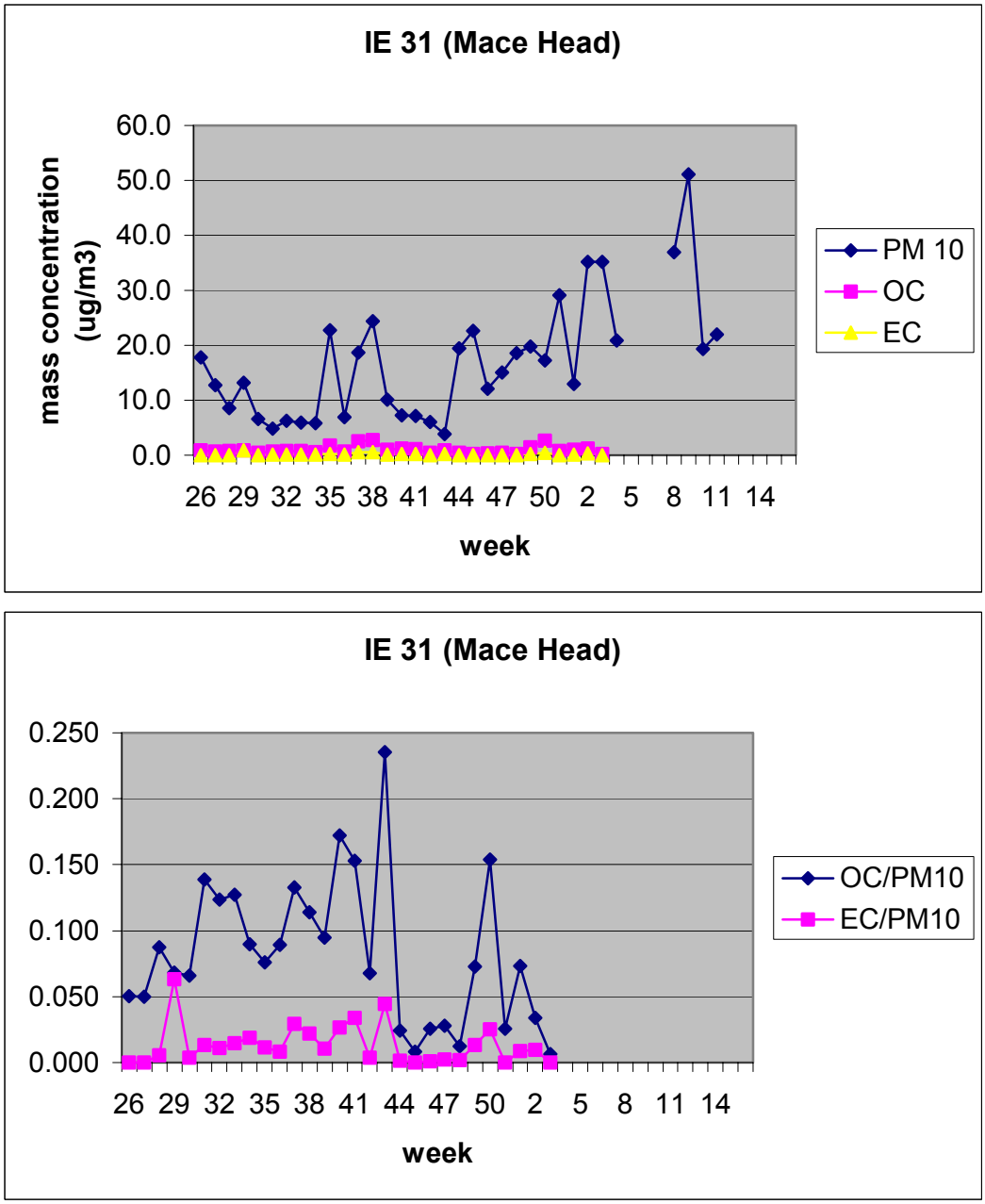

Figure 22: As Figure 16, but for Mace Head (Ireland).

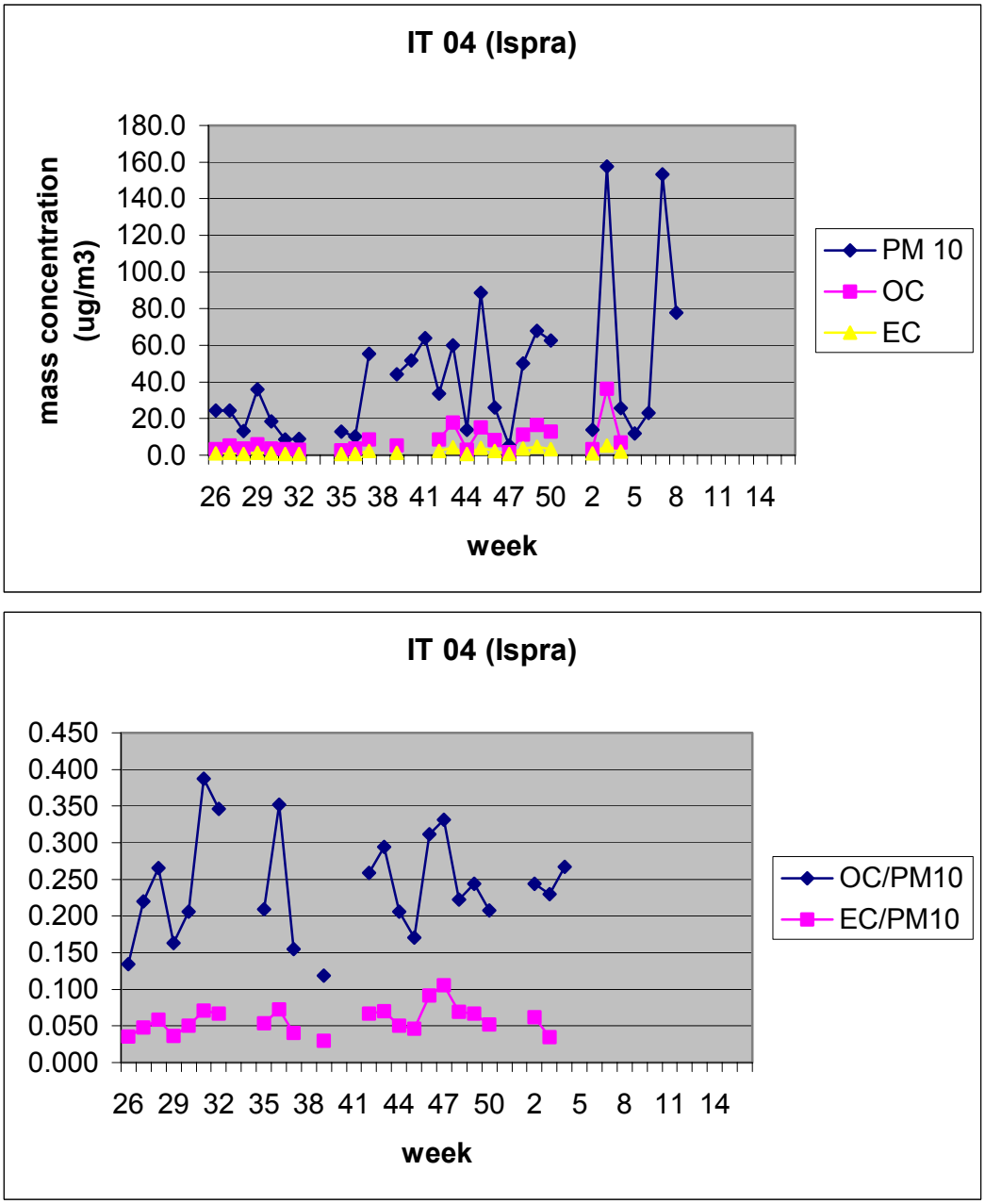

Figure 23: As Figure 16, but for Ispra (Italy).

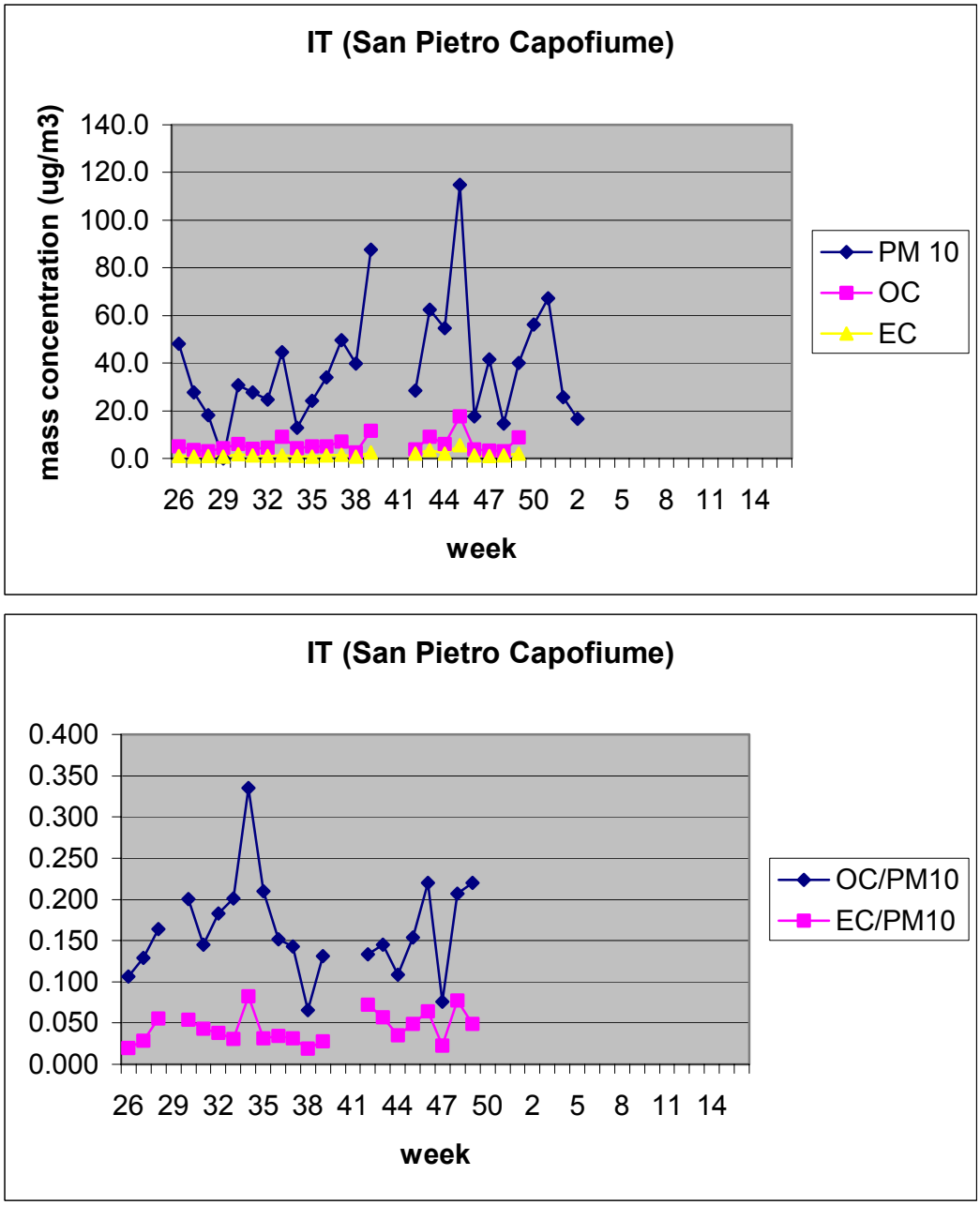

Figure 24: As Figure 16, but for San Pietro Capofiume (Italy).

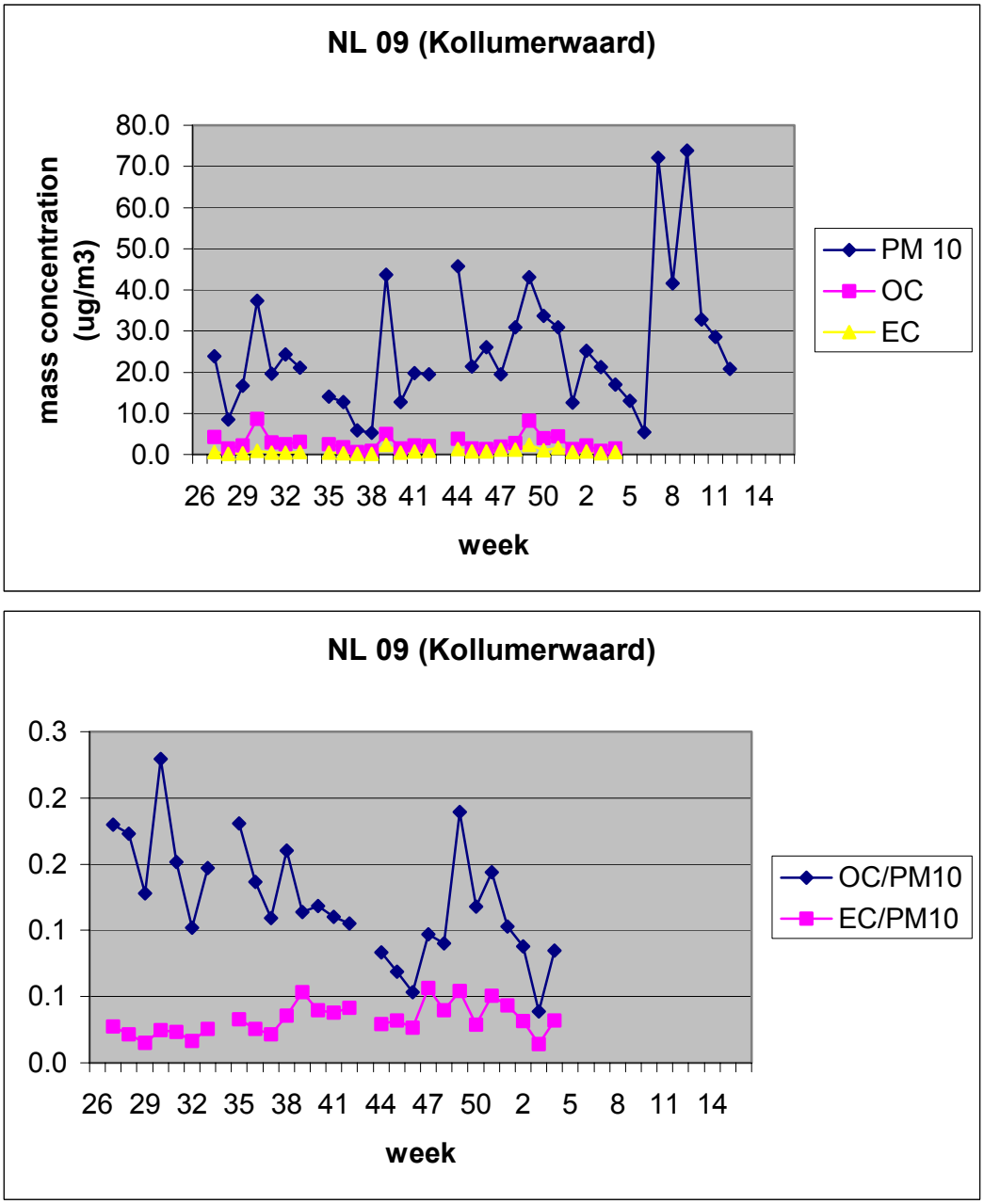

Figure 25: As Figure 16, but for Kollumerwaard (The Netherlands).

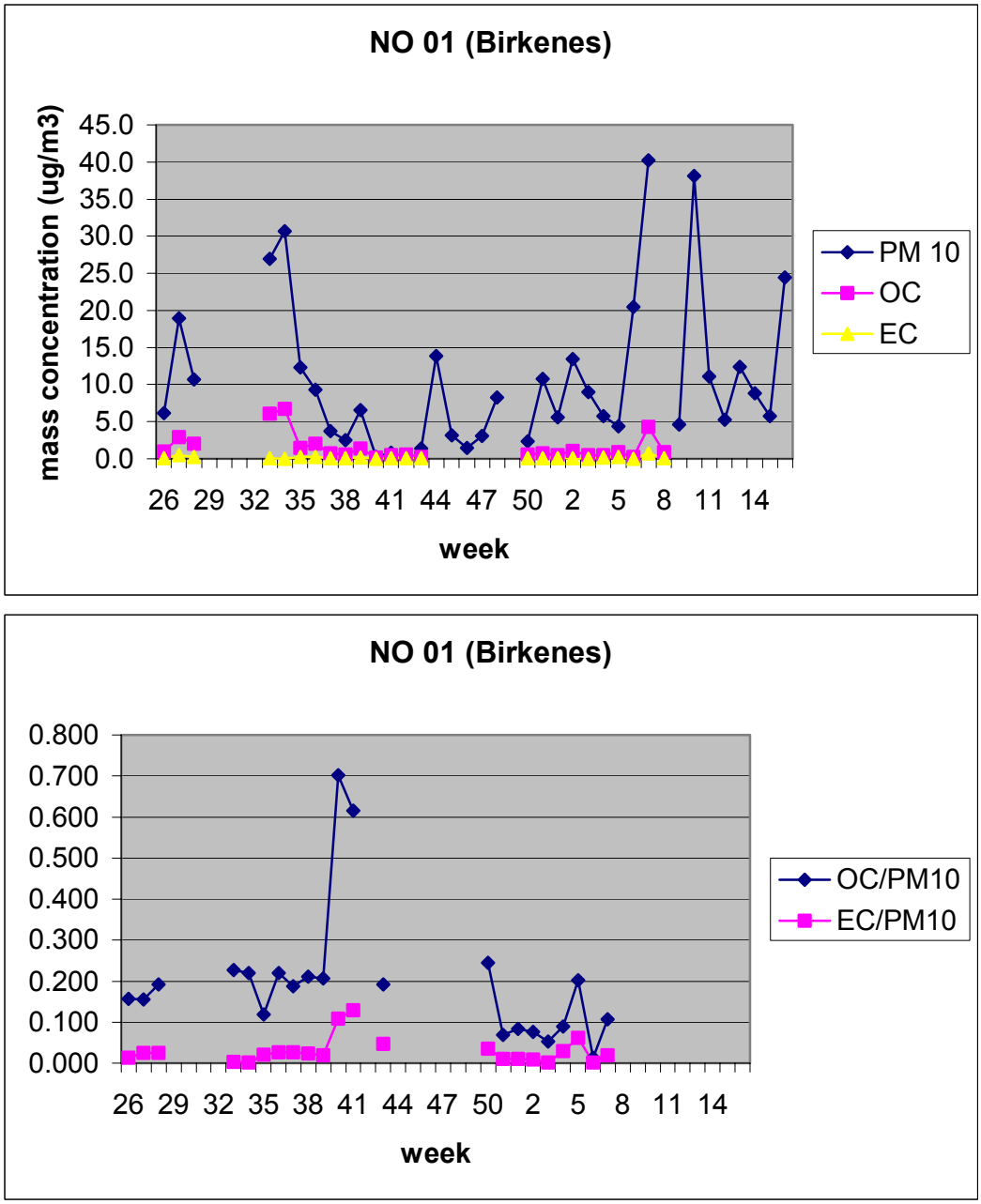

Figure 26: As Figure 16, but for Birkenes (Norway).

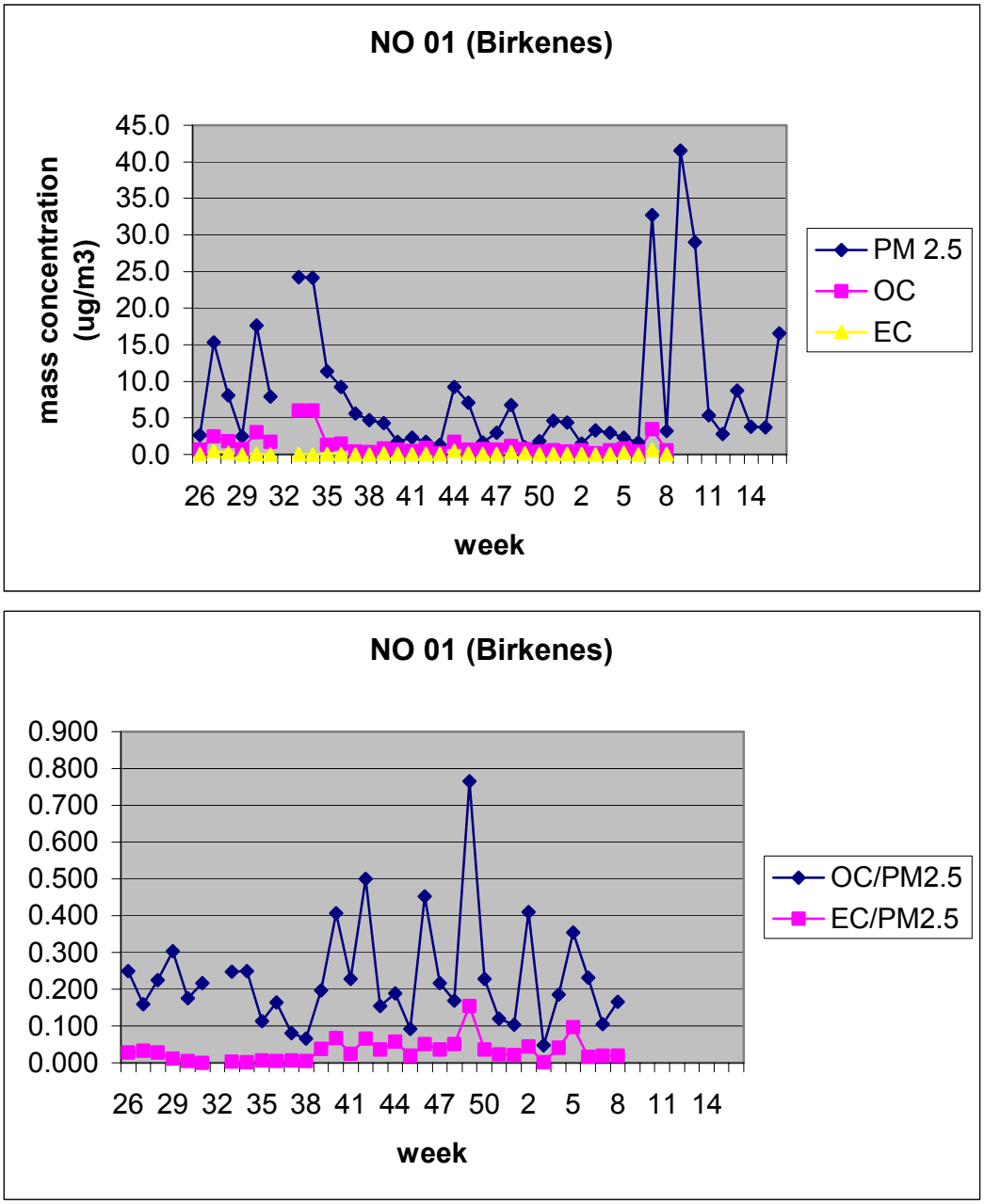

Figure 27: As Figure 26, but for $PM_{2.5}$.

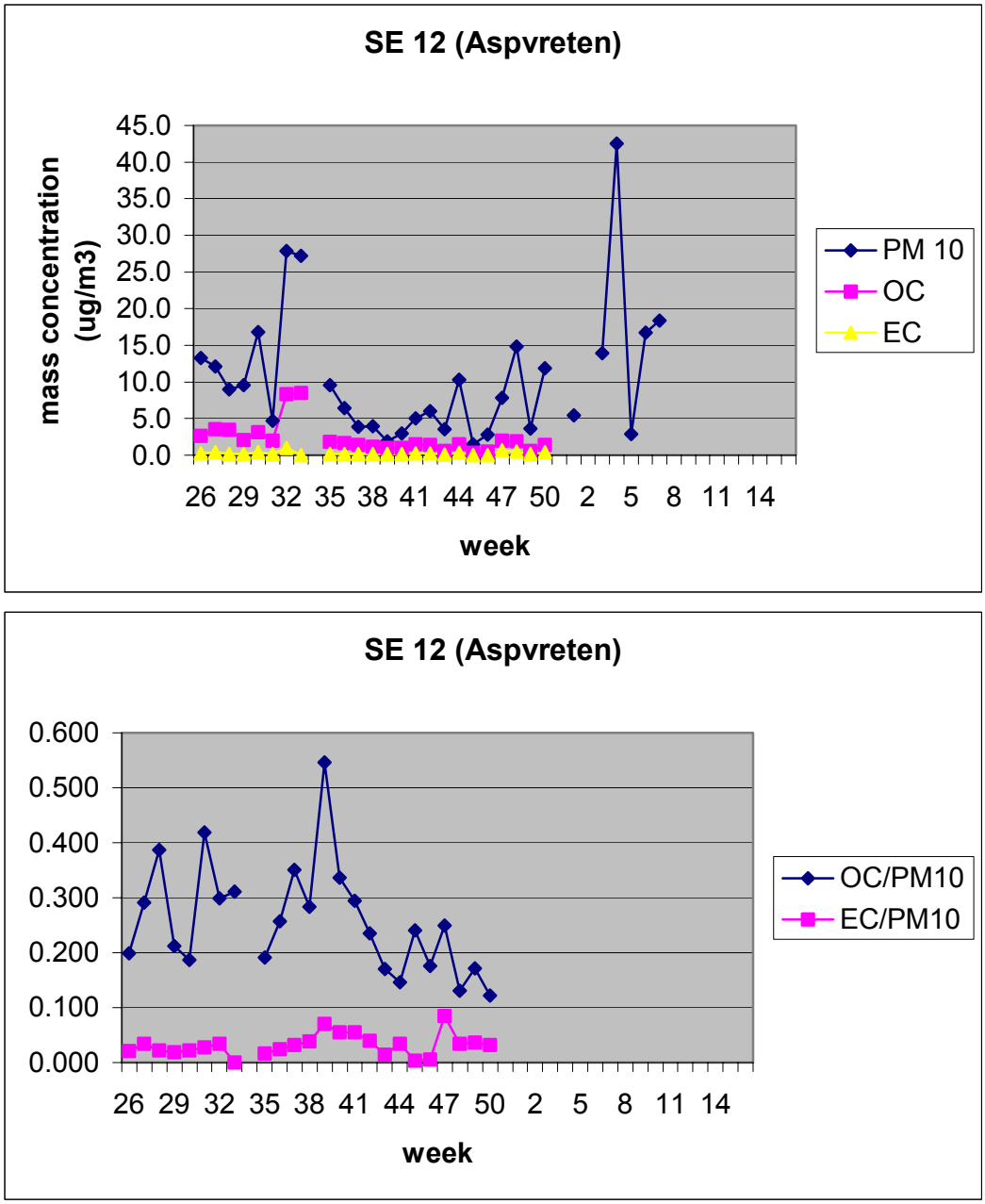

Figure 28: As Figure 16, but for Aspvreten (Sweden).

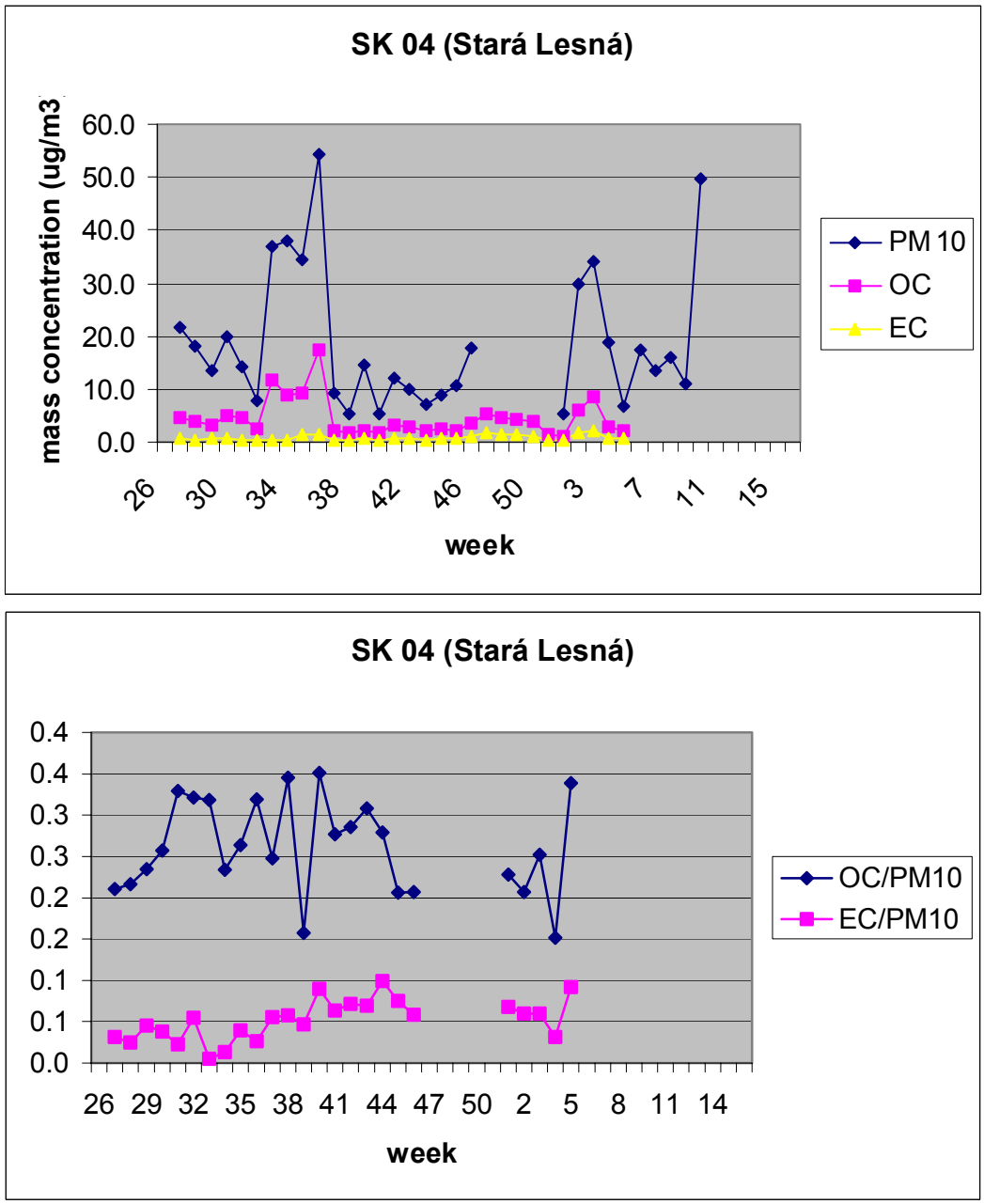

Figure 29: As Figure 16, but for Stará Lesná (Slovakia).

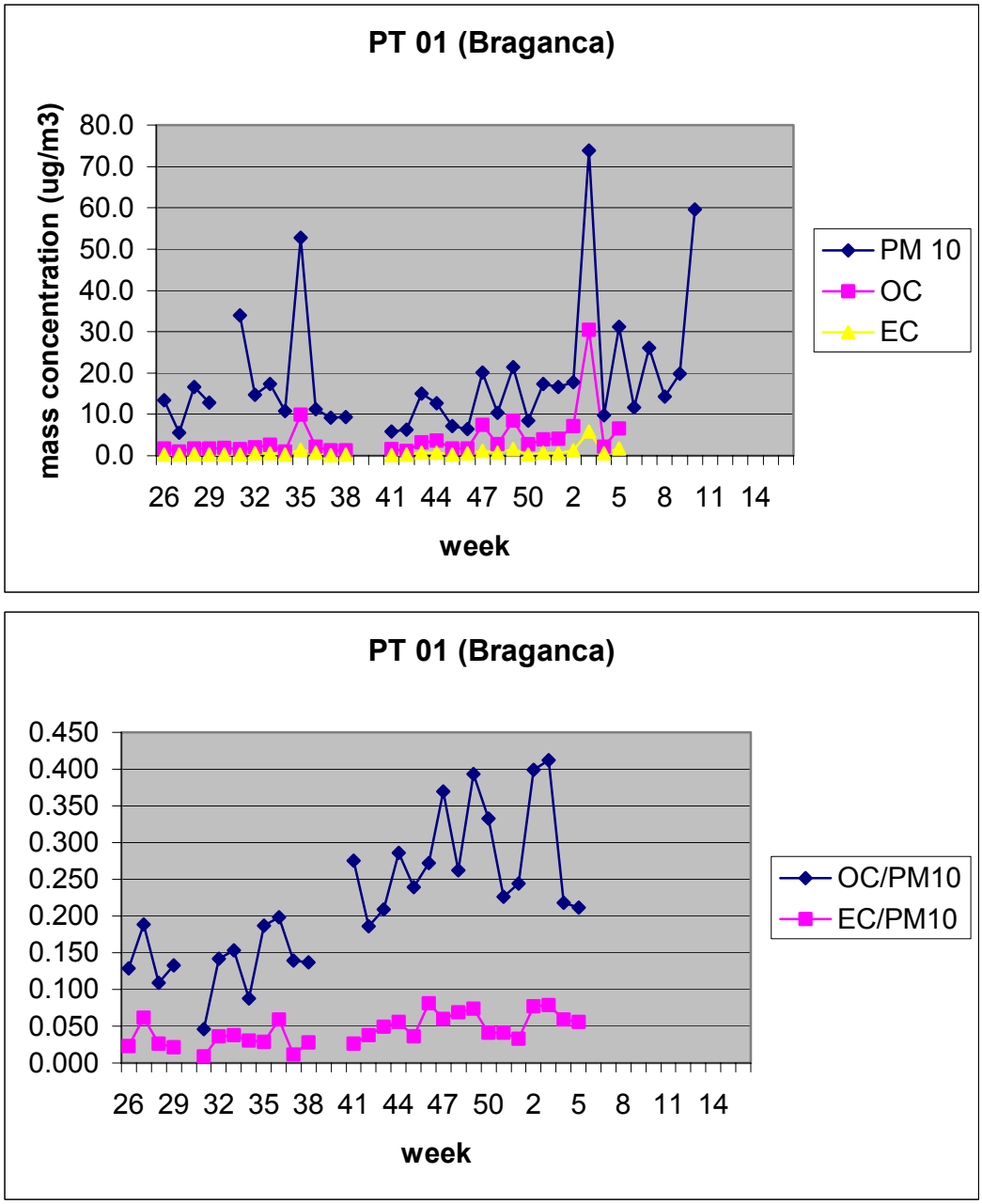

Figure 30: As Figure 16, but for Braganca (Portugal).

Clearly, OC concentrations fluctuate considerably at most measurement sites. Even though peak concentrations of PM_{10} are often accompanied by elevated OC concentrations, the mass ratio OC/PM_{10} is by no means a constant but varies at most stations over a large range. We find episodes during which the (uncorrected) OC mass concentration can account for as little as 3% and for as much as 70% of the PM_{10} mass concentration, with an average of roughly 20%. For large contributions of water-soluble organic species this can amount to a corrected average OC mass fraction of almost 40%, which is quite substantial. Peak values can even lie significantly higher than this. The high variability of OC and its high average and peak contributions to the total PM_{10} mass concentration underline the need to extend OC monitoring with a reasonably high time resolution. The high

fluctuations reflect the complex nature of the organic fraction, consisting of several thousand individual components originating from different natural and anthropogenic sources. However, they also reflect the measurement uncertainties associated with OC quantification. On the other hand, EC concentrations seem to be much more constant over time, accounting on average for roughly 5% of the total PM_{10} mass. Most EC originates from soot emissions, mainly from combustion processes.

These first results of the EC/OC campaign confirm that organic and elemental carbon contribute significantly to the total aerosol mass. The complex behaviour of the organic fraction needs to be carefully analysed and should be monitored on a continuous basis. Obtaining more observational data on the EC/OC content of aerosols will also be critical for making further progress in the development of the EMEP Unified Model. The problems of sampling artefacts due to OC adsorption in the quartz filters and the comparability of OC samples obtained with different sampling equipment need further investigation. Finally, a detailed speciation of the OC fraction in single components and/or a fractioning into different solubility classes is needed for selected sites.

2.4 Conclusions and future challenges

Basic PM monitoring programme

Fulfilling EMEP's objectives poses a significantly larger challenge for particulate matter than for most other single-component pollutants, due to the highly complex and variable nature of particles in air. PM monitoring is still a developing field within the EMEP network. Currently, one of the main shortcomings of the PM monitoring programme is an insufficient overlap between monitoring of PM mass and of chemical compounds in aerosols. In particular, to improve the current programme, high priority should be placed on attaining a significantly better coordination between PM mass measurements and denuder measurements of NO_3 and NH_4. Also, coordination of measurements of (HNO_3+NO_3) and (NH_3+NH_4) with PM_{10} measurements needs to be improved. Ten out of 28 stations reporting PM_{10} data in 2001 did not report any data for the sum of nitric acid and nitrate and for the sum of ammonia and ammonium. Chemical analysis should preferably be performed on PM_{10} rather than TSP samples. The spatial coverage of denuder measurements of nitrate and ammonium also needs to be improved. In fact, one should aim at measuring all the main inorganic components including the sum of nitric acid and nitrate and the sum of ammonium and ammonia at all EMEP sites at which PM_{10} and $PM_{2.5}$ (or PM_1) are sampled to obtain at least a basic characterisation of particulate pollutants. Denuder measurements should be performed at several sites in order to address the problems associated with sampling artefacts due to volatile compounds. According to site-specific conditions, monitoring of, e.g., mineral dust should be added at selected sites at which PM mass and the main inorganic components are measured. High priority should also be placed on obtaining a better characterisation of the EC/OC fraction in the monitoring programme. Weekly EC/OC determinations for the coarse and the fine fraction are desirable for a reasonably high number of sites. Needless to say, sites selected for such EC/OC measurements have to coincide with sites that perform the "standard" PM mass and inorganic measurements.

As discussed in some detail, mass measurements of the fine fraction are indispensable to separate accumulation mode and coarse mode aerosols. From a scientific standpoint, PM_1 would be preferable to $PM_{2.5}$.

More advanced PM measurements

In addition to a basic monitoring programme of PM mass, main inorganic components, and EC/OC content, the collection of additional and more advanced data material into the EMEP database should be considered. In the following, several possible extensions of today's database and/or monitoring programme are discussed.

In addition to EC/OC mass determinations, OC speciation of individual compounds and/or fractioning into different solubility classes (water soluble, water insoluble, other solvents) should be performed for a limited number of sites. At NILU/CCC OC speciation by means of liquid chromatography/high resolution mass spectroscopy as well as solubility classifications are currently in progress for OC samples collected at different Norwegian sites.

More emphasis needs to be placed on particle number distributions and on ultrafine particles (UFP). Particle mass is mostly determined by accumulation and coarse particles, whereas Aitken and nucleation particles make a negligible contribution to PM_{10}, $PM_{2.5}$, or even PM_1 mass. On the other hand, coarse particles contribute little to particle number densities. The main contribution to the particle number concentration comes from UFP, i.e. nucleation and Aitken particles, and to a lesser extent from accumulation particles. A better characterisation of Aitken particles is needed to facilitate our understanding of adverse health effects of aerosols, and of the dynamic growth of Aitken particles to accumulation mode particles by heterogeneous chemical processes. Accurate prediction of aerosol number concentrations is important for estimating the indirect climate forcing of aerosols.

There is accumulating evidence that UFP with a diameter of less than 100 nm can be highly damaging to lung tissue, and that UFP have a much higher ability to damage the lung than particles of similar chemical composition and larger diameters (see Stone and Donaldson, 1998 and references therein). The alveolar macrophages, which play a key role in removing foreign particles from the lung airways and alveoli, are unable to remove UFP as efficiently from the lungs as larger particles. UFP may even damage macrophage cell function. As a result of the long residence time of UFP in the alveoli inflammatory reactions are caused in the lung, and particles and microbes may enter into the delicate lung tissue, where the damage becomes more severe and prolonged. Thus monitoring and modelling number concentrations, particularly of UFP, seems to be at least equally relevant for studying the negative health effects of aerosols as monitoring particle mass.

Secondly, our ability to accurately model cloud processing of aerosols by heterogeneous chemistry depends on an adequate description of the particle number distribution. Even though Aitken particles spend only a short span of their lifetime in cloud droplets, cloud processing plays a significant role in the mass transfer from Aitken to accumulation mode aerosols due to the enhanced chemical reaction rates in the liquid phase.

Another important point pertains to the aerosols' ability to act as cloud condensation nuclei. An increase in the number concentration of cloud condensation nuclei results in a larger number of cloud droplets. Given the same amount of water vapour, this results in a shift of the water droplets' size distribution towards smaller sizes. Thus an increase in the number concentration of cloud condensation nuclei results in more and smaller droplets in the cloud. This change in cloud microphysical properties entails a change in the cloud radiative properties. The characteristic forward-scattering peak in the droplets' phase function increases with droplet size on the expense of side- and backward scattering. Consequently, clouds with smaller droplets show less forward scattering and more side or back scattering and therefore have a larger albedo (i.e. they reflect more visible radiation back into space). An increase in the number concentration of cloud condensation nuclei therefore leads, in general, to an increased negative climate forcing of clouds. This so-called indirect climate forcing effect of aerosols is one of the largest uncertainties in present climate models. Accurate data and model predictions of aerosol number concentrations, especially for fine particles (0.1–1 μm), provide the basis for improving our ability to accurately predict the indirect climate forcing effects of aerosols.

Very limited measurement data on particle number concentrations is available. One of the most extensive networks for measuring particle number distributions in Europe is a Nordic network comprising several Swedish and Finnish stations, and, since autumn 2002, the EMEP station at Birkenes. As an illustration of the information obtained from size distribution data, Figure 31 shows some first results from a newly installed differential mobility particle sizer (DMPS) instrument at Birkenes. The upper panel shows a time series of the particle number distribution for March 2003. One can clearly see several episodes of Aitken particles growing to accumulation size (f.ex. between day 72-75, and again between 80-83), repeatedly fuelled by local nucleation events. Thus DMPS data provide us with valuable information about aerosol dynamical processes. EMEP's PM monitoring programme could greatly benefit from obtaining size distribution information from a limited number of sites. The "CREATE" project under the EC 5th framework programme (contract No. EVK2-CT-2002-00173), in which NILU/CCC leads a work package on building an aerosol database, offers an opportunity to complement EMEP's monitoring database by obtaining more advanced and otherwise unavailable data from research groups around Europe, among them also DMPS data. This is an important step in this direction.

Finally, there lies a great potential in optical aerosol measurements for EMEP, particularly for EMEP's model validation work. Modelling long-range transport of aerosols requires computations in a model atmosphere consisting of multiple layers. Mass and number concentrations of particles on the ground and in upper layers influence each other in various ways. A comprehensive validation of the EMEP unified model should therefore aim in the future at taking information on vertical distributions of particles into account. Ground measurements can provide us with a very detailed physical and chemical characterisation of particulate matter. However, they do not provide us with information about the vertical distribution of particles in the boundary layer and in the free troposphere. Mass and particle concentrations and chemical composition of aerosols measured on the

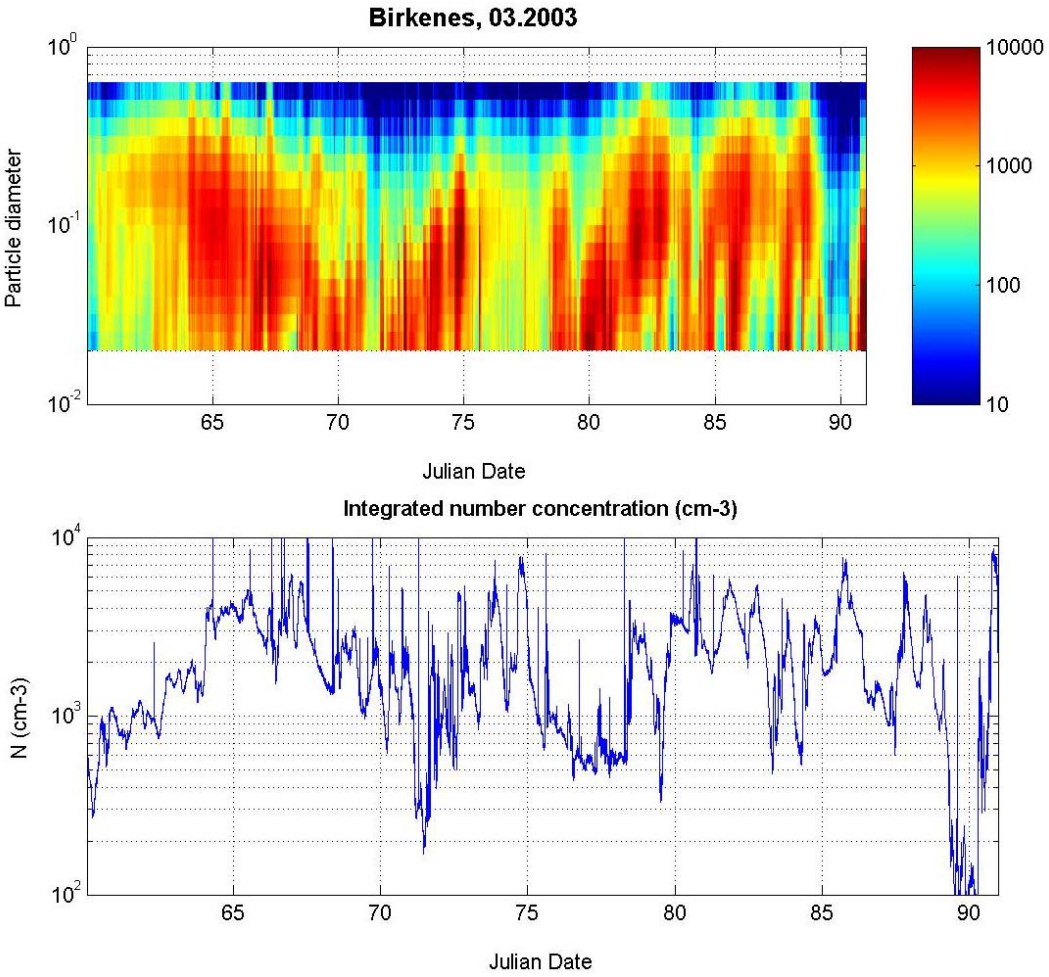

Figure 31: Particle number distribution (upper panel) and total particle number concentration at the EMEP site at Birkenes (Norway) in March 2003.

ground may not be representative for the corresponding particle characteristics at higher altitudes. Additional data are therefore needed. In situ measurements from airborne instruments are expensive and only available on a campaign basis. However, various kinds of optical measurements can serve to retrieve information on the distribution and temporal evolution of particles at higher altitudes.

As an illustration of the usefulness of optical measurements Chapter 5 presents an analysis of sun photometer data obtained at the Zeppelin EMEP site on Spitsbergen (Norway). Another illustration of optical measurements is given in Figure 32-Figure 33. The plots show Raman lidar measurements performed at the Southern Great Planes site of the US Atmospheric Radiation Measurement (ARM) programme and are taken from the ARM website (http://www.nsdl.arm.gov/cgi-bin/quicklook/frame.pl). Lidar backscattering data provide us with a unique range-resolved picture of the vertical distribution of aerosols in the atmosphere and their temporal evolution. In Figure 32, especially in the upper panel, one can clearly discern a high concentration of aerosols in the boundary layer, which expresses itself by a higher scattering ratio in the boundary layer than in the upper tropospheric layers, in which Rayleigh scattering by molecules dominates. The variation of the vertical extent of the aerosol layer over

the two-day period as well as an increase in aerosol concentrations is clearly seen. The high scattering ratios starting to occur at around 0200 UTC on April 21 indicate cloud formation. Also, the variation of the cloud base and the cloud top can be clearly observed in the data visualisation.

The instrument sends out polarised laser light and measures the backscattered light in two perpendicularly polarised channels, thus allowing for the determination of the depolarisation ratio. Since nonspherical particles depolarise light much more strongly than spherical particles, this allows us to discriminate between water and ice clouds. Figure 33 (note the larger vertical scale compared to Figure 32) shows that the clouds forming early on April 21 above the boundary layer have a rather low depolarisation ratio, whereas clouds observed throughout the two days near the tropopause have a high depolarisation ratio. One can conclude that the low-altitude clouds consist of liquid water, whereas the higher clouds are ice or mixed-phase clouds.

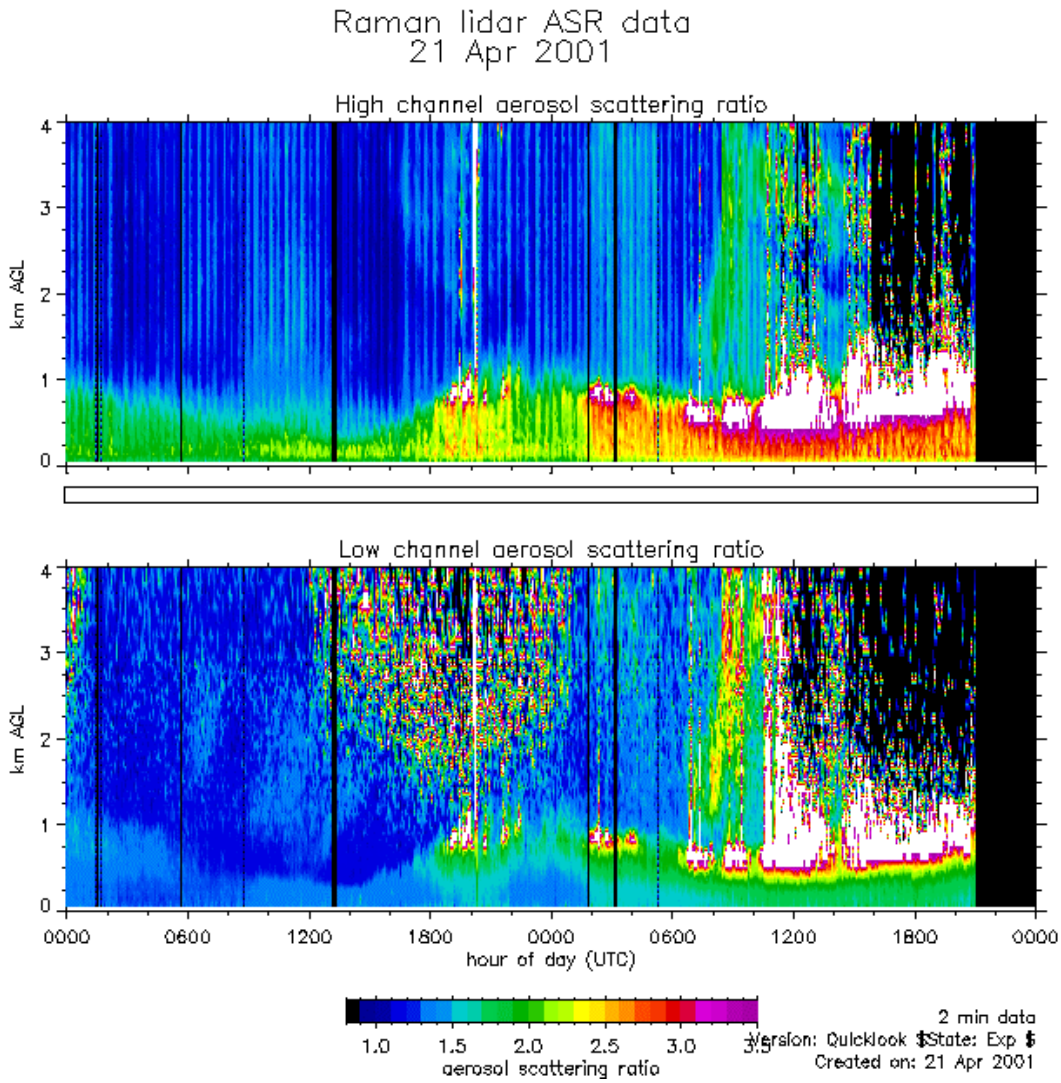

Figure 32: Aerosol backscattering ratio during a two-day period at the SGP ARM site.

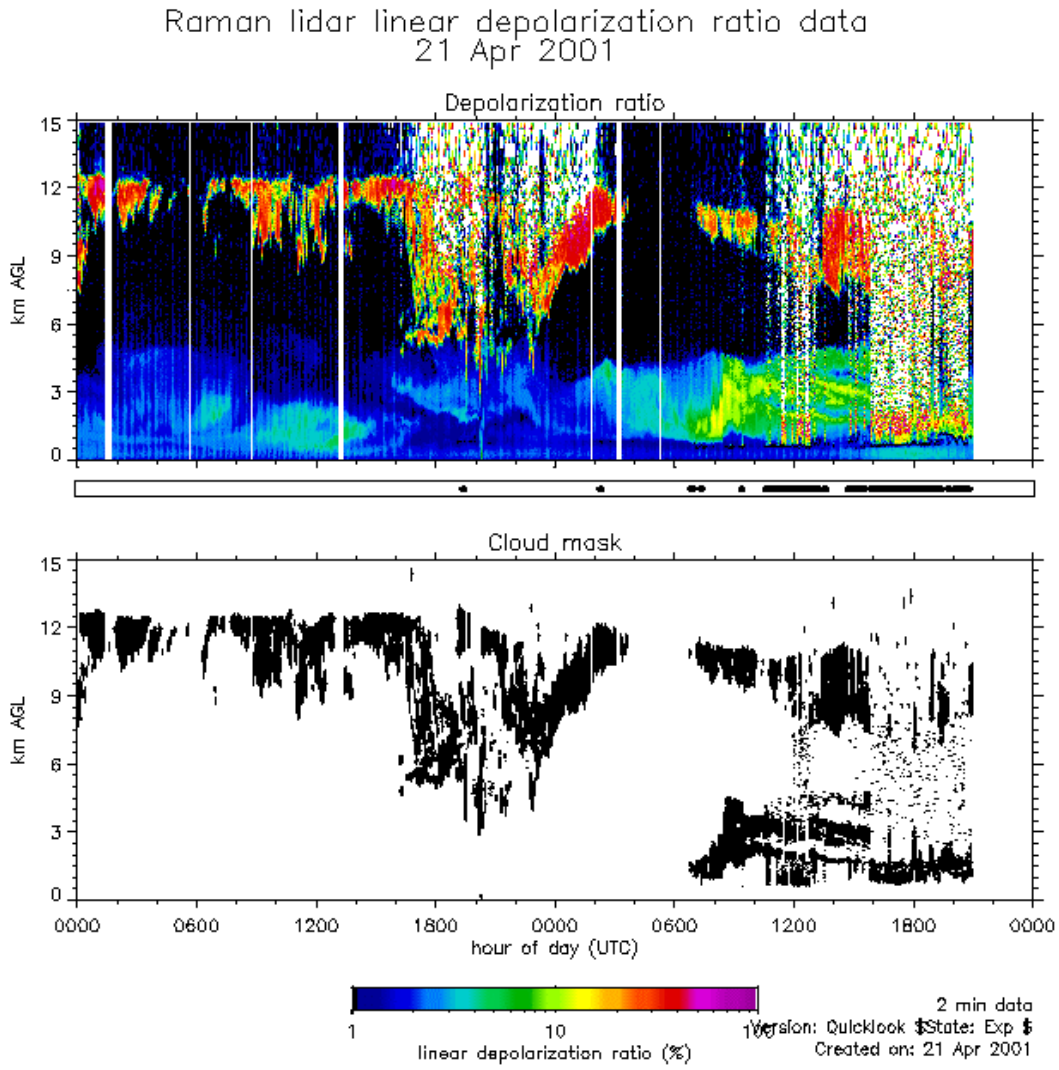

Figure 33: As Figure 32, but for the backscatter depolarisation ratio (upper panel) and for a cloud mask (lower panel).

This example illustrates the wealth of information contained in optical measurements. A lot can be learnt from these data about the transport and evolution of aerosols in the atmosphere since the lidar data reveal the vertical distribution and temporal changes of aerosols. A lot can also be learnt about the aerosols' interaction with clouds, which is important for wet deposition of aerosols, for cloud processing of particles, and not least for climate studies. Optical data would also provide useful information on aerosol loads in the boundary layer and the free troposphere for future model validation studies. It should therefore be considered to include a selected number of optical monitoring data into EMEP's aerosol database, or even to recruit new sites performing continuous optical aerosol monitoring as new EMEP sites.

Acknowledgements

Frank de Leeuw and Steinar Larssen(ETC/ACC) are gratefully acknowledged for making AIRBASE PM_{10} data available, and for providing Figure 4–Figure 6.

3. PM_{10} mass concentrations at Birkenes during 2002

K.E. Yttri
Norwegian Institute for Air Research, P. O. Box 100, 2027 Kjeller, Norway

Airborne particle sources are either of natural or anthropogenic origin, and the particles are emitted directly from the sources as primary particles or created in air from gaseous substances through chemical reactions to secondary particles. The particle chemical composition can be quite complex, and one single particle may contain a large and changing amount of different chemical compounds during transportation due to chemical and physical processes in air. Research is needed in this field in order to fully understand and to model the processes and products. Reliable data on concentrations, compositions, and size distributions are needed in order to control and reduce the emissions of both particles and their precursors. The chemical composition is important since it contains information on sources as well as on the chemical and physical processes that take place in the atmosphere. Particles in air have a direct effect on the radiation balance in the atmosphere and an indirect effect on cloud formation, and different chemical characteristics of particles have different effects. Particles are known to have an adverse health effect. However, the effects due to different chemical compositions are still unclear. The best-known link between airborne particles and adverse health effects is connected to particle size. Fine and ultra-fine particles penetrate deeper into the lungs than larger particles and they have a stronger negative health effect.

The arithmetic average mass concentration of PM_{10} for 2002 at Birkenes was 7.2 μg m^{-3} (Table 3). The monthly averages increased from 4–5 μg m^{-3} in January to 13.1 μg m^{-3} in April followed by a decrease to 7.6 μg m^{-3} in July 2002. The highest monthly average was calculated for August; 14.1 μg m^{-3}, which is the highest monthly average since the measurements started in 1999. During autumn the monthly averages decreased to a minimum of 2.5 μg m^{-3} in October followed by a slight increase to 4.4 μg m^{-3}in December.

The $PM_{2.5}$ mass concentrations were highly correlated to the corresponding PM_{10} concentrations, and were on average 67% of the PM_{10} concentrations in 2002 (Figure 34 and Table 3). The annual average $PM_{2.5}$ mass concentration in 2002 was 4.8 μg m^{-3}, while the corresponding coarse fraction $PM_{10-2.5}$ reached 2.4 μg m^{-3} (Table 3). The $PM_{10-2.5}$ contributed substantially to PM_{10} mass concentrations during certain periods. During February, May, and October the coarse fraction's share of the PM_{10} concentration was 61%, 47% and 46% respectively. The PM_{10} concentrations were, however, rather low during February and October, and the $PM_{10-2.5}$ mass concentrations were not particularly high.

The $PM_{10-2.5}$ and the $PM_{2.5}$ masses are not well correlated at Birkenes, which indicates different sources for the two fractions. This view is supported by different chemical compositions in the fractions; $PM_{2.5}$ is dominated by the mass of SO_4^{2-}, NO_3^-, NH_4^+, K^+, Ca^{2+}, and organic plus elementary carbon (TC). On the other hand, the dominating contribution to the mass of the coarse fraction comes from Cl^-, Mg^{2+}, and Na^+. NO_3^-, Ca^{2+}, and K^+ in both fractions are fairly well

correlated, which may be due to reactions between gaseous nitric acid and sea salt, soil dust, and other constituents of coarse particles.

Table 3: Annual average 2002, and minimum and maximum of $PM_{2.5}$, $PM_{10-2.5}$ and PM_{10} for 2002.

Month	$PM_{2.5}$	$PM_{10-2.5}$	PM_{10}
January	3.2 (0.3-11.2)	1.7 (0.25-6.1)	4.9 (1.2-14.4)
February	1.5 (0.3-8.0)	2.4 (0.2-13.0)	3.9 (0.5-19.1)
March	6.0 (0.7-31.8)	2.4 (0.2-6.9)	8.4 (0.9-34.1)
April	10.1 (1.0-22.2)	3.0 (0.7-5.8)	13.1 (1.7-26.2)
May[1)]	5.2 (1.2-12.9)	4.6 (0.3-12.5)	9.8 (1.7-22.1)
June[2)]	4.8 (0.3-13.6)	3.0 (0.3-8.1)	7.8 (0.7-20.1)
July[3)]	5.1 (0.4-14.9)	2.5 (0.3-6.9)	7.6 (1.0-20.4)
August[4)]	10.4 (1.2-24.4)	3.7 (0.3-7.8)	14.1 (4.3-31.3)
September[5)]	3.3 (0.3-12.7)	2.4 (0.3-6.0)	5.7 (1.0-17.1)
October[6)]	2.3 (0.3-13.3)	2.0 (0.1-18.0)	4.2 (0.7-21.9)
November	1.8 (0.2-7.8)	0.8 (0.1-3.0)	2.5 (0.5-9.1)
December	3.8 (1.3-7.4)	0.6 (0.1-2.2)	4.4 (1.5-8.0)
Annual average	4.8	2.4	7.2

1) 5 samples missing this month
2) 5 samples missing this month
3) 2 samples missing this month
4) 2 samples missing this month
5) 3 samples missing this month
6) 3 samples missing this month

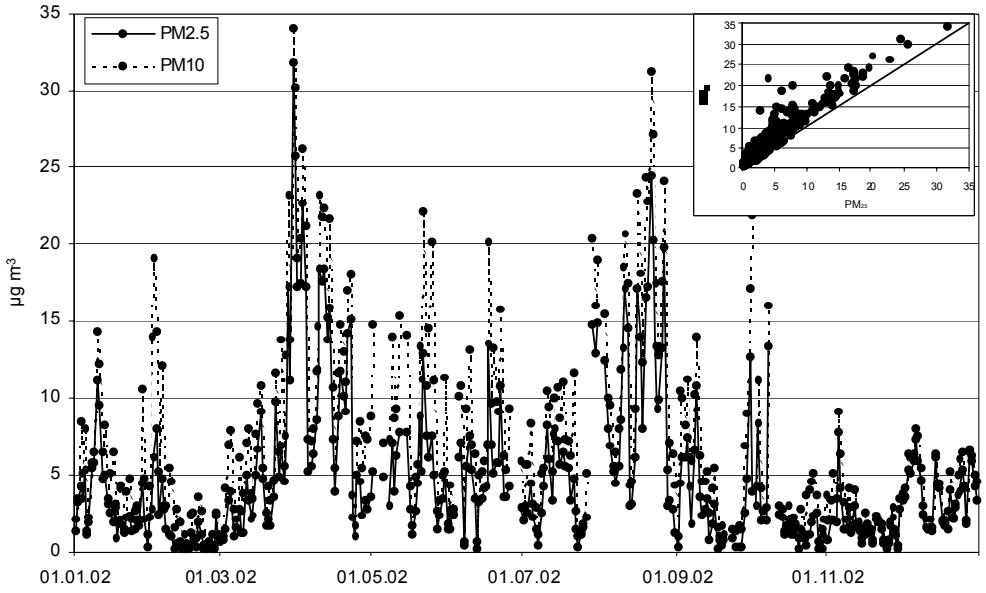

Figure 34: Time series of PM_{10} and $PM_{2.5}$ mass concentrations at Birkenes during 2002, and correlation between PM_{10} and $PM_{2.5}$.

The PM_{10} mass concentrations at Birkenes exceeded 30 µg m^{-3} during episodes of long-range transport. One example of air mass trajectories passing important source regions before arriving at Birkenes is presented in Figure 35a together with

a clean air case with air masses from Greenland and the Arctic. Trajectories were calculated with the FLEXTRA model (Stohl and Koffi, 1998) and the ECMWF data. The EU criteria for 24-hour averages of PM_{10} at 50 µg m^{-3} was never exceeded at Birkenes in 2002, the daily averages were, however, close to the Norwegian national limit value of 35 µg m^{-3}. The highest 24-hour PM_{10} mass average in 2002, 34.1 µg m^{-3}, was recorded during a long-range episode 30.03.02-31.03.02, demonstrating that the PM_{10} anthropogenic long-range part may be as high as 70% of the EU limit value in the southern part of Norway. The $PM_{2.5}$ mass concentration this day, 31.7 µg m^{-3}, was the highest concentration measured during 2002, and reached 92% of the PM_{10} mass. The concentrations of SO_4^{2-}, NO_3^-, and NH_4^+ were high. The Norwegian national 24-hour $PM_{2.5}$ limit is 20 µg m^{-3}. It was exceeded this day and in four other days during 2002.

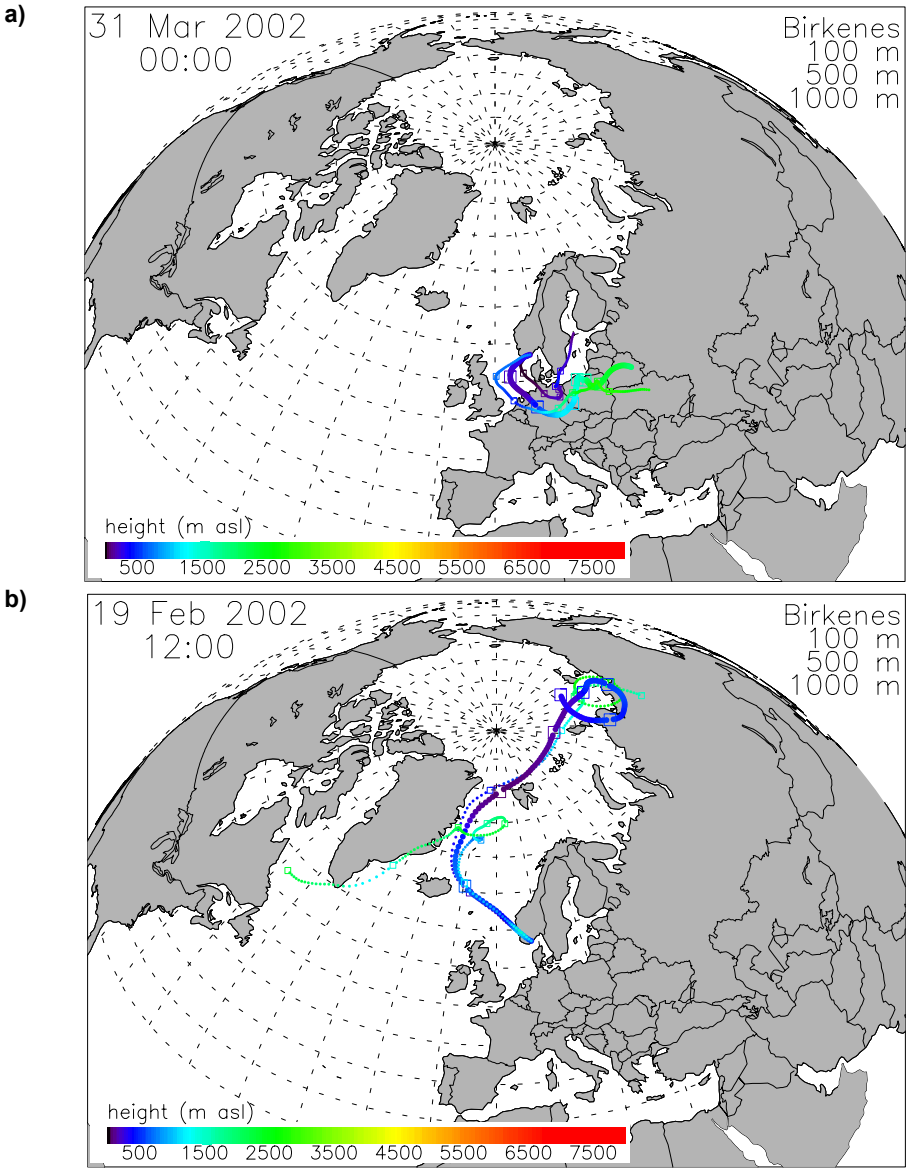

Figure 35: Air mass trajectories representative for two typical episodes with high and low PM_{10} concentrations, respectively;
a) 30.03.02-31.03.02; PM_{10} = 34.1 µg m^{-3}, $PM_{2.5}$ = 31.7 µg m^{-3}.
b) 19.02.02-20.02.02; PM_{10} = 0.87 µg m^{-3}, $PM_{2.5}$ = 0.37 µg m^{-3}.

The mass concentrations of SO_4^{2-}, NO_3^-, NH_4^+, Cl^-, Na^+, Mg^{2+}, K^+, and Ca^{2+} account for 30–90% of the PM_{10} monthly mass concentration averages (Table 4). A high anthropogenic contribution to PM_{10} with high concentrations of SO_4^{2-}, NH_4^+, NO_3^-.was seen to occur when the mass ratio $PM_{2.5}/PM_{10}$ was large. The sea salt's (Cl^-, Mg^{2+}, Na^+) share of the PM_{10} monthly mass averages was 13% on average. The sea salt contribution is highest during autumn and winter, and during February the sea salt contribution was larger than the secondary inorganic part of the PM_{10}. The coarse fraction was larger than the fine fraction during February both in 2002 and in 2001.

Table 4: SO_4^{2-}, NO_3^-, NH_4^+,Cl^-, Na^+, Mg^{2+}, K^+ and Ca^{2+} concentrations during the period 01.01.02–31.12.02, in $\mu g/m^3$.

Month	SO_4^{2-}	NO_3^-	NH_4^+	Cl^-, Na^+, Mg^{2+}	K^+, Ca^{2+}
January	1.18	0.77	0.29	0.83	0.07
February	0.75	0.73	0.17	1.98	0.07
March	1.57	2.24	0.84	1.52	0.11
April	2.91	2.25	1.59	0.58	0.18
May	1.37	3.17	1.02	0.90	0.15
June	1.43	0.52	0.32	0.59	0.16
July	2.18	0.48	0.64	0.47	0.12
August	2.31	0.42	0.71	0.27	0.25
September	1.29	0.52	0.31	0.46	0.11
October	0.66	0.35	0.17	0.55	0.05
November	0.78	0.22	0.22	0.25	0.04
December	1.19	0.11	0.18	0.37	0.06
Annual average	1.45	0.98	0.54	0.73	0.11

The total carbon (TC) contributions to the monthly averages of the PM_{10} mass concentrations varied between 0.4 and 3.9 μg C m^{-3} (Figure 36 and Table 5). This accounted for 6-22% of the total PM_{10} mass collected on the LVS 3.1 Filter. The organic carbon (OC) part of the TC was 80-90% of the PM_{10} in 2002, while the elementary carbon (EC) contributed with 1.9-2.9%. The monthly averages of EC PM_{10} mass were generally lower than 0.2 μg C m^{-3}, where the August EC average of 0.33 μg C m^{-3} was exceptionally high.

The corresponding monthly mass averages of TC in $PM_{2.5}$ varied between 0.3 and 3.1 μg C m^{-3} (Figure 36 and Table 5), which accounted for 9-24% of the total $PM_{2.5}$ mass collected by the LVS 3.1 filter. The OC share of the TC $PM_{2.5}$ mass was 80-90%, just as in the PM_{10} mass.

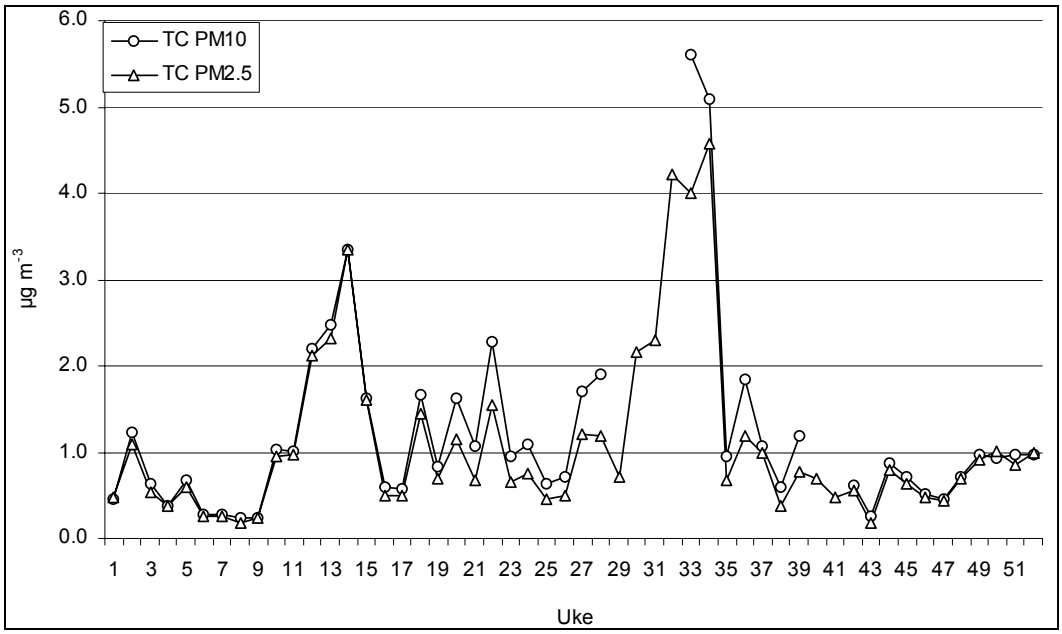

Figure 36: Weekly averages of TC concentrations in the PM_{10} and $PM_{2.5}$ fractions during 2002. Concentrations are given in µg C m^{-3}.

Table 5: Monthly average mass concentration of OC, EC and TC in the PM_{10} and $PM_{2.5}$ fraction at Birkenes during 2002. Concentrations are given in µg C m^{-3}.

	PM_{10}			$PM_{2,5}$		
Month	OC	EC	TC	OC	EC	TC
January	0.53	0.14	0.68	0.50	0.12	0.62
February	0.30	0.06	0.37	0.26	0.05	0.32
March	0.97	0.15	1.12	0.93	0.14	1.07
April	1.79	0.22	2.01	1.76	0.19	1.94
May	1.04	0.11	1.15	0.79	0.10	0.89
June	1.13	0.11	1.23	0.76	0.09	0.86
July	1.27	0.17	1.44	0.84	0.12	0.96
August	3.55	0.33	3.88	2.85	0.23	3.08
September	1.03	0.14	1.17	0.73	0.10	0.83
Oktober	0.37	0.07	0.44	0.31	0.06	0.37
November	0.54	0.11	0.66	0.48	0.12	0.6
December	0.80	0.16	0.96	0.76	0.18	0.94
Annual average	1.11	0.15	1.26	0.91	0.13	1.04

The OC and EC concentrations in the PM_{10} and $PM_{2.5}$ fractions were generally quite similar, and the variation through the year corresponded well with the variation in the PM_{10} and $PM_{2.5}$ mass concentrations. The monthly averages indicate that about 67-98% of the PM_{10} TC was contained in the $PM_{2.5}$ fraction. This is as expected and indicate that the carbon containing particles have an equivalent aerodynamic diameter (EAD) less than 2.5 µm. The carbon mass

fraction in the particles increases with decreasing particle size, since various incineration processes are the main sources. The ratio of OC in the $PM_{2.5}$ relative to the PM_{10} fraction was lower during May to September than in the other months (Table 5). Pollen was one likely source of the OC in the coarse fraction, as May was the start of the pollen season at Birkenes. Other types of biological material as well as re-suspension were other possible sources for the coarse fraction OC.

The analytical methods EGA and IC were capable of determining 69% of the annual average mass in the PM_{10} fraction (Figure 37) at Birkenes in 2002. The undetermined fraction was 31% and consisted most likely of insoluble minerals, partly of known composition. The water content in the samples may likewise have given a contribution to the undetermined part. The organic part may better be estimated by multiplication of the OC with a factor 1.2-1.9 in order to include O, S, N, H, since these elements are not quantified in the EGA analysis. The mass balance above should be considered to be a coarse estimate only. More research is needed on the speciation of the organic fraction.

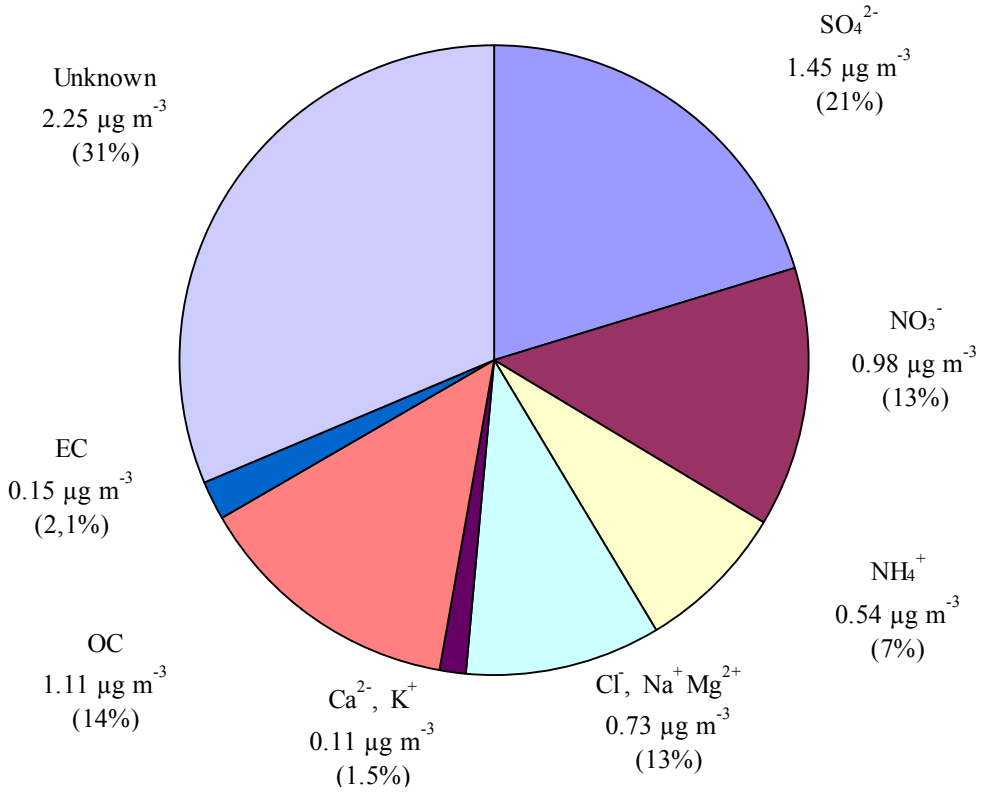

Figure 37: Average PM_{10} composition during 2002. Average PM_{10} mass concentration was 7.2 µg m^{-3}.

The OC is partly water-soluble (WS). It is known that this part can be quite different at different locations and that it varies from one season to the next. The WS part of the OC should be multiplied with a factor in the high end of the range given above (1.2-1.9) in order to best estimate the WS organic mass.

When non-identical sampling equipment with different filter types is co-located, they will normally give different mass concentrations. The PM_{10} and $PM_{2.5}$ results obtained with the Partisol Dichotomous sampler and Teflon filters are lower than those obtained with the LVS 3.1 and heated quartz filters; the Partisol mass amounted to 87% and 80% respectively of the LVS 3.1 mass in the two fractions during comparable periods in 2000. Heated quartz filters are known to adsorb organic gases when exposed to air, which may explain some of the differences. The filter heating generates a chemically more active quartz surface that increases the impact of this positive artefact. These filters may also adsorb water. The measurements may also have negative artefacts. The mass concentration is determined as the weight difference of exposed and non-exposed filters. In both cases the filters will be kept at 20^{o}C and 50% RH for several hours before weighing, and highly volatile compounds collected during cold conditions can easily be lost. Besides loosing volatile organic compounds and ammonium nitrate that may decompose to ammonia and nitric acid, mass may also be lost due to chemical reactions between salts and sulphuric acid that transform particulate matter to gases; nitric acid and hydrochloric acid. The simple sampling systems that normally are applied may therefore give results that are inaccurate due to artefacts such as those mentioned above, besides the general problems related to transportation and storing of samples before analysis. These artefacts are more important at urban sites with higher levels of organic compounds and ammonium nitrate than at regionally representative sites such as Birkenes. More complex samplers that can better handle the artefacts exist, see e.g. Ding et al. (2002), but they are both expensive and less suited for routine networks.

During a short period from October to November attempts were made to quantify the adsorbance of organic gases to heated quartz filters by using a method by McDow and Huntzicker (1990), and by Turpin et al. (1994). This short study indicated that on average 33% of the organic carbon measured on the filters was due to gaseous organics. The method is, however, considered inaccurate in background areas where the organic particles to a high extent are secondary organics, and give too large corrections. The artefacts in background areas clearly seem to be important and should be investigated more thoroughly.

It should also be noted that the filter loading at locations such as Birkenes may be quite low giving less accurate mass concentrations than with heavy filter loading. Results from daily samples in background areas may often be lower than the detection limit. When this occurred, a concentration equal to one half of the detection limit was applied in calculations on the results above.

4. Size resolved mass concentration and elemental composition of atmospheric aerosols over the eastern Mediterranean area

J. Smolík[1], V. Ždímal[1], J. Schwarz[1], M. Lazaridis[3], V. Havránek[2], K. Eleftheriadis[4], N. Mihalopoulos[5], C. Bryant[6], I. Colbeck[6]

[1]Institute of Chemical Process Fundamentals, ASCR, Prague, Czech Republic
[2]Nuclear Physics Institute AS CR, Prague, Czech Republic
[3]Technical University of Crete, Department of Environmental Engineering, 73100 Chania, Greece
[4]N.C.S.R. Demokritos, 15310 Ag. Paraskeui, Attiki, Greece
[5]Environmental Chemical Processes Laboratory (ECPL), Department of Chemistry, University of Crete 71409 Heraklion, Greece
[6]Department of Biological Sciences, University of Essex, UK

(The current work will be published in the Atmospheric Physics and Chemistry Discussions Journal)

4.1 Introduction

Intensive aerosol and gaseous pollutant measurement campaigns have been performed at Finokalia on the island of Crete (Greece) in combination with boat measurements in the eastern part of the Mediterranean area as part of the SUB-AERO project. The measurements were performed with the participation of 9 European research institutions. The above measurements together with regional/mesoscale/subgrid modelling studies were utilised to investigate the dynamics/characteristics of photochemical and fine particle pollutants in the Mediterranean area. The research work was performed under the auspices of the European Union Fifth Framework Programme (project SUB-AERO).

Under this research framework gaseous phase measurements for a number of photo-oxidants, fine particle concentration measurements and detailed PM_1 and PM_{10} particulate matter characterisation were carried out in the eastern Mediterranean area during summer 2000 and winter 2001. The experimental data were compared with modelling studies of the dynamics of photochemical gaseous species and particulate matter.

To the north of the Mediterranean Sea are the highly populated European countries with industrial, semi-industrial, and rural economies, whilst to the south is Africa. A detailed wind trajectory analyses shows that more than 60% of the air masses that arrive in the eastern Mediterranean come from the N-NW and 13-16% from the Sahara (Guerzoni et al., 1990). Air masses from the N-NW contain particles related to industrial and urban inputs; those from the Sahara carry predominantly mineral dust. Transport of Sahara dust occurs mostly during spring and summer and causes non-continuous crustal aerosol pulses to the Mediterranean area (e.g. Bergametti et al., 1989b; Moulin et al., 1998). On the other hand, precipitation scavenging during the rainy season between October and May reduces aerosol concentrations (e.g. Dulac et al., 1987; Bergametti et al., 1989a). The summer time is also characterised by low-inversion layers, and strong sunlight, causing photochemical smog. Moreover, forest fires, which occur during the summer months in the Mediterranean region and in North Africa, increase black carbon and fine particle emissions. Thus, the Mediterranean Sea constitutes

an area where atmospheric particles originating from continental natural and anthropogenic sources, marine sources and gas-to-particle conversion simultaneously exist. Furthermore, specific meteorological conditions result in high temporal variability of aerosol concentrations. Consequently, the Mediterranean area offers unique conditions for modelling/measurement studies.

Most of the studies on the chemical composition of Mediterranean particulate aerosol have been conducted in the western and north-western region (e. g. Dulac et al., 1987; Bergametti et al., 1989a,b; Dulac et al., 1989; Migon et al., 1991; Migon et al., 1993; Sandroni and Migon, 1997) or on the eastern coast including Turkey and Israel (e. g. Mamane et al., 1980; Ganor et al., 1991; Kubilay et al., 1994; Luria et al., 1996; Maenhaut et al., 1999; Güllü et al., 2000; Yatin et al., 2000; Erduran and Tuncel, 2001). However relatively few studies have been undertaken in the southern part of the eastern Mediterranean and Greece (e.g. Chester et al., 1993; Mihalopoulos et al., 1997; Danalatos and Glavas, 1999; Chabas and Lefèvre, 2000). Here we report on the atmospheric aerosol measurement on the island of Crete (south-eastern Mediterranean) using cascade impactors and the characterisation of the collected particulate matter. Emphasis is placed on the mass and elemental size distributions and the temporal variability of PM_1 and PM_{10}.

4.2 Experimental

4.2.1 Sampling site

Aerosol samples were collected on Crete during the periods 10–31 July 2000 and 7–14 January 2001. According to an analysis of 10 years of air mass back trajectories (WMO, 1985; Guerzoni et al., 1990; Chester et al., 1993) 39% of all air masses arrive at Crete from the north across Greece, eastern Europe and the former USSR, 28% arrive from the west-northwest crossing western Europe, 16% come from the south carrying with them aerosols from the Sahara and from Northern Africa deserts, and 17% come from the east crossing the Middle Eastern desert regions. Mihalopoulos et al. (1997) report similar figures. The main sampling site was located at Finokalia (35º19´N, 25º40´E), a coastal remote site east of Heraklion on the top of a hill (~ 150 m a.s.l.) facing the sea within the sector of 270º to 90º. The sampling was carried out in open terrain about 3 m above the ground. In addition samples of atmospheric aerosol were also collected during the period 25–29 July 2000 aboard the research vessel "AEGAIEO". The vessel cruised in the Aegean Sea along selected tracks calculated by forward and back trajectory modelling with the Finokalia sampling site as the end point.

4.2.2 Sampling

Samples of atmospheric particulate matter were collected and size-segregated into 10 size fractions by two Berner type low pressure cascade impactors BLPI 25/0,018/2, one from ICPF Prague and the second one from "Demokritos", Athens. The impactors were used alternately at Finokalia station during the period 10-19. July 2000. After that the measurements at Finokalia continued with an impactor from Prague, and the impactor from "Demokritos" was used aboard the "AEGAION" vessel. Both impactors were used alternately during the winter campaign (7-14 January 2001). In order to determine the real cut diameters and shapes of collection efficiency curves the impactor from Prague was calibrated at

the Finnish Meteorological Institute by the method described by Hillamo and Kauppinen (1991). It was found that real cut diameters (D_{50} values) for stages 1-10 were 0.026, 0.062, 0.110, 0.173, 0.262, 0.46, 0.89, 1.77, 3.4, and 6.8 µm. Further, it was found that all stages of the impactor have reasonably sharp collection efficiency curves, which makes the impactor response suitable for use with a data inversion technique (Hillamo et al., 1999). Prior to both campaigns the impactors were compared during 2-day measurements of mass size distributions of urban aerosol in Athens. For this purpose both impactors were connected in parallel to the same vacuum pump and two 24-hour samples were taken. The results of the intercomparison are shown in Figure 38, where D_{ae} is the geometric mean aerodynamic diameter. As can be seen the instruments were practically identical.

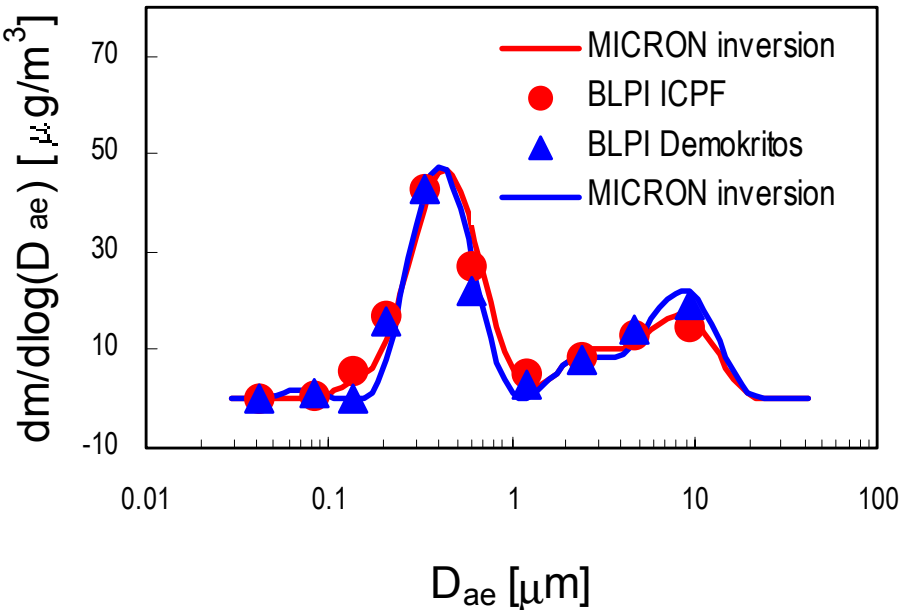

Figure 38: Intercomparison of two BLPI cascade impactors. The raw mass size data were inverted into smooth mass size distributions by the MICRON code.

The sampling at Finokalia was carried out on top of the roof of a small building. The impactor, with an inlet providing approximately 15 µm upper cut-off particle size, was positioned at a height of about 3 m above the ground. To reduce particle bounce the samples were deposited on Nuclepore polycarbonate foils greased with Apiezon L vacuum grease. Sampling was carried out in approximately 24-hour intervals with a flow rate of 25 l/min (in some cases the real time was shorter due to electrical current interruptions). The first sample was taken from 10 July 2000, 10:00 to 11 July 2000, 10:00 local time. Due to some technical problems samples on the boat were not taken at standard times, as at Finokalia, and sampling times were usually shorter. In total five samples were collected aboard the boat over the following time intervals 25 July (23:10)–26 July (09:53), 26 July (11:15)–27 July (10:20), 27 July (11:12)–28 July (09:15), 28 July (10:45)–29 July (01:15), and on 29 July between 09:00–18:43. During the winter sampling started at about 14:00. Thus the first sample was taken between 7 January 2001, (14:00) and 8 January 2001, (14:00). In total 21 samples from the summer campaign, five samples from

the boat and seven samples from the winter measurements were obtained, with each sample consisting of ten size fractions.

4.2.3 Gravimetric analysis

The mass size distributions were obtained from the mass of particulate matter deposited on the individual stages of the impactor, volume flow rate of aerosol and total time of sampling. The electronic microbalances ATTA Cahn and Sartorius BP211D with a maximum attainable precision of 10 μg were used for weighing the aerosol samples from the summer campaign. During the winter campaign Sartorius M5P-000V001 electronic microbalances with maximum attainable precision of 1 μg were used. Foils were transported from the sampling site in Petri dishes and equilibrated in the weighing room for at least 24 hours before weighing at conditions R.H. 56±13% and temperature 24.7±1.0°C (summer), R.H. 62.8±2.5% and temperature 26.8±1.0°C (boat) and R.H. 69.2±1.8 and temperature 21.4±0.8 (winter). Internal calibration of the balance was performed regularly, at least once at the beginning of each weighing run. To check reproducibility of the weighing procedure, a control aluminum foil was weighed at least once during each weighing run. Before and after each weighing run another control substrate (blank made of the same polycarbonate foil processed the same way but without a sample) was weighed to check the influence of possible temperature and RH fluctuations.

4.2.4 Elemental analysis

All samples were analysed by particle-induced X-ray emission (PIXE). Analyses were performed on the 3MeV Van de Graaff electrostatic accelerator at the Nuclear Physics Institute in Řež in Prague. The samples consisted of annular deposit of individual spots, with the number of spots depending on the stage. For stage 1 an 8 mm collimator of the proton beam was used, and for stages 2-10 a 3 mm collimator was used. Usually 6 spots from stage 1, 2 spots from stage 2, and 1 spot from stages 3-10 were analysed. To obtain the elemental concentrations for individual size fractions deposited on impaction foils, the results of the analysis were related to the actual number of spots on each stage. Two proton beam energies of 1.31 MeV and 2.35 MeV were used to irradiate the samples. The 3 mm diameter collimator of the proton beam was chosen for stages 1-9. Stage 10 was analysed with the 8 mm collimator. Usually a proton fluence of about 10 μC and 50 μC were used for the 1.31 MeV and 2.35 MeV measurements, respectively. The typical time for one irradiation was about 5 min. The 1 mm polyethylene absorption filter was used for the 2.35 MeV irradiation to reduce the intensive low energy X-rays from sample. In samples from the summer campaign Al, Si, K, Ca, Ti, Mn, Fe, Sr, S, Cl, Ni, V, Cu, Cr, Zn, and Pb were determined. During the winter campaign a new set of polycarbonate foils with low blank of Br was used. This allowed the determination of Br in the samples. Elements up to Ti were determined from 1.31 MeV, while the remaining elements were determined from the 2.35 MeV measurement. The influence of the observed matrix effect due to the deposit thickness was corrected using the Equivalent Layer Thickness Model (Havránek et al., 1999). The ratio of the Fe signal from 1.35 MeV and 2.35 MeV irradiation was used to estimate the effective thickness of aerosol deposit for individual spots.

4.3 Results and discussion

4.3.1 Mass size distributions

A total of 21 mass size distributions from the summer campaign, five mass size distributions from the boat, and seven mass size distributions from the winter measurements were obtained. The distributions were predominantly bimodal with mode mean diameters around 0.4 and 5 μm and with a minimum between both modes at around 1 μm. The raw mass size data were inverted into smooth mass size distributions by the MICRON code (Wolfenbarger and Seinfeld, 1990). The inverted distributions were integrated to obtain PM_1 and PM_{10} mass concentrations. The time series of PM_1 and PM_{10} for both summer and winter campaigns are shown in Figure 39. As can be seen PM_1 and PM_{10} mass concentrations show both short-term (daily) and long-term (seasonal) variations. In our case the daily PM_{10} mass concentration, measured at Finokalia during the summer, ranged from 20.7 to 40 $\mu g/m^3$ (10–18 July 2000). After that it was practically constant at approximately 29 $\mu g/m^3$ (19–25 July 2000), before increasing up to 67.2 $\mu g/m^3$ (27 July 2000), and finally decreasing to 37 $\mu g/m^3$ (30 July 2000). A similar increase of PM_{10} concentration was observed in samples collected aboard the boat, with a maximum of 75.1 $\mu g/m^3$ (28 July 2000). The daily PM_1 mass concentration, measured during the summer, ranged from 3.7 to 20.2 $\mu g/m^3$ and from 11.6 to 25.9 $\mu g/m^3$ at Finokalia and aboard the boat, respectively. During the winter the daily PM_1 and PM_{10} concentrations varied from 2.4 to 8.6 $\mu g/m^3$ and from 10.1 to 19.5 $\mu g/m^3$, respectively. The short-term variation in aerosol mass and composition, is observed frequently in the Mediterranean area and surrounding regions. It is caused mainly by changes in air mass transport arriving from different sectors toward the sampling point (e.g. Dulac et al., 1987; Bergametti et al., 1989a,b, 1992; Guerzoni et al., 1990; Ganor et al., 1991; Hacisalihoğlu et al., 1991, 1992; Migon et al., 1993; Kubilay et al., 1994, 1995; Luria et al., 1996; Mihalopoulos et al., 1997; Sandroni and Migon, 1997; Güllü et al., 2000; Danalatos and Glavas, 1999; Chabas and Lefèvre, 2000; Yatin et al., 2000; Erduran and Tuncel, 2001).

To estimate the effect of air mass transport we computed the backward trajectories (HYSPLIT4 Trajectory Model with 6 hours time steps 72 hours backward in time for two transport layers 300-2000 m and 1500-3000 m). The results showed that the air masses arriving in Crete changed direction several times between north and west during the first period (10–18 July 2000). Higher PM_{10} concentrations were observed with air masses originating over the Atlantic Ocean and Western Europe (10, 13, and 16 July 2000). The relatively constant PM_{10} concentration observed during 19–25 July 2000 corresponded to air masses originating from the western coast of the Black Sea. The peak PM_{10} mass concentrations, observed during the end of the summer campaign, corresponded to air masses from Northern Africa. During the winter campaign higher mass concentrations were observed with air masses originating over the Atlantic Ocean and arriving via Northern Africa and the Mediterranean Sea (9 January 2001). Higher mass concentrations were also observed with air masses originating from southern Greece and the Ionian Sea, that recirculated above Crete (7 January 2001) or originated above the Mediterranean Sea and recirculated above the North African coast. However, for similar meteorological conditions low aerosol mass concentrations were also found (8 January 2001).

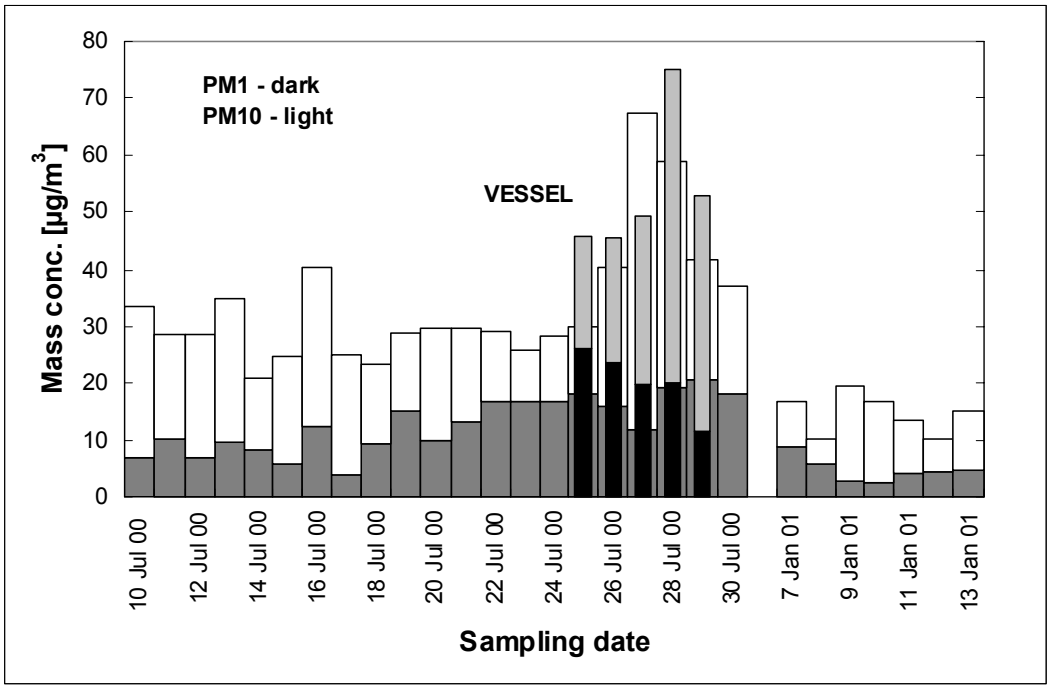

Figure 39: Daily PM_1 and PM_{10} mass concentrations at Finokalia and aboard the research vessel "AEGAIEO".

The long-term (seasonal) variation results in different average aerosol concentrations observed during the different seasons. In our case the geometric mean PM_1 and PM_{10} mass concentrations, measured at Finokalia during the summer, were 11.44 and 32.09 µg/m^3, respectively. Corresponding winter mass concentrations were 4.22 and 14.17 µg/m^3, respectively. A similar seasonal variability of aerosol concentrations in the Mediterranean region was observed by other authors (e. g. Bergametti et al., 1989a,b; Güllü et al., 2000; Chabas and Lefèvre, 2000). This may be attributed to the scavenging by precipitation during transport from source areas, which is more frequent during the rainy period in autumn and winter.

4.3.2 Elemental size distributions

As already mentioned earlier, Al, Si, K, Ca, Ti, Mn, Fe, Sr, S, Cl, Ni, V, Cu, Cr, Zn, and Pb were determined in the BLPI samples using PIXE. In addition a new set of polycarbonate foils with low blank values of Br were used during the winter campaign, which allowed us to determine Br. Typically samples collected on stages 1-6 (i.e. with particles <1 µm in diameter) were black indicating the presence of soot from combustion. The samples with coarse particles were beige in colour corresponding to mineral dust. Principally three types of elemental size distributions were observed. A monomodal distribution with particle size >1µm and a mode centred at about 4 µm was typical for Al, Si, Ca, Ti, Mn, Fe, and Sr. Also Cl exhibited a monomodal distribution with particle size >1 µm and a mode maximum at around 5 µm. S, Br, K, V, and Ni exhibited bimodal distributions with modes around 0.3 and 3 µm and a minimum at about 1 µm. Cu, Cr, Zn, and Pb showed rather flat multimodal distributions centred at approximately 1 µm. The raw elemental size data were inverted into smooth elemental size

distributions by the MICRON code, and the inverted distributions were integrated to obtain PM_1 and PM_{10} elemental concentrations. The geometric mean mass and elemental concentrations in the PM_1 and PM_{10} fractions of atmospheric aerosols collected at Finokalia during the summer and winter campaigns are compared in Table 6. As can be seen the winter values are considerably lower (except for Cl). Further, Table 7 shows a comparison of mass and elemental concentrations in PM_1 and PM_{10} aerosols collected during corresponding days at Finokalia and aboard the "AEGAIEO" vessel. Both mass and elemental concentrations found at Finokalia and aboard the vessel are comparable (with the exception of Cl, V, and Ni).

Table 6: Geometric mean mass ($\mu g/m^3$) and elemental (ng/m^3) concentrations in PM_1 and PM_{10} fractions of atmospheric aerosol collected at Finokalia during the summer (10.-31.7.2000) and winter (7.-14.1.2001) campaigns.

	PM_1		PM_{10}	
	Summer	Winter	Summer	Winter
Mass	11	4	32	14
Al	44	27	251	99
Si	130	69	1106	257
S	1837	575	2167	740
Cl	0	6	724	825
K	81	78	269	138
Ca	21	7	549	153
Ti	2	0	22	2
V	4	2	6	3
Cr	0	0	1	0
Mn	1	0	6	1
Fe	19	5	246	34
Ni	1	1	2	2
Cu	0	0	2	1
Zn	6	2	10	3
Sr	0	0	2	1
Pb	8	3	12	6
Br	nd	3	nd	5

Table 7: Geometric mean mass (μg/m^3) and elemental (ng/m^3) concentrations in PM_1 and PM_{10} fractions of atmospheric aerosol collected at Finokalia station and aboard the research vessel "AEGAIEO" during 25.–29.7.2000.

	PM_1		PM_{10}	
	Finokalia	Vessel	Finokalia	Vessel
Mass	17	20	46	53
Al	39	35	496	426
Si	294	167	2866	2838
S	2705	2703	2913	3043
Cl	0	0	155	417
K	109	87	455	468
Ca	62	25	1093	896
Ti	9	6	79	87
V	7	13	11	18
Cr	1	1	1	1
Mn	2	2	16	16
Fe	80	51	800	828
Ni	2	6	3	7
Cu	1	1	2	2
Zn	9	10	15	20
Sr	0	0	5	4
Pb	10	13	16	20
Br	nd	Nd	nd	nd

In addition the PM_{10} mass and elemental concentrations, determined from 21 summer samples collected at Finokalia were used in principal component analysis (Varimax rotated factor analysis) to identify possible sources of individual elements. The results are given in Table 8. The first factor contains the group of crustal elements Ca, Al, Fe, Mn, K, Ca, Ti, Cr and Sr and explains 39% of the total system variance. The second factor, mainly associated with Cl, represents the marine factor and explains 19% of the variance. Thus the cumulative variance from crustal and marine influence explains up to 60% of the variability, indicating a greater influence of natural sources compared to anthropogenic ones in the region. The third factor includes Pb, S, Cu and Zn and is attributed to pure anthropogenic sources. Finally the last factor contains V and Ni, which have mixed origins from both anthropogenic and crustal sources. As can be seen the results of the factor analysis agree fairly well with the individual elemental size distributions. Coarse modes observed for crustal elements and chlorine correspond to mineral dust and sea-salt particles produced by bursting of bubbles. The size distribution of sulphur, where the accumulation mode dominates, shows that particulate sulphur is mainly a product of gas-to-particle conversion (Finlayson-Pitts and Pitts, 2000). Bimodal distributions for K, Ni, and V indicate that these elements are both anthropogenic and natural in origin. Potassium in submicrometer particles results from biomass burning, nickel and vanadium come from oil combustion. Rather broad distributions of Cu, Cr, Zn and Pb with not too well-defined peaks indicate more sources and an aged aerosol.

Table 8: Factor loadings of concentrations of elements in PM_{10} particulate matter.

Factor isolated	Factor 1	Factor 2	Factor 3	Factor 4
Mass	**0.799**	0.038	0.392	0.309
Sr	**0.961**	0.110	0.010	0.135
Si	**0.959**	-0.133	0.183	0.125
Al	**0.953**	-0.082	0.087	-0.024
Fe	**0.953**	-0.147	0.160	0.176
Ti	**0.953**	-0.140	0.133	0.205
K	**0.928**	0.068	0.287	0.037
Mn	**0.927**	-0.175	0:234	0.183
Ca	**0.926**	0.023	0:259	0.080
Cr	**0.730**	0.019	0.285	0.117
V	**0.670**	-0.139	0.342	**0.603**
Ni	**0.544**	-0.093	0.265	**0.755**
Cl	-0.237	**0.812**	-0.343	-0.137
Pb	0.133	-0.103	**0.925**	0.017
Cu	0.355	0.125	**0.880**	-0.060
S	0.284	-0.207	**0.841**	0.164
Zn	0.190	-0.265	**0.791**	0.234
Eigenvalues	9.87	4.63	5.16	2.01
Fractional variance	0.39	0.19	0.21	0.08

The next Figures show the temporal variation of PM_1 and PM_{10} for several elements characteristic for individual groups of elements as found from factor analysis and also for different types of the above mentioned elemental size distributions. Figure 40a shows the time series of PM_1 and PM_{10} for Si as a typical crustal element. As can be seen PIXE revealed another peak in the concentration of Si on 12 July 2000. According to backward trajectories and Meteosat pictures this increase was caused by Saharan dust. Figure 40b shows the temporal variation of another crustal element, potassium, which exhibited a bimodal distribution. Here the higher concentrations correspond both to Saharan dust, in which potassium is present in illite (e.g. Ganor et al., 1991; Molinaroli, 1996), and to forest fires. This follows from satellite pictures showing forest fires in Greece and surrounding areas that occurred at the beginning of the summer campaign, and from higher concentrations of potassium in the PM_1 fraction found in the corresponding samples. The latter is typical for wood combustion (e. g. Valmari et al., 1998) and biomass burning (e.g. Jaffrezo et al., 1998). Figure 40c shows the temporal variation of chlorine. For chlorine we have not observed any specific dependence on the air mass trajectories, but rather on the velocity of air mass transport. Higher chlorine concentrations were observed for air masses which originated over the Atlantic Ocean and were transported with a higher velocity across Europe (10, 13-17 July 2000, 9 and 10 January 2001) or originated above the western coast of the Black Sea (20 and 21 July 2000). Low chlorine concentrations were found for calm days. Chlorine in atmospheric aerosol is mainly contained in sea-salt particles produced by bursting of air bubbles at the ocean surface. The number of sea-salt particles depends approximately exponentially on the wind speed (Lovett, 1978; Monahan et al., 1986; Smith et al., 1993). This shows the exponential dependence of marine elements concentrations

on the local wind speed observed in the Mediterranean area (e.g. Bergametti et al., 1989a; Chabas and Lefèvre, 2000). Since we have not found any correlation with the local wind speed, the observed chlorine concentrations depend on the distant marine source strength and on long-range transport to Crete, and both should also be related to the wind speed. Figure 40d shows the behaviour of sulphur. As can be seen sulphur was predominantly found in submicron particles. Concentrations of sulphur determined in the PM_1 and PM_{10} fractions by PIXE were well correlated with the concentrations determined in the soluble fraction by ion chromatography (Bardouki et al., 2002) with a slope of unity. It shows that sulphur was present as sulphate. Lower concentrations were observed for air masses that originated over the Ligurian Sea and the Mediterranean Sea to the west of Crete. Higher concentrations were observed for air masses arriving from the west coast of the Black Sea or from Western Europe that later recirculated above the west coast of the Black Sea and arrived from the North. Figure 40d shows the seasonal variation in sulphur, with higher concentrations being observed in the summer. This is in agreement with other results from this region (Tsitouridou and Samara, 1993; Luria et al., 1996; Mihalopoulos et al., 1997; Danalatos and Glavas, 1999). Higher sulphate concentrations in the summer may be caused by higher phytoplanktonic activity producing gaseous dimethylsulphide that is later oxidised to methanesulphonic acid and sulphur dioxide (Finlayson-Pitts and Pitts, 2000), and by larger conversion rates due to higher concentrations of oxidising species (Danalatos and Glavas, 1999).

As found earlier at Finokalia, the biogenic sulphur can account for 0.6 to 28.3% of the total non-sea sulphate concentrations (Mihalopoulos et al., 1997), with higher values observed during the summer. Also the long-range transport of sulphates may have greater influence in the summer because precipitation events are rare in the region during this period (Luria et al., 1996). In our case the non-sea sulphate concentrations followed the ^{222}Rn variation, and this indicates air of continental origin (Bardouki et al., 2002). This can be supported by the similar behaviour of time series found for sulphur and anthropogenic elements Cu, Pb, and Zn. The temporal variation of vanadium is shown in Figure 40e. As found from factor analysis vanadium should have mixed origin, it is produced by fuel oil combustion, but it is also produced by crustal elements (Finlayson-Pitts and Pitts, 2000). As a result vanadium is found both in submicron and coarse particles. The effect of oil combustion is clearly seen from the high concentration of vanadium found aboard the boat, coming from oil driven engines of both the “AEGAIEO” and other vessels cruising in the area. Also the concentration of vanadium in Saharan dust towards the end of the summer campaign (Schütz and Rahn, 1982; Bonelli et al., 1996).

It follows that the atmospheric input of trace elements into the central and eastern Mediterranean is a complex phenomenon that depends on the transport of pollutants from their sources. This includes air mass movement, strength and spatial distribution of sources, precipitation scavenging by distant and local rain events, and for some elements such as halogens even on chemical reactions. Thus, it is very difficult to draw general conclusions, and continuing long-term measurements of size- and time resolved chemical composition of atmospheric particles is needed.

a)

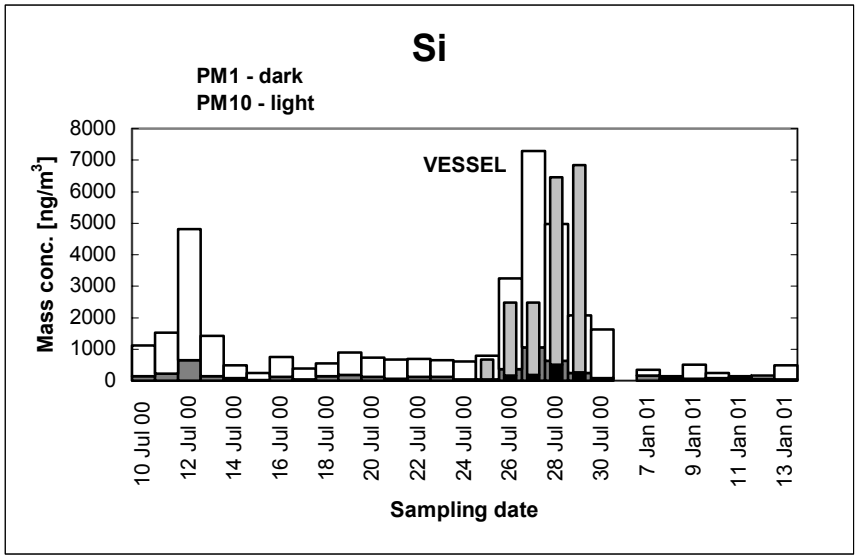

b)

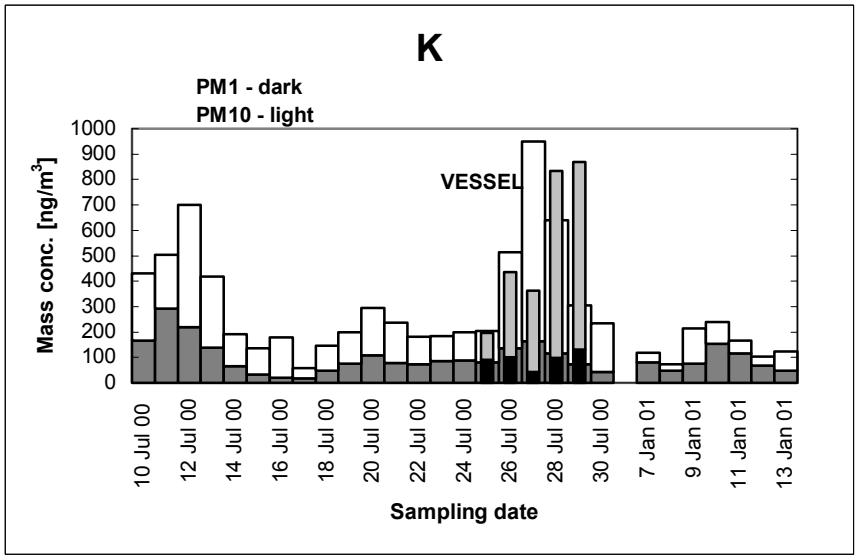

c)

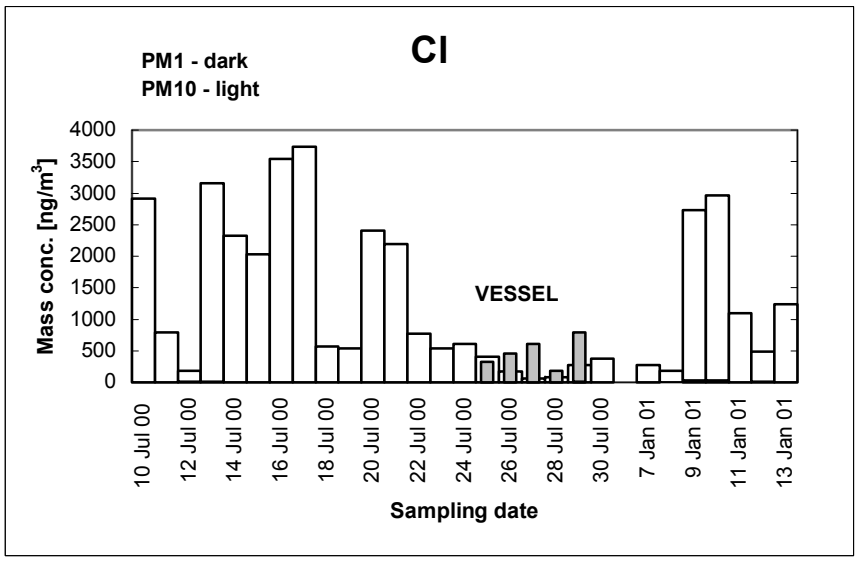

Figure 40: Daily concentrations of a) Si, b) K, c) Cl, d) S, and e) V in PM_1 and PM_{10} at Finokalia and aboard of the research vessel "AEGAIEO".

d)

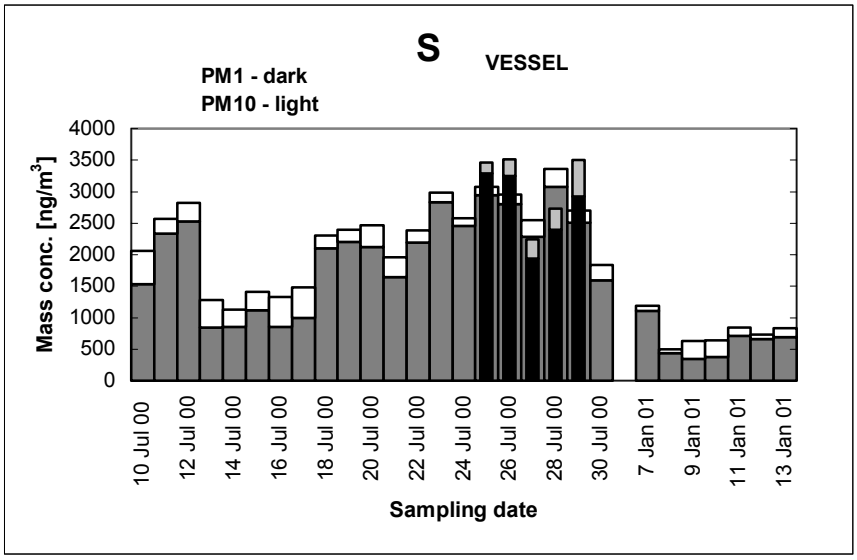

e)

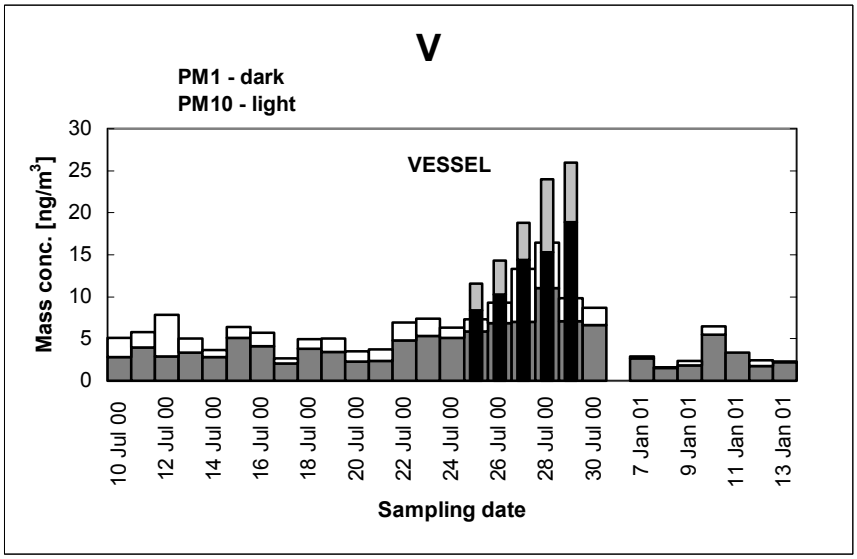

Figure 40, cont.

4.4 Conclusions

Size resolved aerosol samples were collected at Finokalia, a coastal site in Crete and aboard the research vessel "AEGAIO" cruising in the Aegean Sea during two periods in July 2000 and January 2001. Gravimetric analysis of samples yielded PM_1 and PM_{10} temporal variations. The elemental composition of samples was determined by PIXE. The time series for PM_1 and PM_{10} showed both daily and seasonal variation. The daily variation was caused mainly by air masses arriving at Crete from different directions including two incursions of Saharan dust. The seasonal variation was probably caused by precipitation scavenging, which is more frequent in winter. The elemental analysis showed practically monomodal distributions for crustal elements, chlorine, and sulphur. Sulphur has most of its mass in the submicron size range, crustal elements and chlorine in the supermicron fractions. Three elements, namely, K, V, and Ni, which are of both anthropogenic and crustal origins, exhibited bimodal distributions. Higher concentrations of potassium in submicron particles corresponded to forest fires,

and vanadium and nickel to oil combustion. High concentrations of vanadium and nickel in submicron particles, produced probably by oil driven engines of both "AEGAION" and other vessels, was found in samples collected aboard the boat. Anthropogenic elements Cr, Cu, Pb, and Zn exhibited broad and not well defined distributions. Higher concentrations of these elements were found for air masses originating from the west coast of the Black Sea and advected across northern Greece and western Turkey. The time series for Cu, Pb, and Zn, resemble those for sulphur, which indicates a similar source.

Acknowledgements

The authors gratefully acknowledge the help of G. Kouvarakis in factor analysis. This work was supported by the European Commission under grant ENVK2-1999-00052.

5. Sun photometer measurements at Ny-Ålesund

J. Schaug
Norwegian Institute for Air Research, P.O. Box 100, N-2027 Kjeller

Optical measurements can provide information about aerosols in the atmospheric column above the observation site with a high time-resolution. From sun photometer data, for instance, one can retrieve information about aerosol loads and aerosol sizes. In this chapter some first results from sun photometer measurements at Ny-Ålesund on Spitsbergen (Norway) are presented. The sun photometer is a Precision-Filter-Radiometer (PFR) that accurately measures direct solar radiation in four wavelengths; 368, 411, 501, and 862 nm. The sun photometer is directed towards the sun and follows the sun across the sky during the day. The signals that are recorded every minute are the averages of ten single measurements taken within 1.25 seconds. The aerosol optical depths (AOD) at the four wavelengths are important parameters for aerosol optical characterisation that can be compiled from the sun photometer measurements. The precipitable water amount (PW) is another important parameter for aerosol optical characteristics that can be measured with sun photometers at 936 nm, but this is not measured on Spitsbergen. The sun photometer at Ny-Ålesund is part of the large global network AERONET (http://aeronet.gsfc.nasa.gov/) with routine observations that are important for the assessment of the global radiation budget and climate change in combination with satellite measurements.

Haze and visibility degradation is due to scattering and absorption of visible light by gases and airborne particles, where scattering is generally more important than absorption. Rayleigh scattering of sunlight by the permanent gases in air is the largest single physical process reducing the light intensity at the sun photometer in Ny-Ålesund. The scattering by particles in the visible part of the spectrum, 0.4-0.7 μm, is more efficient for short wavelengths than for longer. The particle size that gives the largest contribution to the scattering at a wavelength λ is given by $r/\lambda \approx 0.5$ where r is the particle radius according to Junge (1963). The only light absorption by gaseous species relevant for the wavelengths observed by the sun photometer is due to ozone, mostly at 501 nm. In the calculations below, 230 D.U. were used. The variation in the O_3 column content during the measurement period has not been taken into account. The AOD as observed by the instrument depends on the amount of particle in the slant atmospheric column above the instrument (~ sea level) to the top of the atmosphere on a slant path towards the sun. The AOD is wavelength-dependent, because the optical cross sections of the particles generally depend on the size parameter $x=2\pi r/\lambda$ and on the complex refractive index of the particles, which again is a function of wavelength. It should be kept in mind that the AOD is estimated as the difference between the total scattering and the molecular Rayleigh scattering. Under typical conditions encountered on Spitsbergen this is a fairly small difference between to large numbers, which introduces a certain uncertainty.

A sun photometer needs a clear sky towards the sun in order to give useful data, and this limits the data capture at Ny-Ålesund. The photometer measurements were started on 1st May 2002, and the photometer was operated until 15th October 2002. Useful data were obtained on 66 days only. On the other hand, the

photometer could, in principle, measure both day and night on clear days during the Arctic summer due to the midnight sun.

Figure 41 shows monthly AOD arithmetic averages of all accepted measurements during 2002. A high AOD indicates a high number of particles, and the results from Ny-Ålesund are generally very low indicating low concentrations of particles in the atmosphere there. The AOD at a short wavelength is normally higher than that measured at a longer wavelength, indicating that the particle size distribution is dominated by small particles.

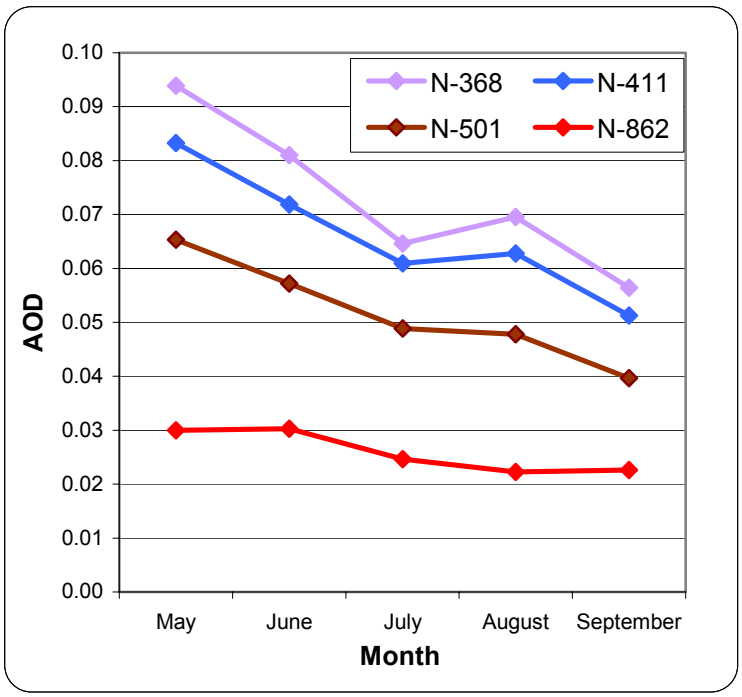

Figure 41: Monthly average AOD at 368, 411, 501, and 862 nm during May–September 2002 at Ny-Ålesund.

According to Junge (1963) most of the scattering is due to particles between about 0.4–0.8 μm at those wavelengths observed at Ny-Ålesund.

The aerosol number concentration is low at Spitsbergen compared to continental sites with larger emissions and production of particles. Figure 42a and Figure 42b compare the AOD results from Ny-Ålesund with corresponding measurements at Gotland in Sweden and measurements at the Joint Research Centre at Ispra near Lago Maggiore in north-western Italy. The wavelengths compared are nearly, but not quite identical. Gotland is located in the Baltic Sea, while the Ispra site in northern Italy is located in a region with considerable anthropogenic activities and correspondingly high gas and particle concentrations. Both locations have regular EMEP sites. Both the number of measurements and measurement days are different, thus making a direct comparison of the AOD at the sites difficult. But the results indicate that aerosol concentrations in Ispra are higher by a factor of ten than in Ny-Ålesund, while Gotland, as expected, lies in-between.

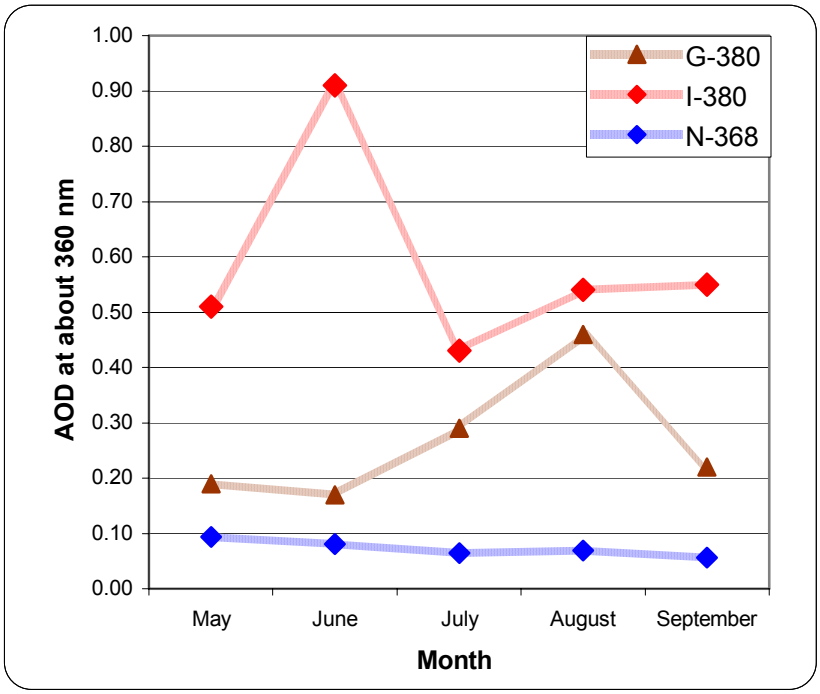

Figure 42a: Monthly averages of AOD at Gotland (G-380) and Ispra (I-380) at 380 nm with Ny-Ålesund (N-368) at 368 nm.

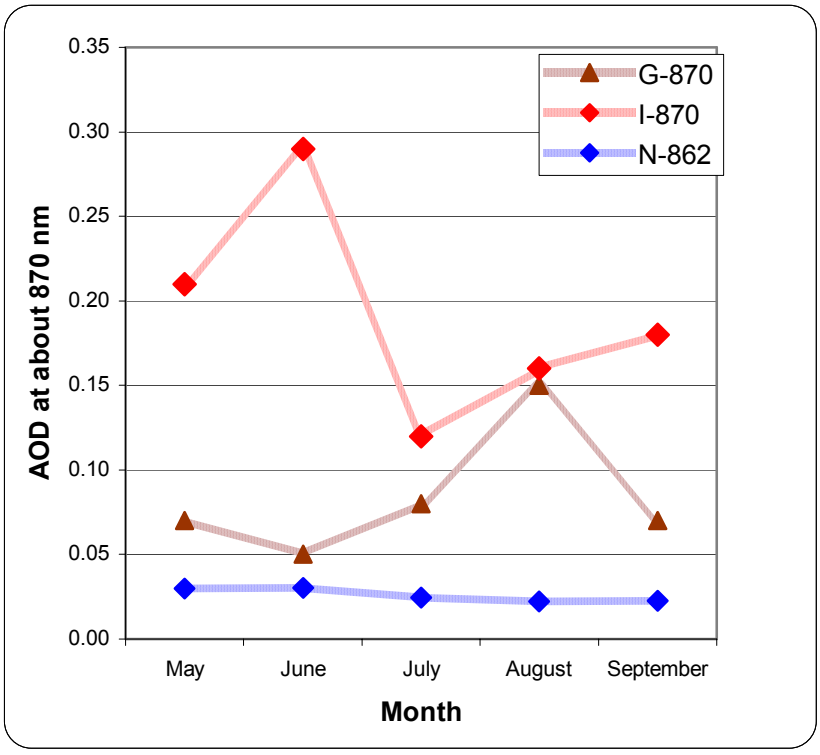

Figure 42b: Monthly averages of AOD at Gotland (G-870) and Ispra (I-870) at 870 nm with Ny-Ålesund (N-862) at 862 nm.

The Ångström exponent, α, which can be calculated from the AOD, is sensitive to the aerosol size distribution. A small α indicates a high number of the larger particles; normally this exponent will vary between 2.0 and 0.5. A time series of α will therefore give information on the variation in the particle size distribution during the measurement period. Figure 43 presents the daily averages of Ångström's α, which in general are higher than 0.5 except for 16th September.

Figure 44 shows a time series of the aerosol optical depth (AOD) on 16th September retrieved from the same photometer data. Larger particles scatter mainly the longer wavelengths. One can clearly see how the low α values on September 16 in Figure 43 coincide with a strong increase in the AOD during the morning hours in the long-wave channel at 863 nm. Thus we can deduce from the sun photometer data that the size distribution of the particles passing the atmospheric column shifts to larger particles during the morning hours of 16th September.

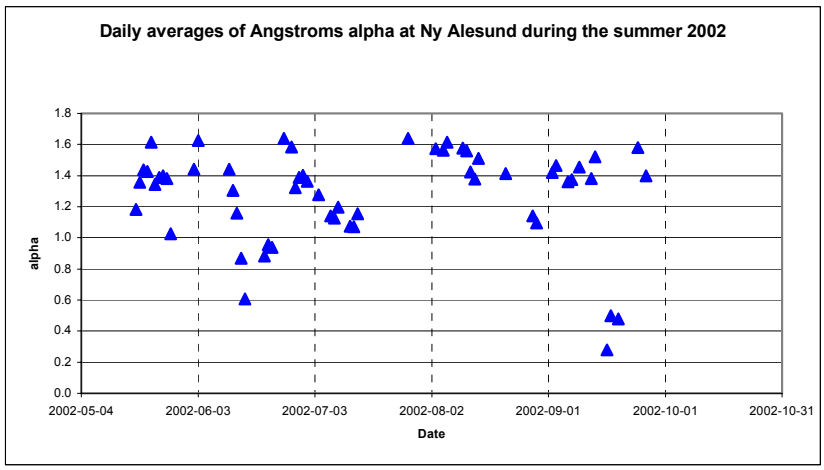

Figure 43: Daily averages of Ångström α at Ny-Ålesund during summer 2002.

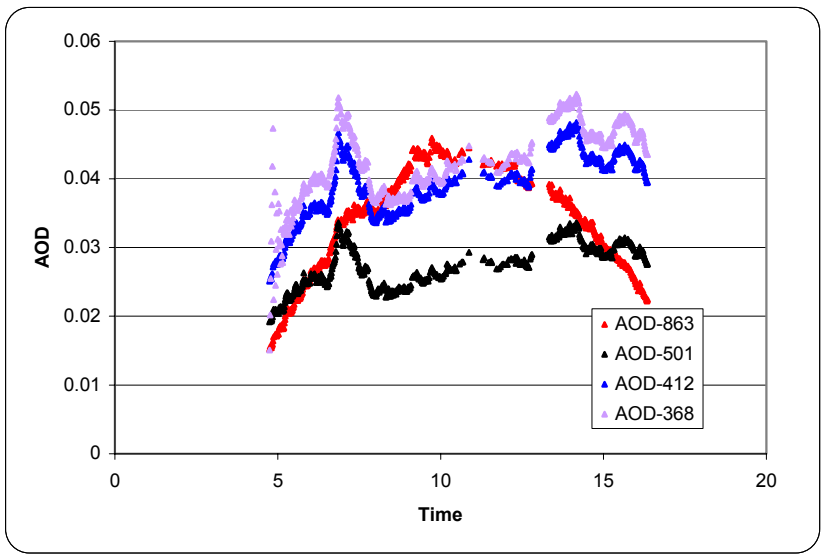

Figure 44: AOD at Ny-Ålesund on 16th September 2002.

The particle sources may be anthropogenic or natural, and trajectories (calculated with HYSPLIT) do not give a clear answer to this. Air masses arriving at high altitude (3000–5000 m) in the morning started 6–7 days earlier in the northern Pacific and have swept over the Asian continent and Russia, arriving over Spitsbergen in the morning/at noon when the episode culminated. Analysis of weather maps may be useful for a further assessment of this event. One possible explanation may be the forest fires in Russia in the Moscow region at that time when hundreds of fires in forests and peat bugs caused immense amounts of smoke and problems in the region.

Acknowledgements

The AOD data from Gotland and Ispra have been kindly provided by Dr. Bertil Hakansson (SMHI) and Dr. Giuseppe Zibordi (JRC, Ispra). The NOAA Air Resources Laboratory (http://www.arl.noaa.gov/ready/hysplit4.html) is gratefully acknowledged for use of their Hybrid Single-Particle Lagrangian Integrated Trajectory (HYSPLIT) model.

6. References

Bardouki, H., Liakakou, H., Economou, C., Sciare, J., Smolík, J., Ždímal, V., Eleftheriadis, K., Lazaridis, M. and Mihalopoulos, N. (2003) Chemical composition of size resolved atmospheric aerosols in the eastern Mediterranean during summer and winter. *Atmos. Environ., 37,* 195-208.

Bergametti, G., Dutot, A.-L., Buat-Ménard, P., Losno, R. and Remoudaki, E. (1989a) Seasonal variability of the elemental composition of atmospheric aerosol particles over the northwestern Mediterranean. *Tellus, 41B,* 353-361.

Bergametti, G., Gomes, L., Remoudaki, E., Desbois, M., Martin, D. and Buat-Ménard, P. (1989b) Present transport and deposition patterns of African dust to the North-Western Mediterranean. In: *Paleoclimatology and paleometeorology: modern and past patterns of global atmospheric transport*. Ed. by M. Leinen and M. Sarthein. Dordrecht, Kluwer. pp. 227-252.

Bonelli, P., Braga Marcazzan, G.M. and Cereda, E. (1996) Elemental composition and air trajectories of African dust transported in northern Italy. In: *The impact of desert dust across the Mediterranean*. Ed. by S. Guerzoni and R. Chester. Dordrecht, Kluwer. pp. 275-283.

Chabas, A. and Lefèvre, R.A. (2000) Chemistry and microscopy of atmospheric particulates at Delos (Cyclades-Greece). *Atmos. Environ., 34,* 225-238.

Chester, R., Nimmo, M, Alarcon, M., Saydam, C., Murphy, K.J.T., Sanders, S.G. and Corcoran, P. (1993) Defining the chemical character of aerosols from the atmosphere of the Mediterranean Sea and surrounding regions. *Oceanologica Acta, 16,* 231-246.

Danalatos, D. and Glavas, S. (1999) Gas phase nitric acid, ammonia and related particulate matter at a Mediterranean coastal site, Patras, Greece. *Atmos. Environ., 33,* 3417-3425.

Ding, Y., Pang, Y. and Eatough, D.J. (2002) High-volume diffusion denuder sampler for the routine monitoring of fine particulate matter. I. Design and optimization of the PC-BOSS. *Aerosol Sci. Techn*., *36,* 369-382.

Dulac, F., Buat-Ménard, P., Arnold, M., Ezat, U. and Martin, D. (1987) Atmospheric input of trace metals to the western Mediterranean Sea: 1. Factors controlling the variability of atmospheric concentrations. *J. Geophys. Res., 92,* 8437-8453.

Dulac, F., Buat-Ménard, P., Ezat, U. and Melki, S. (1989) Atmospheric input of trace metals to the western Mediterranean: uncertainties in modelling dry deposition from cascade impactor data. *Tellus, 41B,* 362-378.

EMEP/CCC (2001) Measurements of particulate matter in EMEP. Ed. by M. Lazaridis. Kjeller, Norwegian Institute for Air Research (EMEP/CCC-Report 5/2001).

EMEP/CCC (2002) Measurements of particulate matter: status report 2002. Ed. by M. Kahnert. Kjeller, Norwegian Institute for Air Research (EMEP/CCC-Report 4/2002).

Erduran, M.S. and Tuncel, S.G. (2001) Gaseous and particulate air pollutants in the northeastern Mediterranean Coast. *Sci. Total Environ., 281,* 205-215.

Finlayson-Pitts, B.J. and Pitts, J.N., Jr. (2000) Chemistry of the upper and lower atmosphere: theory, experiments, and applications. San Diego, Academic Press.

Ganor, E., Foner, H.A., Brenner, S., Neeman, E. and Lavi, N. (1991) The chemical composition of aerosols settling in Israel following dust storms. *Atmos. Environ., 25A,* 2665-2670.

Guerzoni, S., Correggiari, I. and Miserocchi, S. (1990) Wind-blown particles from ships and land-based stations in the Mediterranean See: A review of trace metal sources. In: *EROS 2000: second workshop on the northwest Mediterranean Sea 1990.* Ed. by J.-M. Martin and H. Barth. Brussels, Commission of the European Communities (Water Poll. Res. Rep., 20). pp. 377-386.

Güllü, G., Ölmez, İ. and Tuncel, G. (2000) Temporal variability of atmospheric trace element concentrations over the eastern Mediterranean Sea. *Spectrochimica Acta, B 55,* 1135-1150.

Hacisalihoğlu, G., Balkaş, T.İ., Tuncel, S.G., Herman, D.H., Ölmez, İ. and Tuncel, G. (1991) Trace element composition of the Black Sea aerosols. *Deep-Sea Res., 38,* S1255-S1266.

Hacisalihoğlu, G., Eliyakut, F., Ölmez, İ., Balkas, T.İ., and Tuncel, G. (1992) Chemical composition of particles in the Black Sea atmosphere. *Atmos. Environ., 26A,* 3207-3218.

Havránek, V., Kučera, J., Horáková, J., Voseček, V., Smolík, J., Schwarz, J. and Sýkorová, I. (1999) Matrix effects in PIXE analysis of aerosols and ashes. *Biol. Trace Elements Res., 71-72,* 431-442.

Hillamo, R.E. and Kauppinen, E.I. (1991) On the performance of the Berner low pressure impactor. *Aerosol Sci. Technol., 14,* 33-47.

Hillamo, R.E., Makela, T., Schwarz, J. and Smolík, J. (1999) Collection characteristics of the model 25/0,018/2 Berner low pressure impactor. *J. Aerosol Sci., 30(S1),* 901-902.

Jaffrezo, J.L., Davidson, C.I., Kuhns, H.D., Bergin, M.H., Hillamo, R., Maenhaut, W., Kahl, J.W. and Harris, J.M. (1998) Biomass burning signatures in the atmosphere of central Greenland. *J. Geophys. Res., 103,* 31067-31078.

Junge, C. (1963) Air chemistry and radioactivity. New York, Academic Press.

Kubilay, N., Yemenicioglu, S. and Saydam, C. (1994) Trace metal characterization of airborne particles from the northeastern Mediterranean. *Fresenius Envir. Bull., 3,* 444-448.

Kubilay, N., Yemenicioglu, S. and Saydam, C. (1995) Airborne material collections and their chemical composition over the Black Sea. *Marine Pollution Bull., 30,* 475-483.

Lovett, R.F. (1978) Quantitative measurements of airborne sea-salt in the north Atlantic. *Tellus, 30,* 358-363.

Luria, M., Peleg, M., Sharf, G., Tov-Alper, D.S., Spitz, N., Ben Ami, Y., Gawii, Z., Lifschitz, B., Yitzchaki, A. and Seter, I. (1996) Atmospheric sulfur over the east Mediterranean region. *J. Geophys. Res., 101,* 25,917-25,930.

Maenhaut, W., Ptasinski, J. and Cafmeyer, J. (1999) Detailed mass size distributions of atmospheric aerosol species in the Negev desert, Israel, during ARACHNE-96. *Nucl. Instrum. Meth., B 150,* 422-427.

Mamane, Y., Ganor, E. and Donagi, A.E. (1980) Aerosol composition of urban and desert origin in the Eastern Mediterranean. I. Individual particle analysis. *Water Air Soil Pollut., 14,* 29-43.

Matta, E., Facchini, M.C., Decesari, S., Mircea, M., Cavalli, F., Fuzzi, S., Putaud, J.-P. and Dell'Acqua, A. (2003) Mass closure on the chemical species in size-segregated atmospheric aerosol collected in an urban area of the Po Valley, Italy. *Atmos. Chem. Phys., 3*, 623-637.

McDow S.R. and Huntzicker, J.J. (1990) Vapor adsorption artifact in the sampling of organic aerosol - face velocity effects. *Atmos. Environ., A 24,* 2563-2571.

Migon, C., Morelli, J., Nicolas, E. and Copin-Montegut, G. (1991) Evolution of total atmospheric deposition of Pb, Cd, Cu and Zn to the Ligurian Sea. *Sci. Total Environ., 105,* 135-148.

Migon, C., Alleman, L., Leblond, N. and Nicolas, E. (1993) Evolution of atmospheric lead over the northwestern Mediterranean between 1986 and 1992. *Atmos. Environ., 27A,* 2161-2167.

Mihalopoulos, N., Stephanou, E., Kanakidou, M., Pilitsidis, S. and Bosquet, P. (1997) Tropospheric aerosol ionic composition in the Eastern Mediterranean region. *Tellus, 49B,* 314-326.

Molinaroli, E. (1996) Mineralogical characterisation of Saharan dust with a view of its final destination in Mediterranean sediments. In: *The impact of desert dust across the Mediterranean*. Ed. by S. Guerzoni and R. Chester. Dordrecht, Kluwer. pp. 153-162.

Monahan, E.C. and MacNiocaill, G. (1986) Oceanic whitecaps and their role in air-sea exchange processes. Dordrecht, Reidel.

Moulin, C., Lambert, C.E., Dayan, U., Masson, V., Ramonet, M., Bousquet, P., Legrand, M., Balkanski, Y.J., Guelle, W., Marticorena, B., Bergametti, G. and Dulac, F. (1998) Satellite climatology of African dust transport in the Mediterranean atmosphere. *J. Geophys. Res., 103,* 13,137-13,144.

Sandroni, V. and Migon, C. (1997) Significance of trace metal medium-range transport in the western Mediterranean. *Sci. Total Environ., 196,* 83-89.

Schütz, L. and Rahn, K.A. (1982) Trace-element concentrations in erodible soil. *Atmos. Environ., 16,* 171-176.

Smith, M.H., Park, P.M. and Consterdine, I.E. (1993) Marine aerosol concentration and estimated fluxes over seas. *Q. J. R. Meteorol. Soc.,* 809-824.

Stohl, A. and Koffi, N.E. (1998) Evaluation of trajectories calculated from ECMWF data against constant volume balloon flights during ETEX. *Atmos. Environ*., *32*, 4151-4156.

Stone, V. and Donaldson, K. (1998) Small particles – Big problem. *The Aerosol Society Newsletter, 33,* 12-14.

Tsitouridou, R. and Samara, C. (1993) First results of acidic and alkaline constituents determination in air particulates of Thessaloniki, Greece. *Atmos. Environ., 27B,* 313-319.

Turpin, B.J., Huntzicker, J.J. and Hering, S.V. (1994) Investigation of organic aerosol sampling artifacts in the Los-Angeles basin. *Atmos. Environ., 28,* 3061-3071.

Valmari, T., Kaupinnen, E.I., Kurkela, J., Jokiniemi, J.K., Sfiris, G. and Revitzer, H. (1998) Fly ash formation and deposition during fludized bed combustion of willow. *J. Aerosol Sci., 29,* 445-459.

WMO (1985) Atmospheric transport of contaminants into the Mediterranean region. World Meteorological Organization (GESAMP Report and Studies 26). 53 pp.

Wolfenbarger, J.K. and Seinfeld, J.K. (1990) Inversion of aerosol size distribution data. *J. Aerosol Sci., 21,* 227-247.

Yatin, M., Tuncel, S., Aras, N.K., Ölmez, İ., Aygün, S. and Tuncel, G. (2000) Atmospheric trace elements in Ankara, Turkey: 1. factors affecting chemical composition of fine particles. *Atmos. Environ., 23,* 1305-1318.

Appendix A

Time series of particulate matter mass concentrations (μg/m^3) at EMEP stations in 2000 and 2001

PM_{10} mass concentrations in 2000:

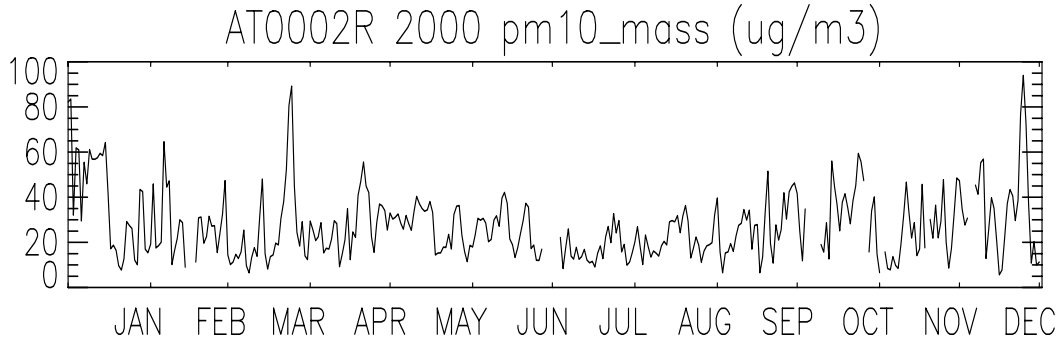

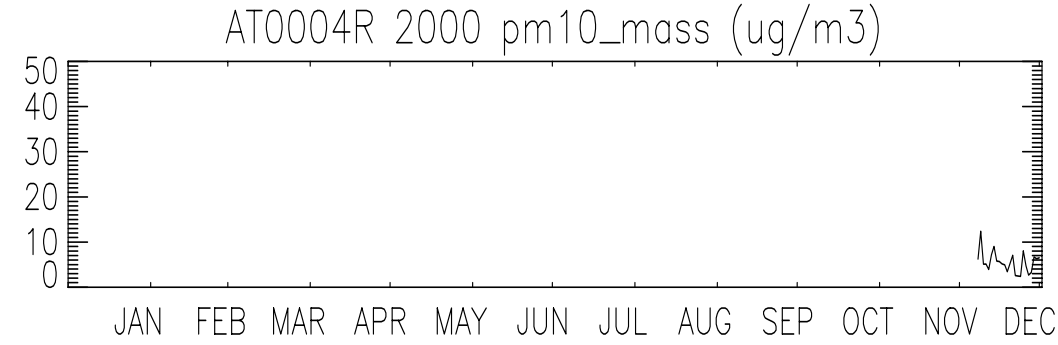

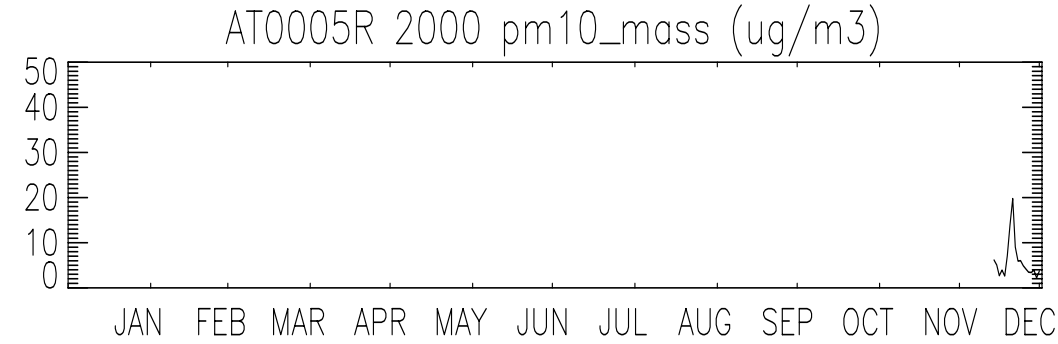

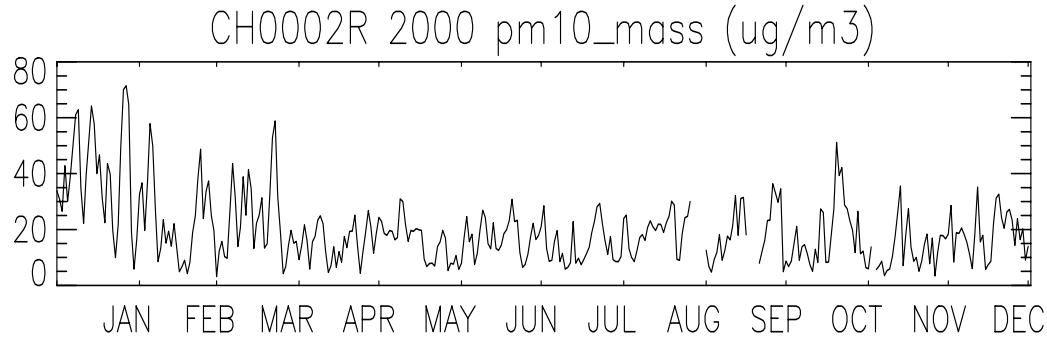
CH0002R 2000 pm10_mass (ug/m3)
80
60
40
20
0
JAN FEB MAR APR MAY JUN JUL AUG SEP OCT NOV DEC

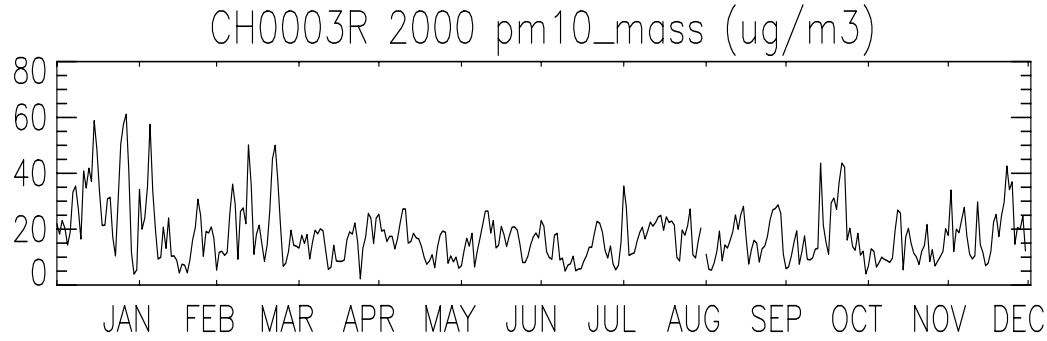
CH0003R 2000 pm10_mass (ug/m3)
80
60
40
20
0
JAN FEB MAR APR MAY JUN JUL AUG SEP OCT NOV DEC

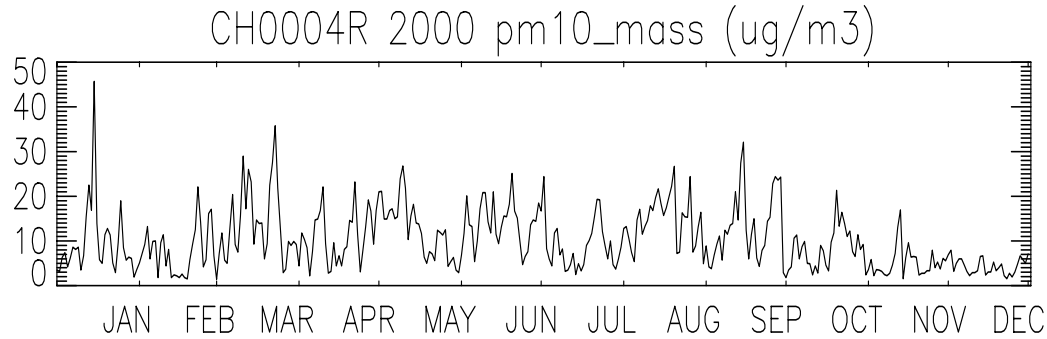
CH0004R 2000 pm10_mass (ug/m3)
50
40
30
20
10
0
JAN FEB MAR APR MAY JUN JUL AUG SEP OCT NOV DEC

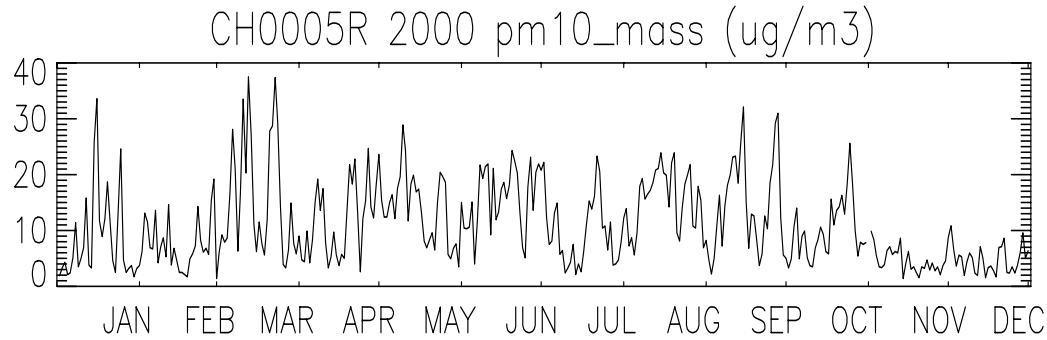
CH0005R 2000 pm10_mass (ug/m3)
40
30
20
10
0
JAN FEB MAR APR MAY JUN JUL AUG SEP OCT NOV DEC

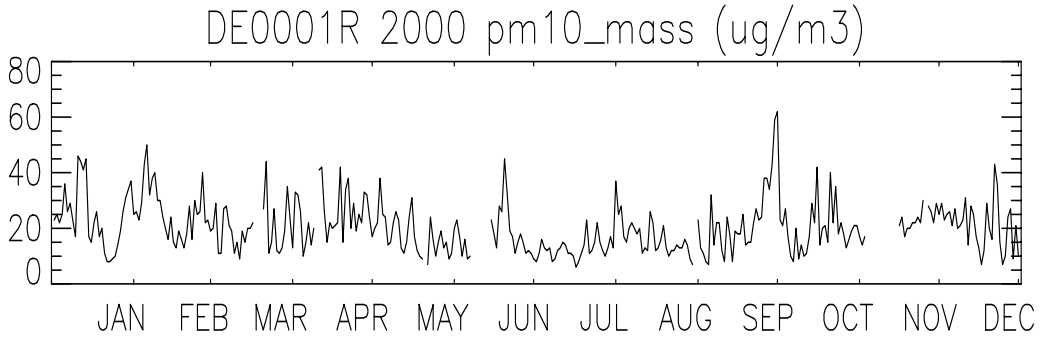
DE0001R 2000 pm10_mass (ug/m3)
80
60
40
20
0
JAN FEB MAR APR MAY JUN JUL AUG SEP OCT NOV DEC

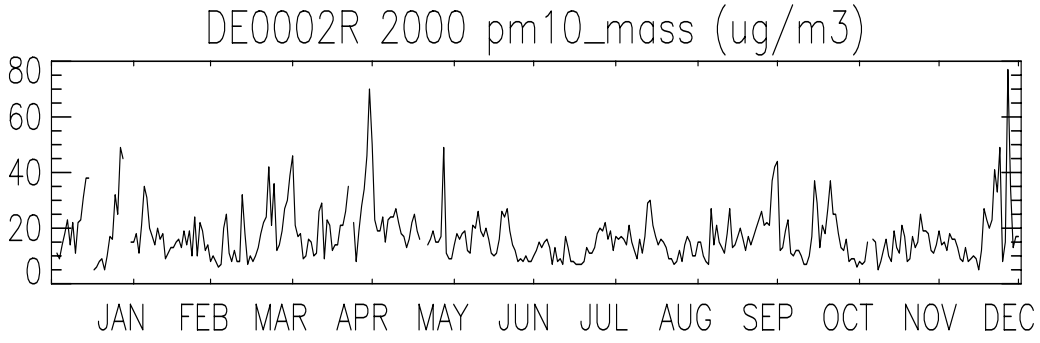
DE0002R 2000 pm10_mass (ug/m3)
80
60
40
20
0
JAN FEB MAR APR MAY JUN JUL AUG SEP OCT NOV DEC

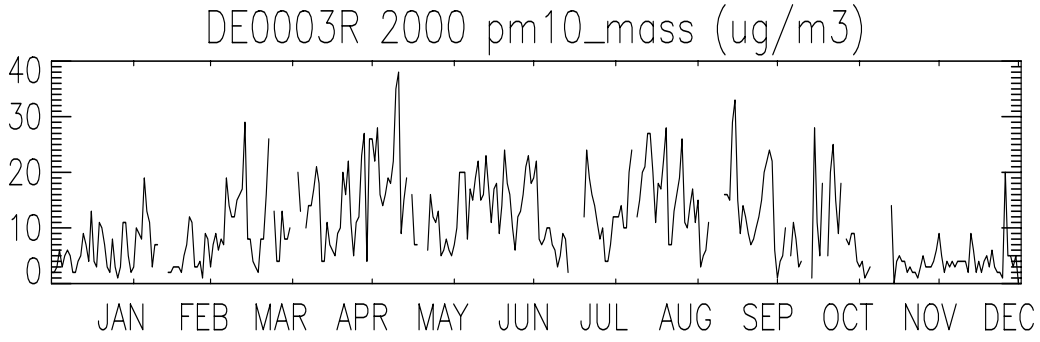
DE0003R 2000 pm10_mass (ug/m3)
40
30
20
10
0
JAN FEB MAR APR MAY JUN JUL AUG SEP OCT NOV DEC

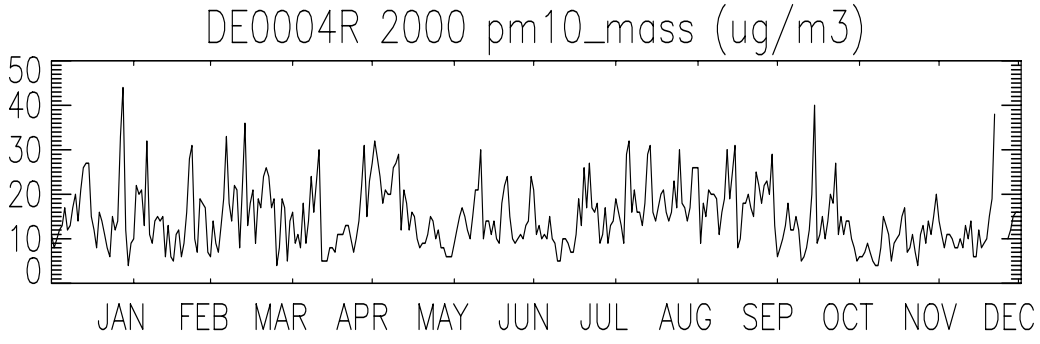
DE0004R 2000 pm10_mass (ug/m3)
50
40
30
20
10
0
JAN FEB MAR APR MAY JUN JUL AUG SEP OCT NOV DEC

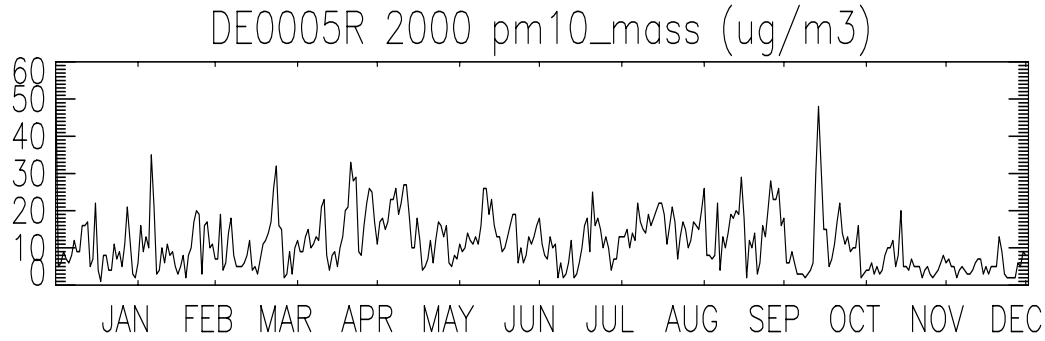
DE0005R 2000 pm10_mass (ug/m3)
60
50
40
30
20
10
0
JAN FEB MAR APR MAY JUN JUL AUG SEP OCT NOV DEC

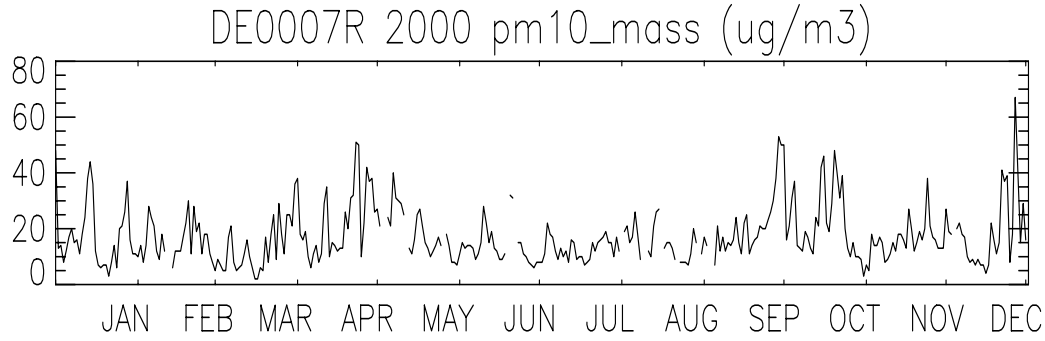
DE0007R 2000 pm10_mass (ug/m3)
80
60
40
20
0
JAN FEB MAR APR MAY JUN JUL AUG SEP OCT NOV DEC

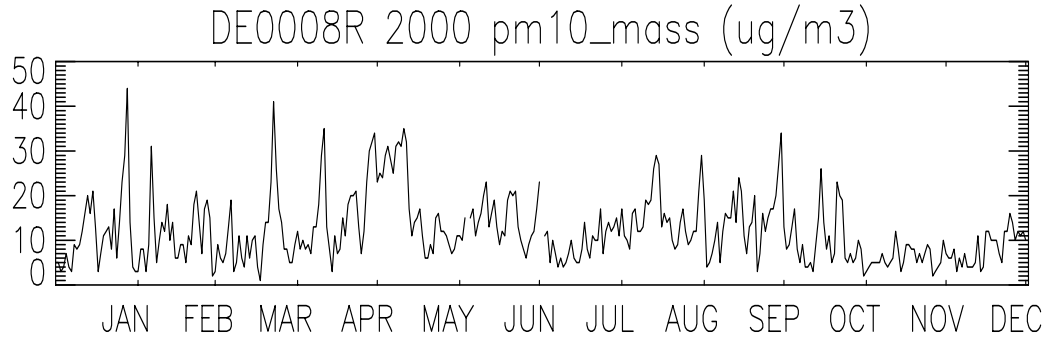
DE0008R 2000 pm10_mass (ug/m3)
50
40
30
20
10
0
JAN FEB MAR APR MAY JUN JUL AUG SEP OCT NOV DEC

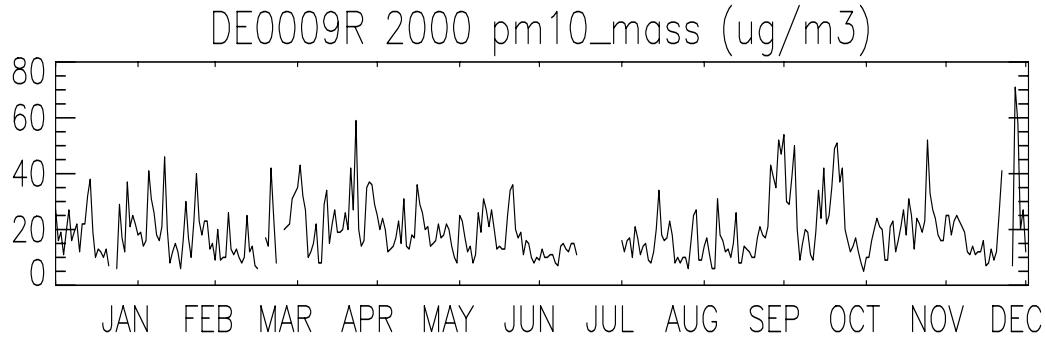
DE0009R 2000 pm10_mass (ug/m3)
80
60
40
20
0
JAN FEB MAR APR MAY JUN JUL AUG SEP OCT NOV DEC

$PM_{2.5}$ mass concentrations in 2000:

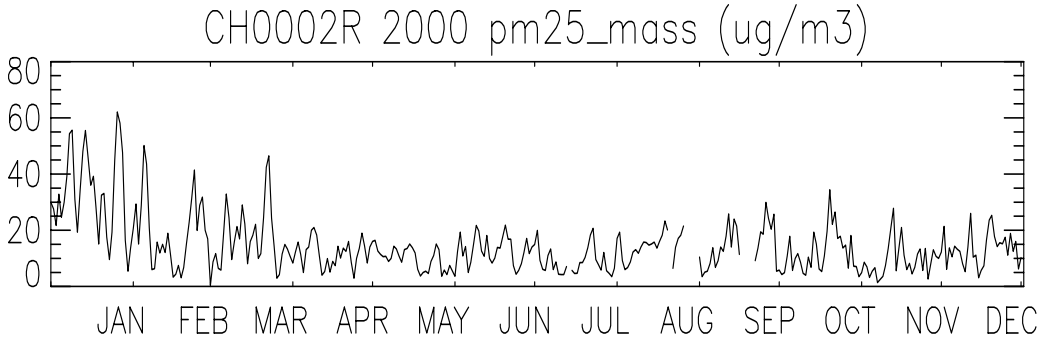

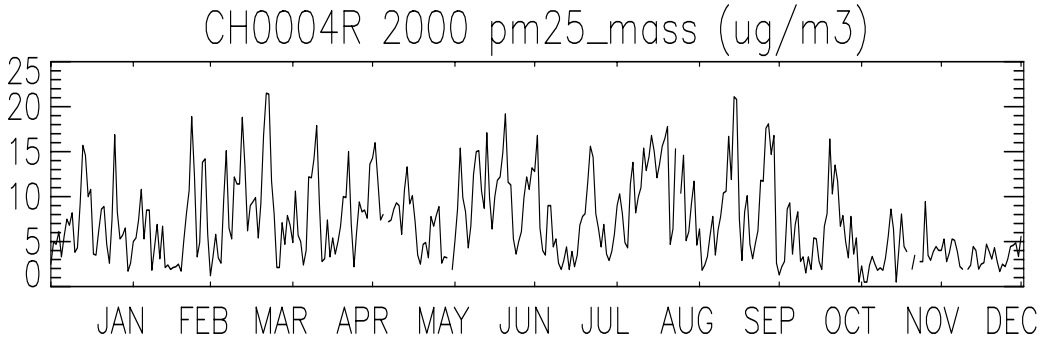

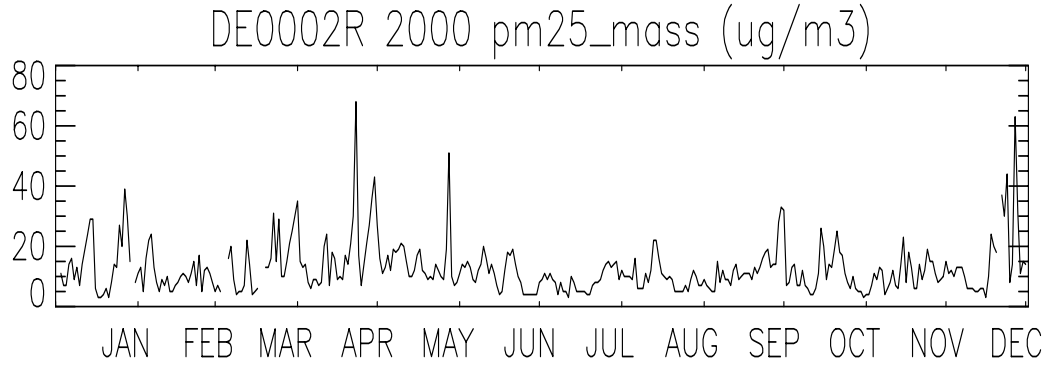
DE0002R 2000 pm25_mass (ug/m3)
80
60
40
20
0
JAN FEB MAR APR MAY JUN JUL AUG SEP OCT NOV DEC

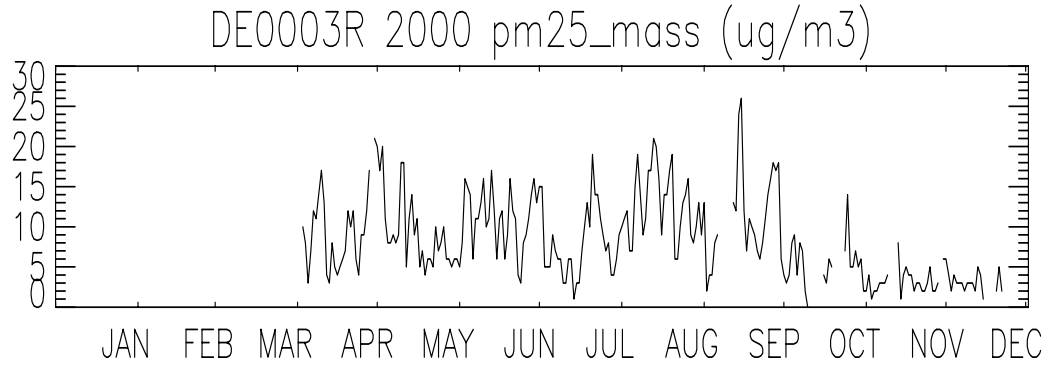
DE0003R 2000 pm25_mass (ug/m3)
30
25
20
15
10
5
0
JAN FEB MAR APR MAY JUN JUL AUG SEP OCT NOV DEC

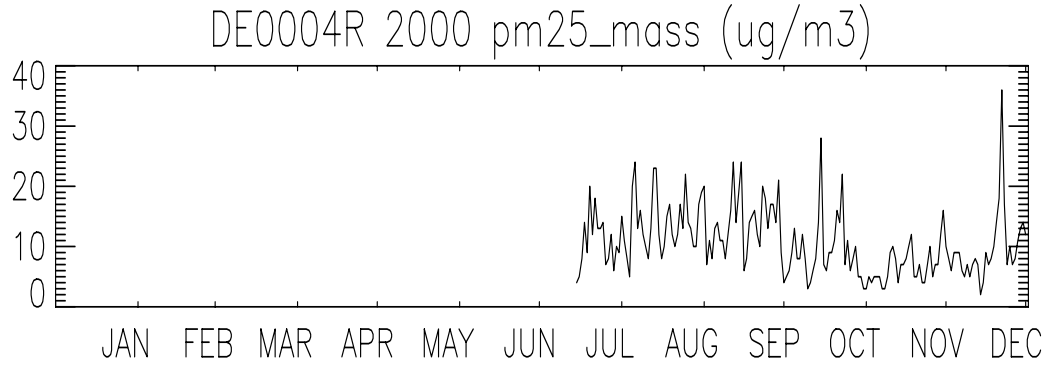
DE0004R 2000 pm25_mass (ug/m3)
40
30
20
10
0
JAN FEB MAR APR MAY JUN JUL AUG SEP OCT NOV DEC

TSP mass concentrations in 2000:

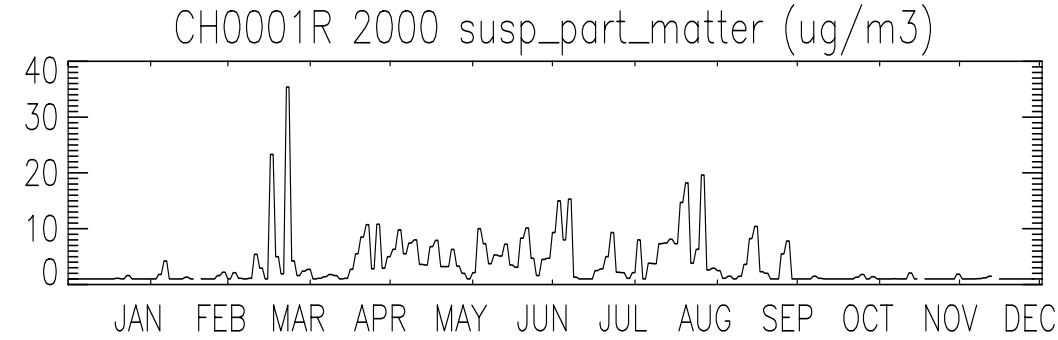

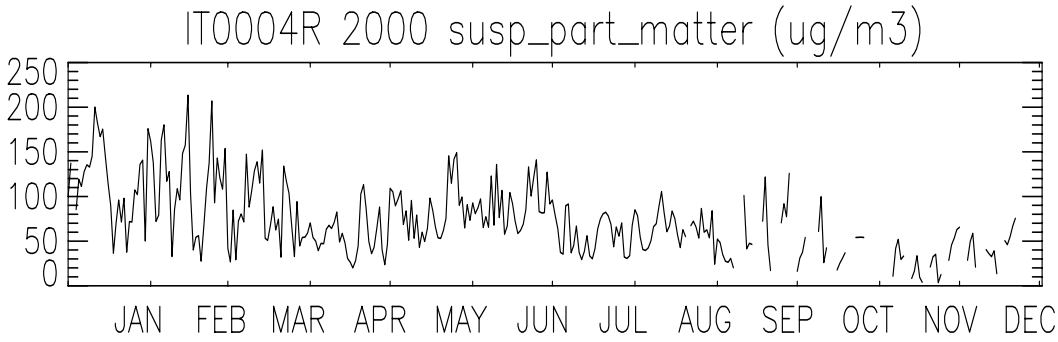

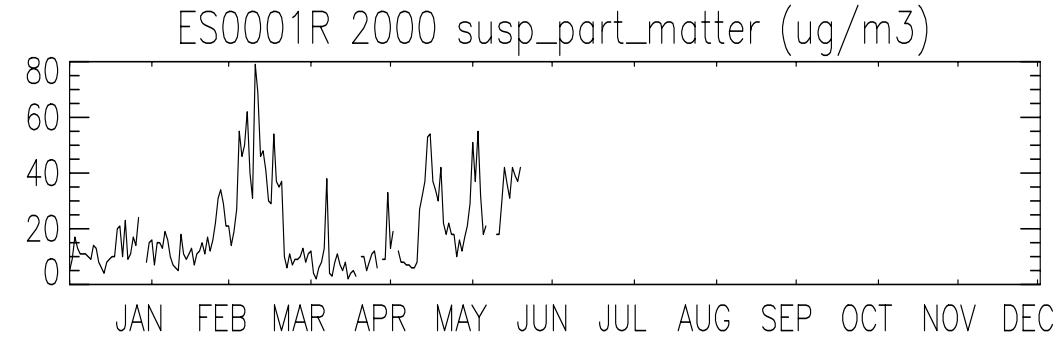
ES0001R 2000 susp_part_matter (ug/m3)
80
60
40
20
0
JAN FEB MAR APR MAY JUN JUL AUG SEP OCT NOV DEC

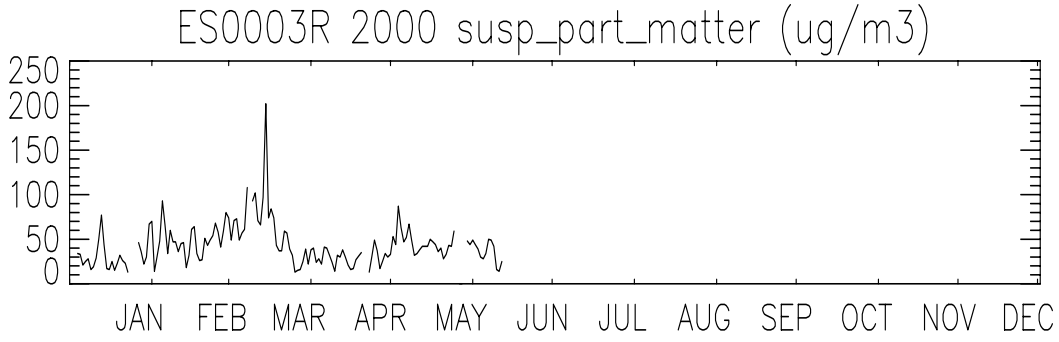
ES0003R 2000 susp_part_matter (ug/m3)
250
200
150
100
50
0
JAN FEB MAR APR MAY JUN JUL AUG SEP OCT NOV DEC

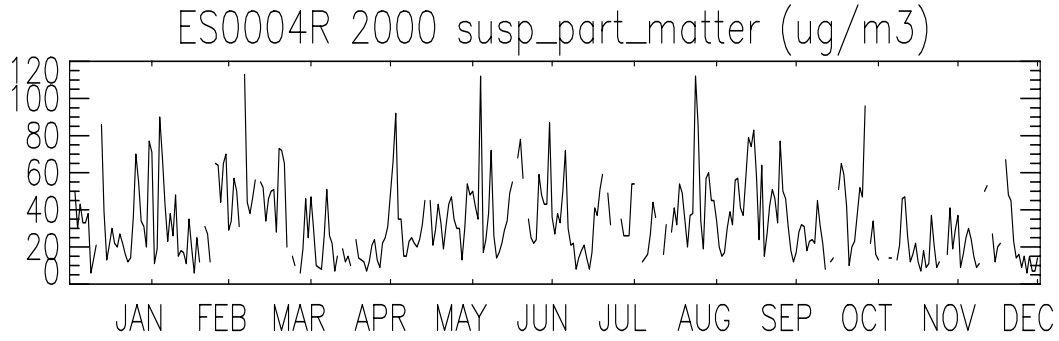
ES0004R 2000 susp_part_matter (ug/m3)
120
100
80
60
40
20
0
JAN FEB MAR APR MAY JUN JUL AUG SEP OCT NOV DEC

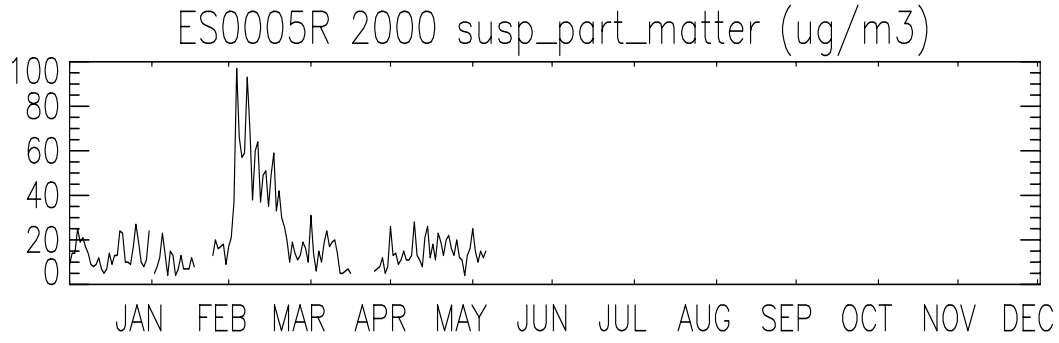
ES0005R 2000 susp_part_matter (ug/m3)
100
80
60
40
20
0
JAN FEB MAR APR MAY JUN JUL AUG SEP OCT NOV DEC

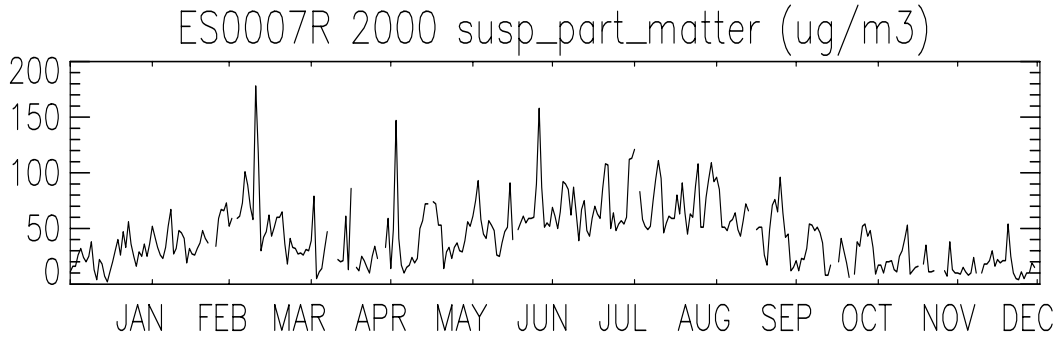
ES0007R 2000 susp_part_matter (ug/m3)
200
150
100
50
0
JAN FEB MAR APR MAY JUN JUL AUG SEP OCT NOV DEC

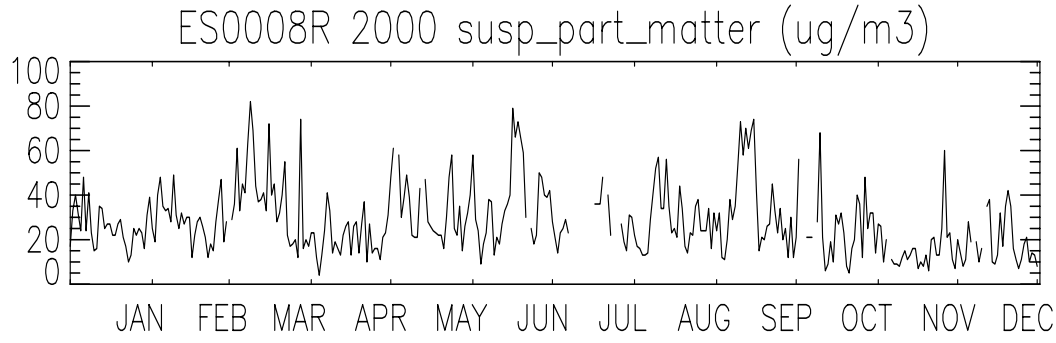
ES0008R 2000 susp_part_matter (ug/m3)
100
80
60
40
20
0
JAN FEB MAR APR MAY JUN JUL AUG SEP OCT NOV DEC

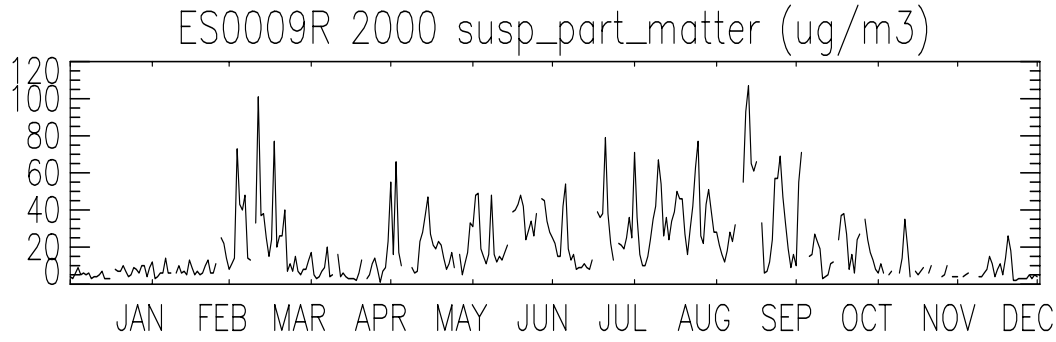
ES0009R 2000 susp_part_matter (ug/m3)
120
100
80
60
40
20
0
JAN FEB MAR APR MAY JUN JUL AUG SEP OCT NOV DEC

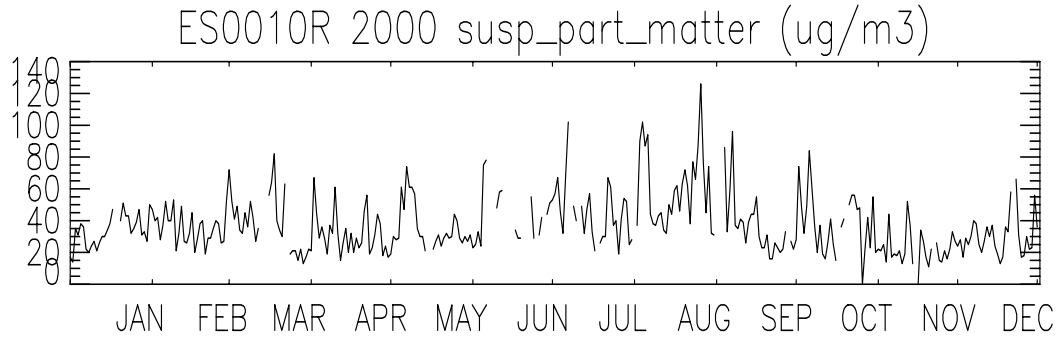
ES0010R 2000 susp_part_matter (ug/m3)
140
120
100
80
60
40
20
0
JAN FEB MAR APR MAY JUN JUL AUG SEP OCT NOV DEC

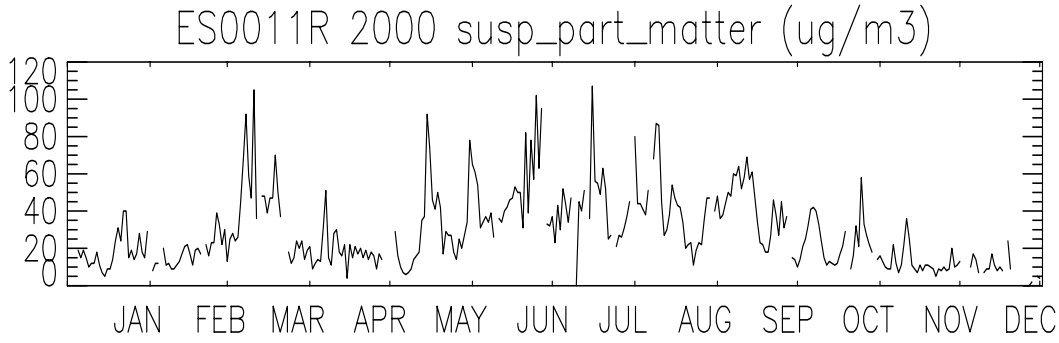
ES0011R 2000 susp_part_matter (ug/m3)
120
100
80
60
40
20
0
JAN FEB MAR APR MAY JUN JUL AUG SEP OCT NOV DEC

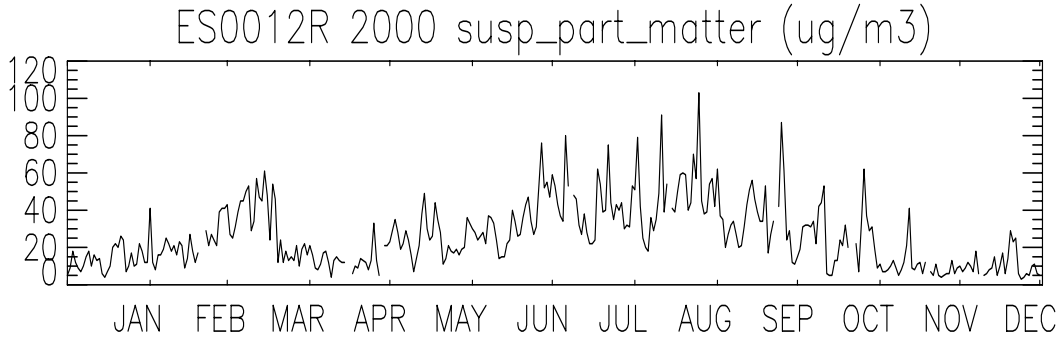
ES0012R 2000 susp_part_matter (ug/m3)
120
100
80
60
40
20
0
JAN FEB MAR APR MAY JUN JUL AUG SEP OCT NOV DEC

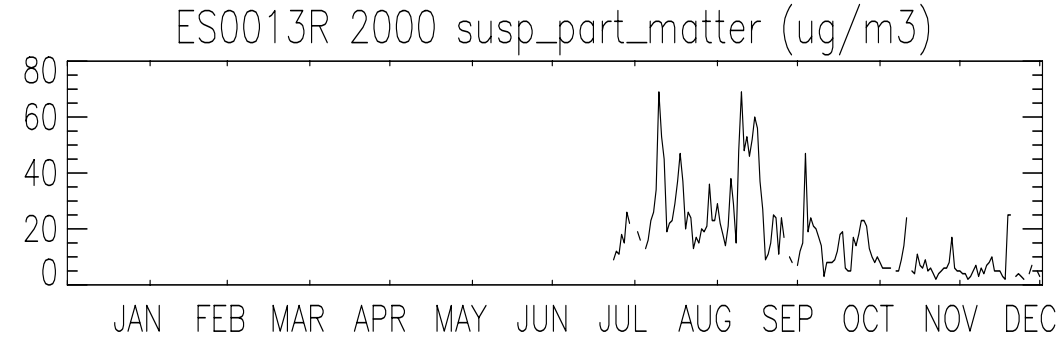
ES0013R 2000 susp_part_matter (ug/m3)
80
60
40
20
0
JAN FEB MAR APR MAY JUN JUL AUG SEP OCT NOV DEC

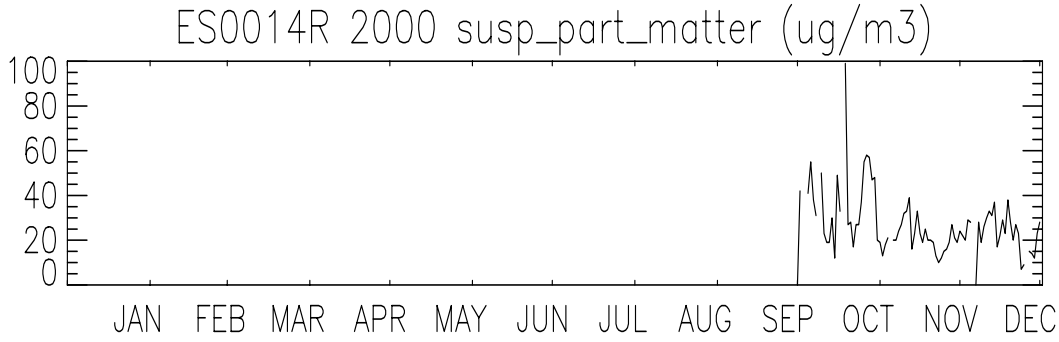
ES0014R 2000 susp_part_matter (ug/m3)
100
80
60
40
20
0
JAN FEB MAR APR MAY JUN JUL AUG SEP OCT NOV DEC

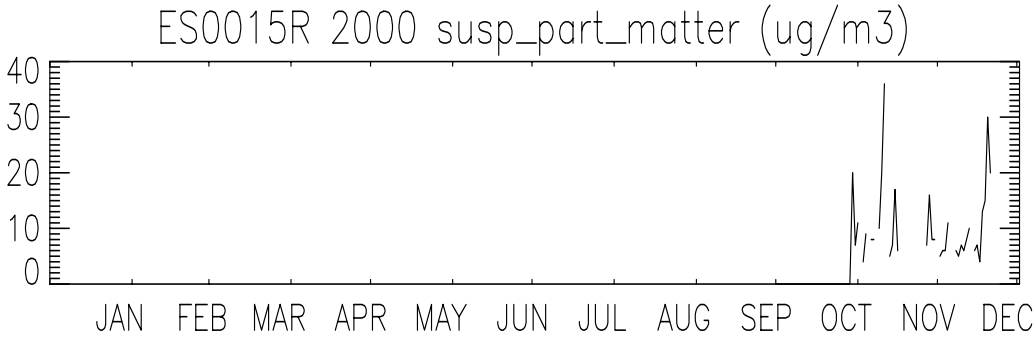
ES0015R 2000 susp_part_matter (ug/m3)
40
30
20
10
0
JAN
FEB
MAR
APR
MAY
JUN
JUL
AUG
SEP
OCT
NOV
DEC

PM_{10} mass concentrations in 2001:

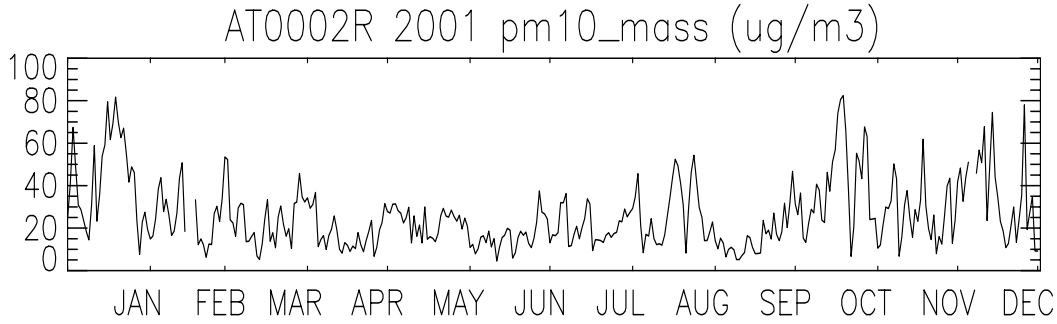

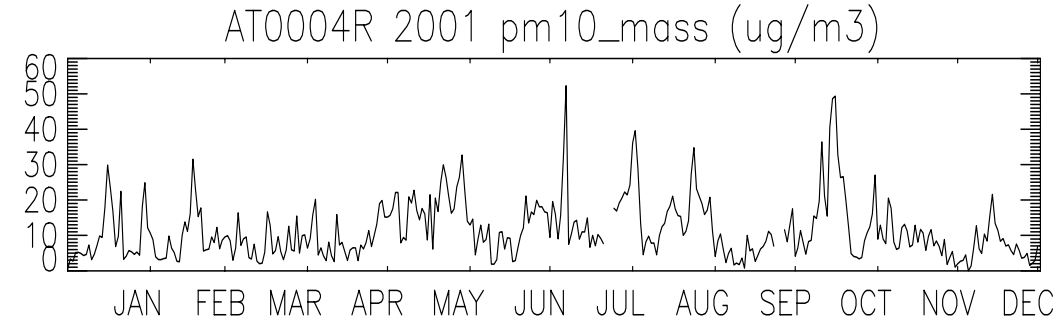

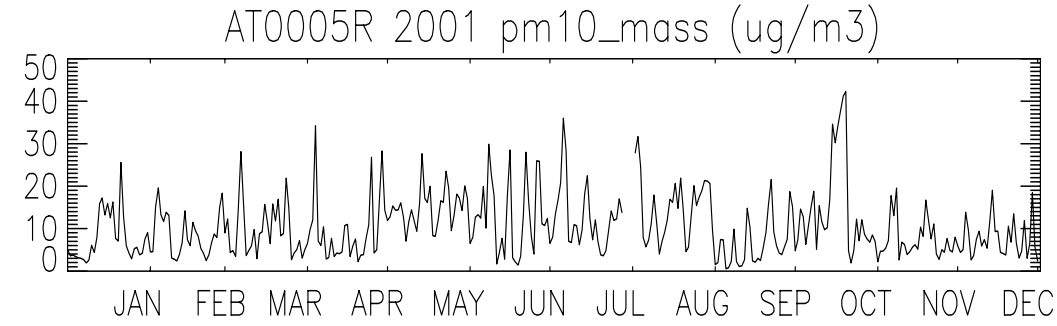

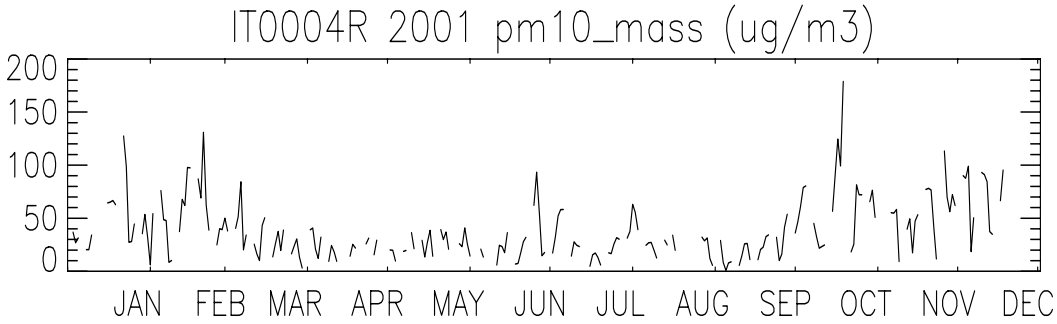

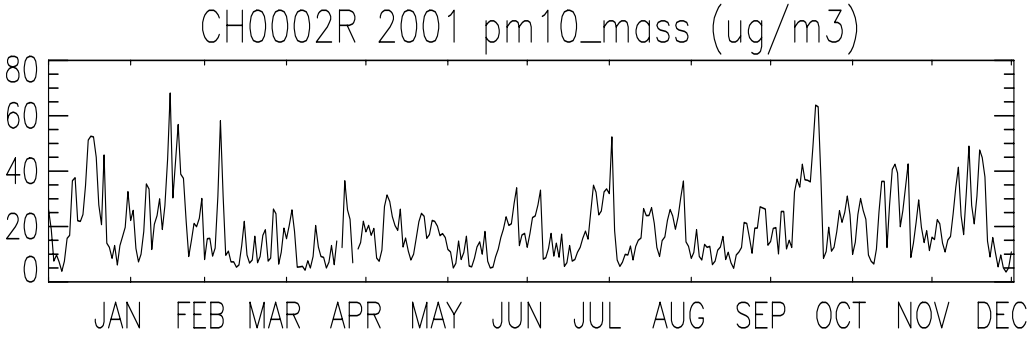
CH0002R 2001 pm10_mass (ug/m3)
80
60
40
20
0
JAN FEB MAR APR MAY JUN JUL AUG SEP OCT NOV DEC

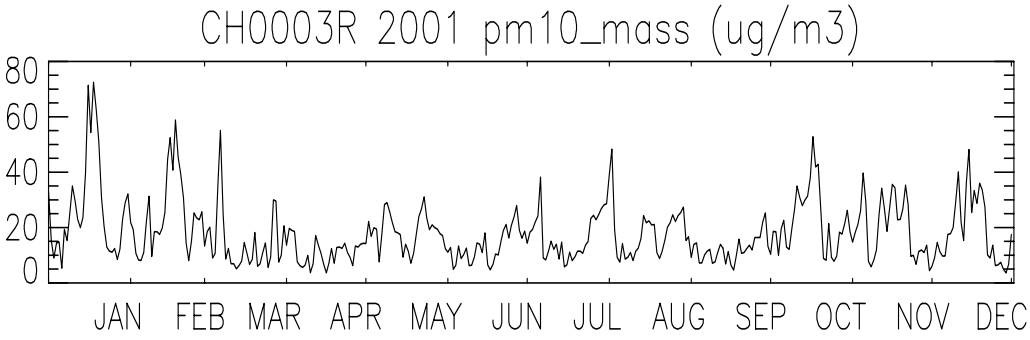
CH0003R 2001 pm10_mass (ug/m3)
80
60
40
20
0
JAN FEB MAR APR MAY JUN JUL AUG SEP OCT NOV DEC

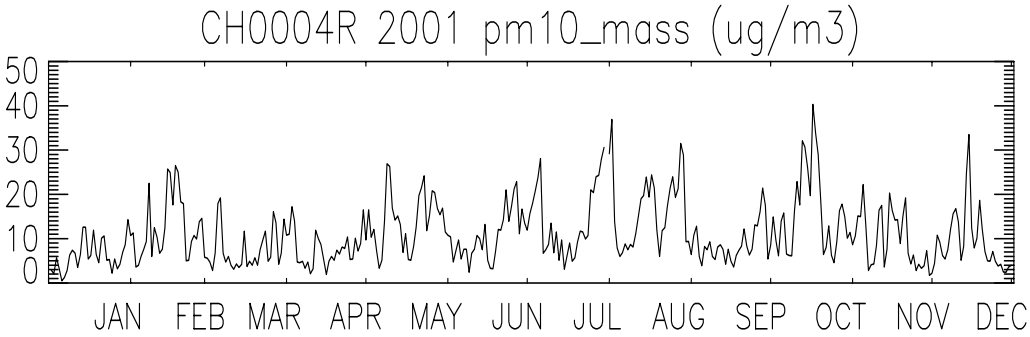
CH0004R 2001 pm10_mass (ug/m3)
50
40
30
20
10
0
JAN FEB MAR APR MAY JUN JUL AUG SEP OCT NOV DEC

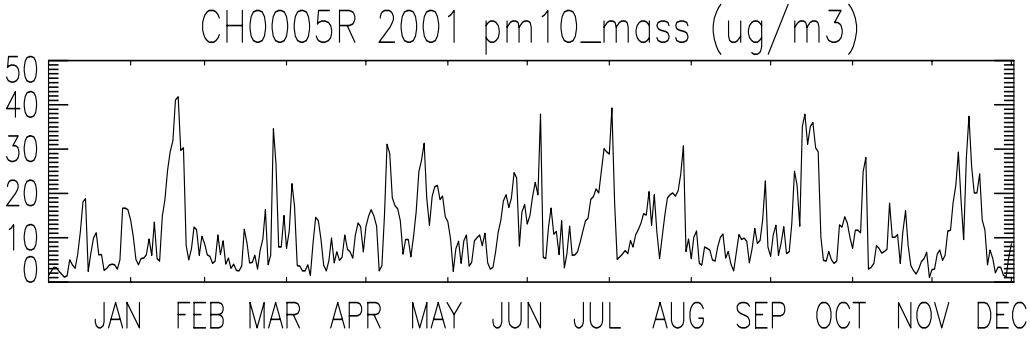
CH0005R 2001 pm10_mass (ug/m3)
50
40
30
20
10
0
JAN FEB MAR APR MAY JUN JUL AUG SEP OCT NOV DEC

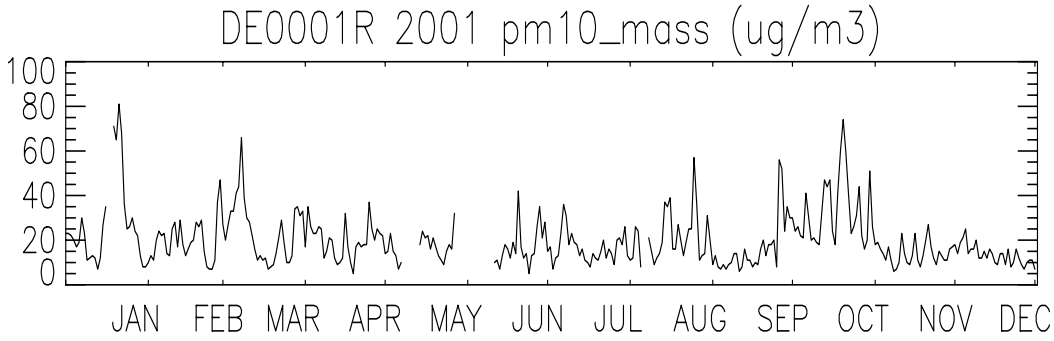
DE0001R 2001 pm10_mass (ug/m3)
100
80
60
40
20
0
JAN FEB MAR APR MAY JUN JUL AUG SEP OCT NOV DEC

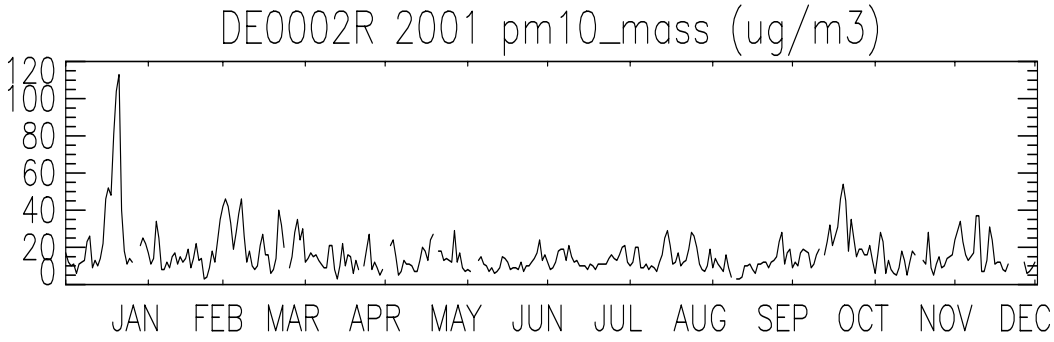
DE0002R 2001 pm10_mass (ug/m3)
120
100
80
60
40
20
0
JAN FEB MAR APR MAY JUN JUL AUG SEP OCT NOV DEC

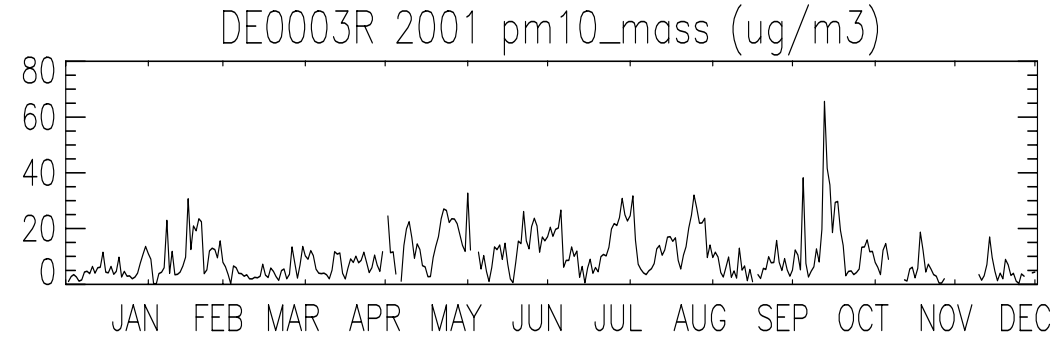
DE0003R 2001 pm10_mass (ug/m3)
80
60
40
20
0
JAN FEB MAR APR MAY JUN JUL AUG SEP OCT NOV DEC

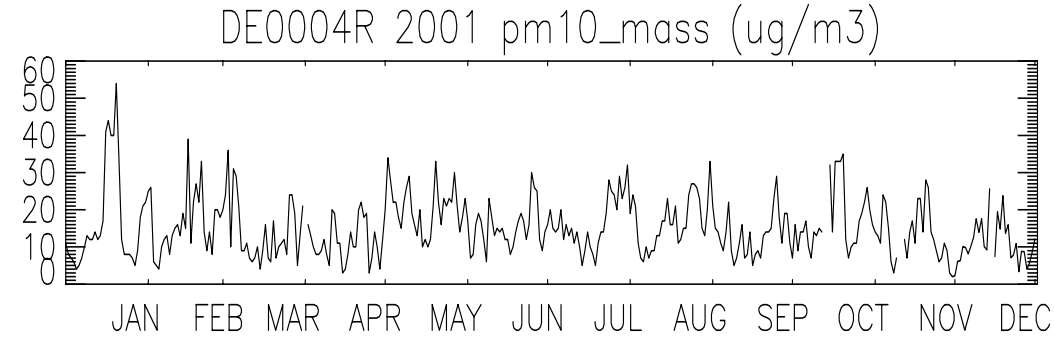
DE0004R 2001 pm10_mass (ug/m3)
60
50
40
30
20
10
0
JAN FEB MAR APR MAY JUN JUL AUG SEP OCT NOV DEC

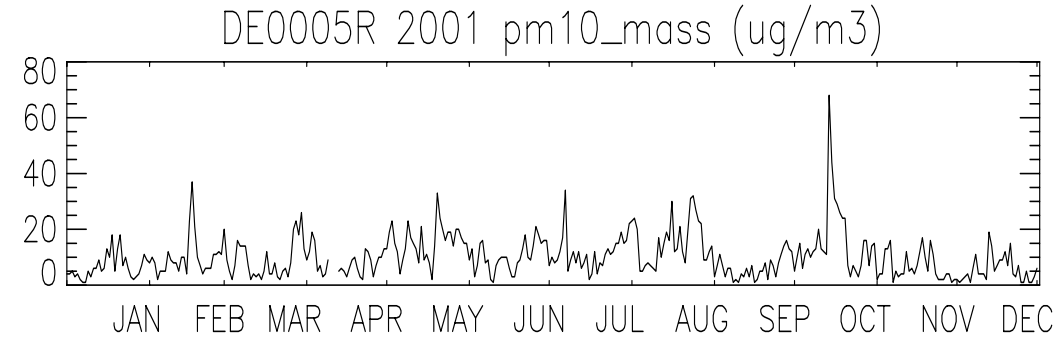
DE0005R 2001 pm10_mass (ug/m3)
80
60
40
20
0
JAN FEB MAR APR MAY JUN JUL AUG SEP OCT NOV DEC

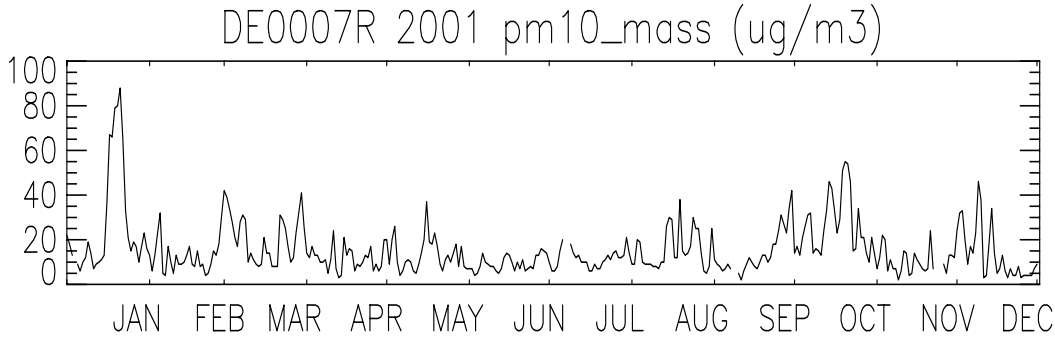
DE0007R 2001 pm10_mass (ug/m3)
100
80
60
40
20
0
JAN FEB MAR APR MAY JUN JUL AUG SEP OCT NOV DEC

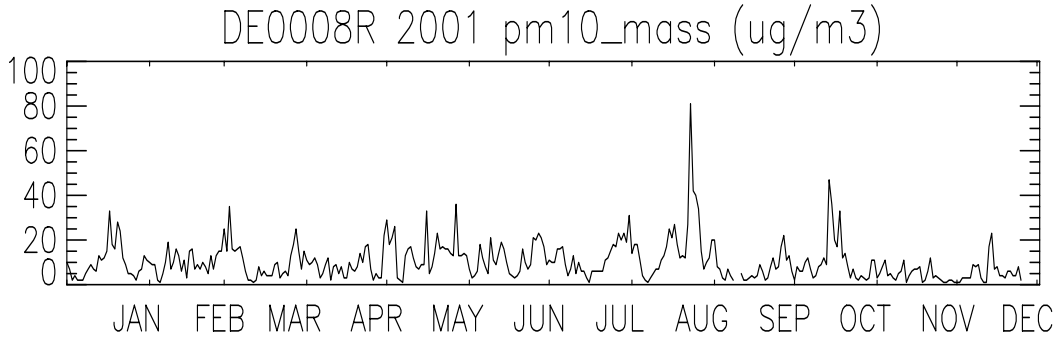
DE0008R 2001 pm10_mass (ug/m3)
100
80
60
40
20
0
JAN FEB MAR APR MAY JUN JUL AUG SEP OCT NOV DEC

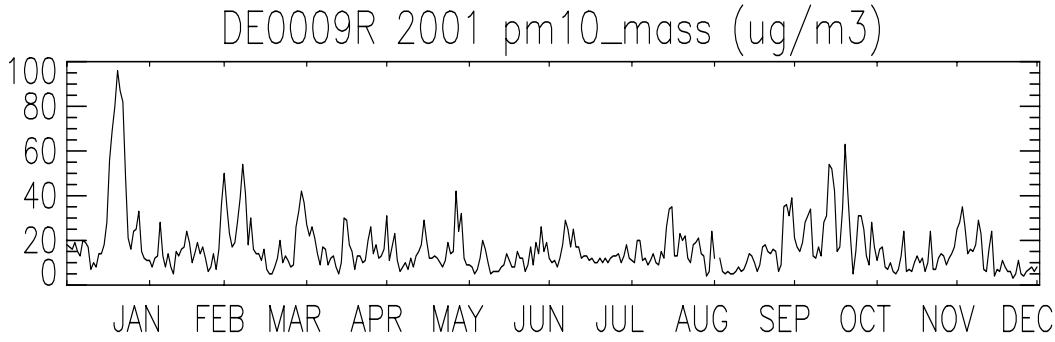
DE0009R 2001 pm10_mass (ug/m3)
100
80
60
40
20
0
JAN FEB MAR APR MAY JUN JUL AUG SEP OCT NOV DEC

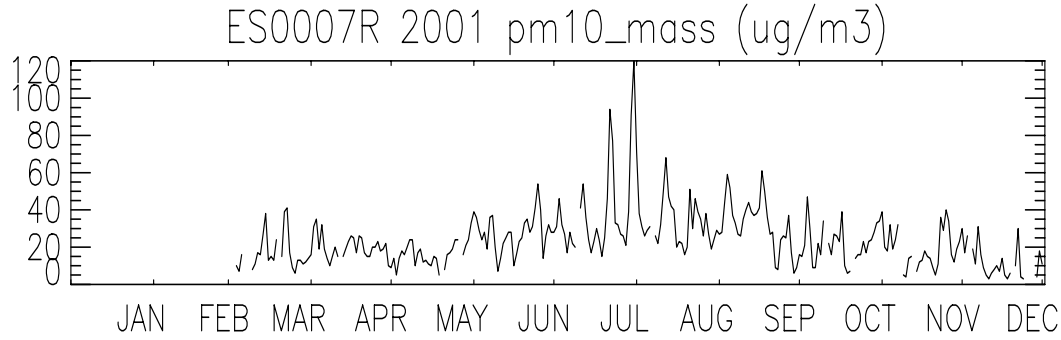
ES0007R 2001 pm10_mass (ug/m3)
120
100
80
60
40
20
0
JAN FEB MAR APR MAY JUN JUL AUG SEP OCT NOV DEC

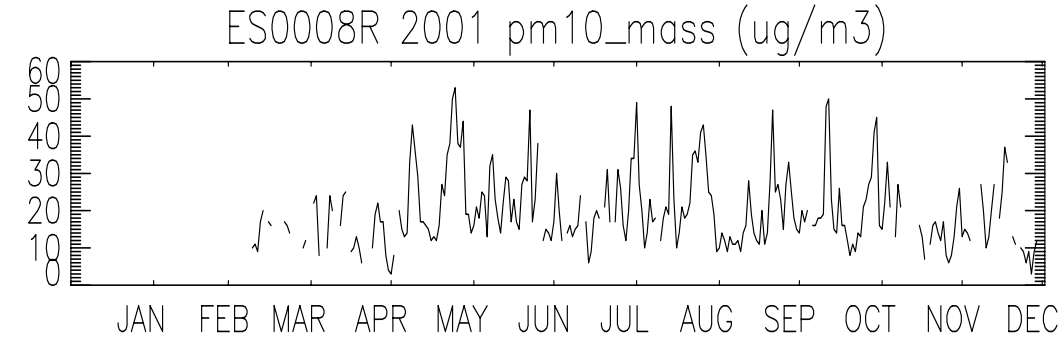
ES0008R 2001 pm10_mass (ug/m3)
60
50
40
30
20
10
0
JAN FEB MAR APR MAY JUN JUL AUG SEP OCT NOV DEC

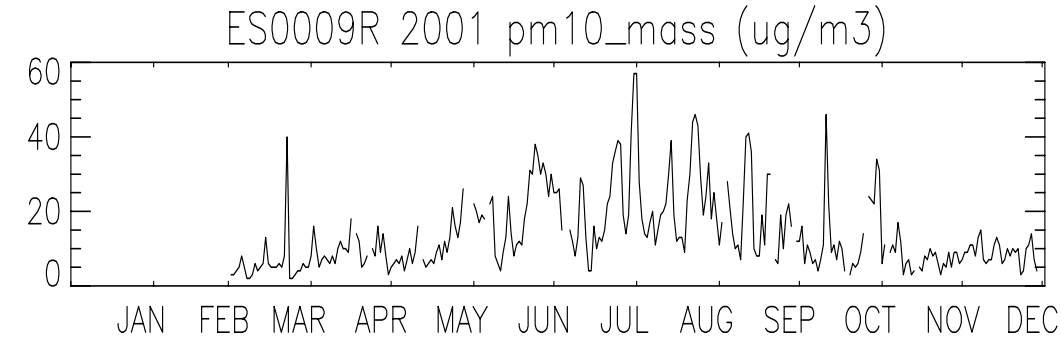
ES0009R 2001 pm10_mass (ug/m3)
60
40
20
0
JAN FEB MAR APR MAY JUN JUL AUG SEP OCT NOV DEC

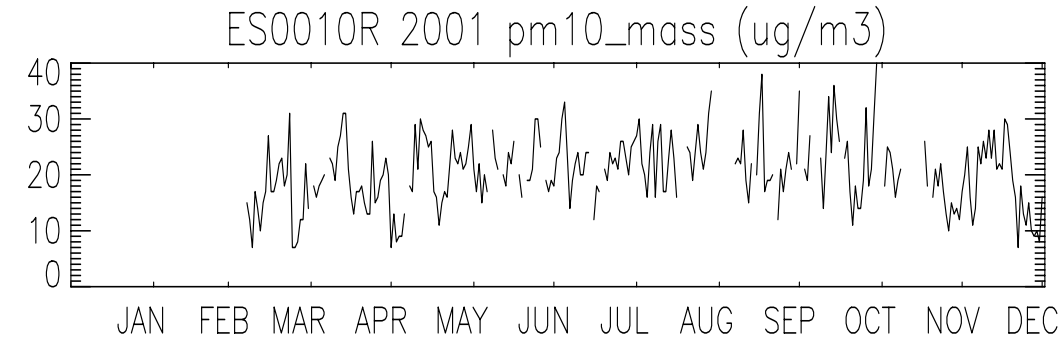
ES0010R 2001 pm10_mass (ug/m3)
40
30
20
10
0
JAN FEB MAR APR MAY JUN JUL AUG SEP OCT NOV DEC

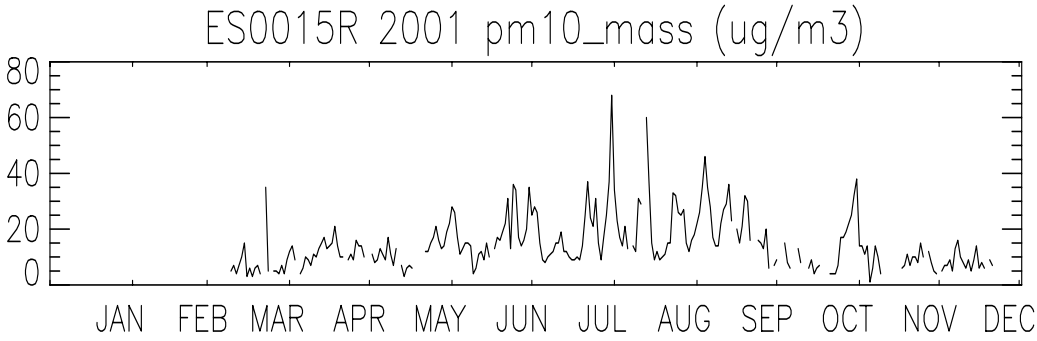
ES0015R 2001 pm10_mass (ug/m3)
80
60
40
20
0
JAN FEB MAR APR MAY JUN JUL AUG SEP OCT NOV DEC

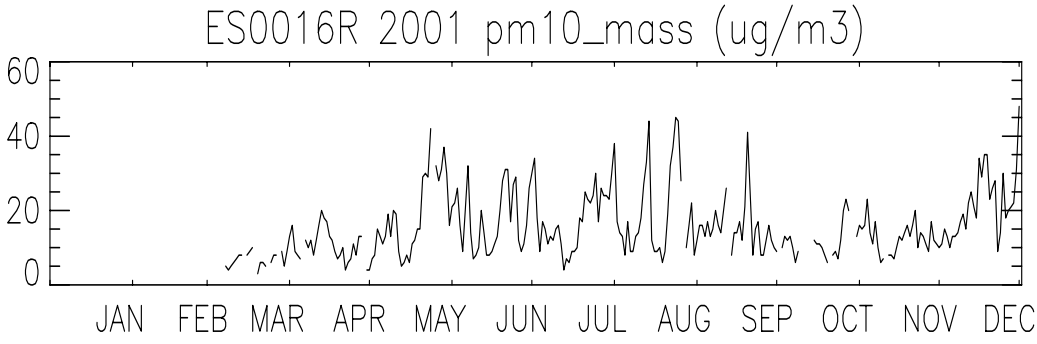
ES0016R 2001 pm10_mass (ug/m3)
60
40
20
0
JAN FEB MAR APR MAY JUN JUL AUG SEP OCT NOV DEC

($PM_{10} - PM_{2.5}$) mass concentrations in 2001:

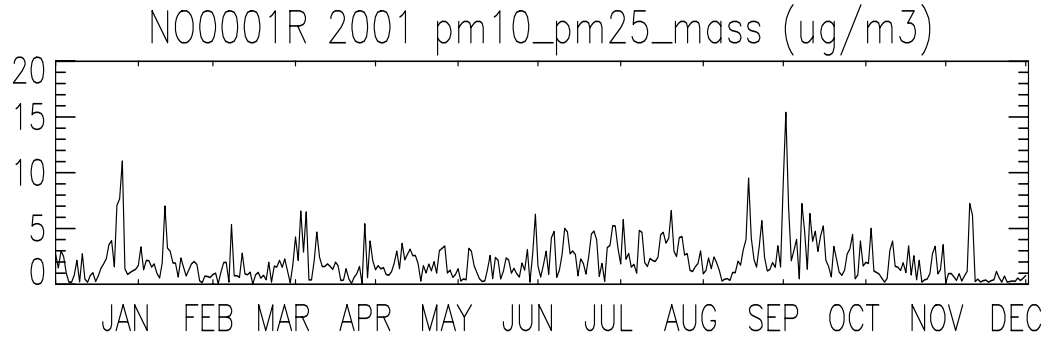

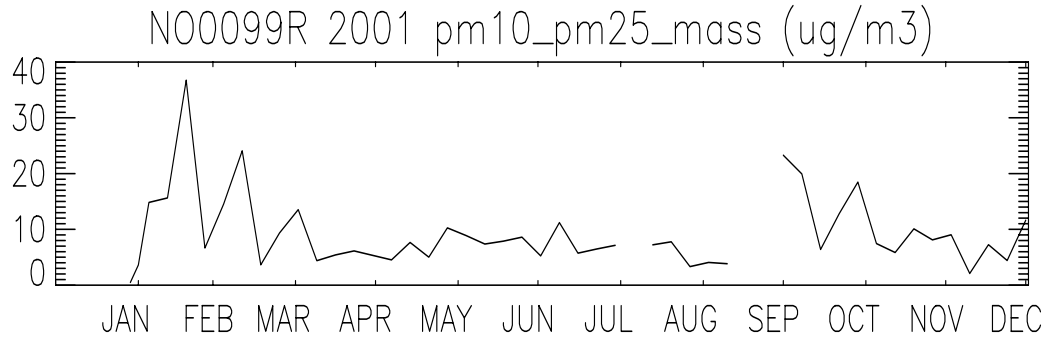

$PM_{2.5}$ mass concentrations in 2001:

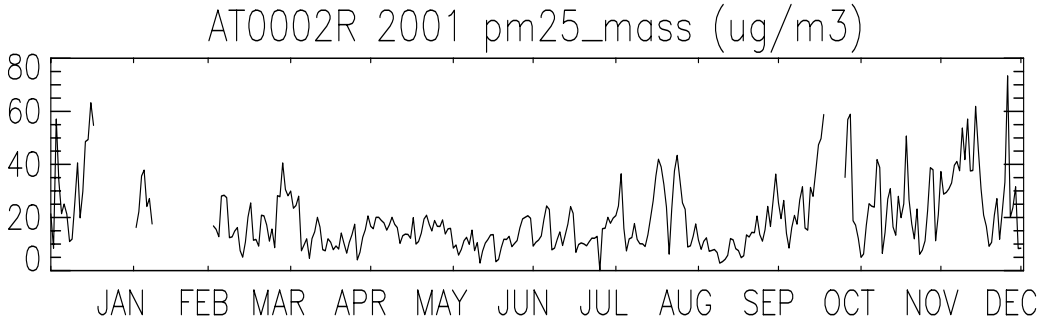

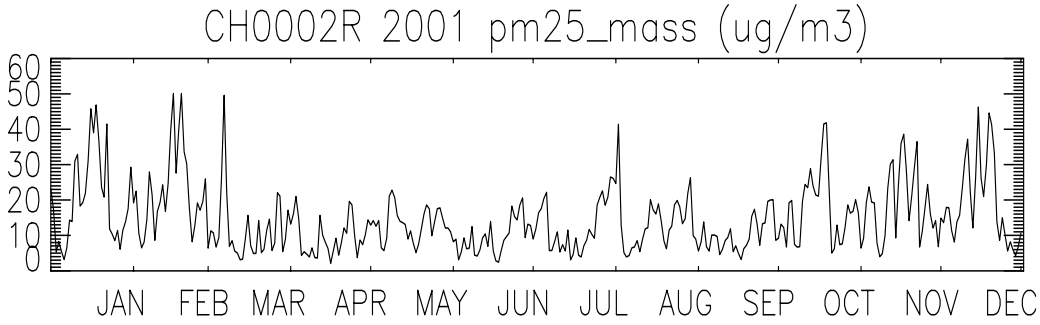

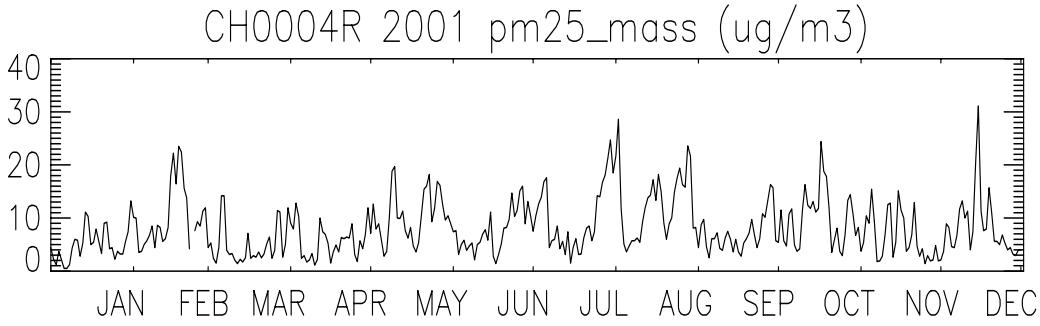

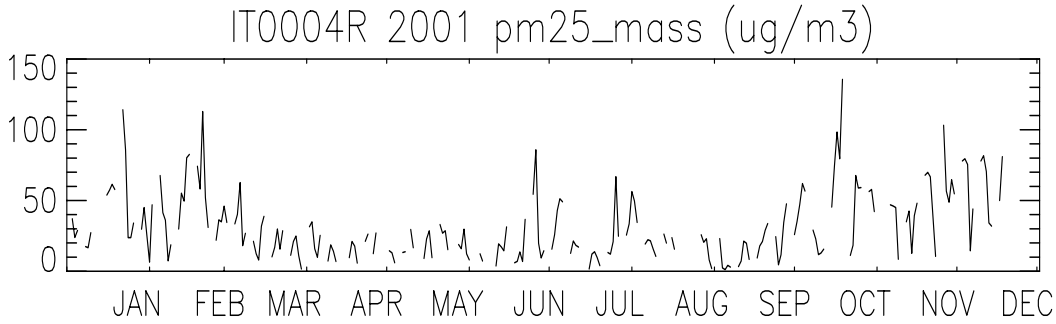

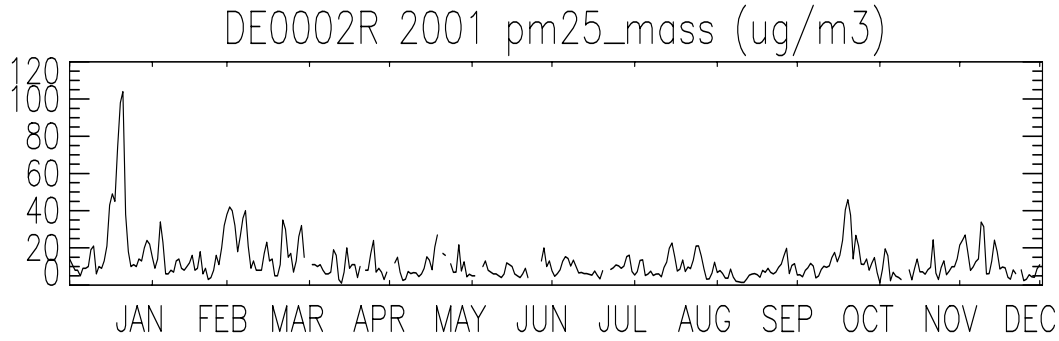
DE0002R 2001 pm25_mass (ug/m3)
120
100
80
60
40
20
0
JAN FEB MAR APR MAY JUN JUL AUG SEP OCT NOV DEC

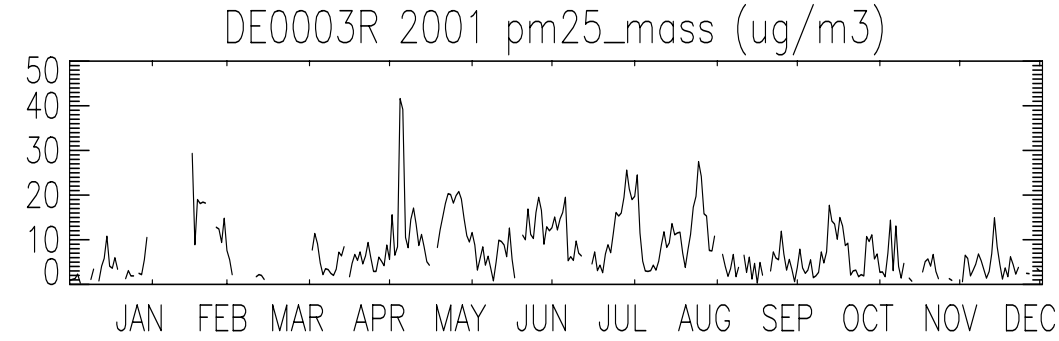
DE0003R 2001 pm25_mass (ug/m3)
50
40
30
20
10
0
JAN FEB MAR APR MAY JUN JUL AUG SEP OCT NOV DEC

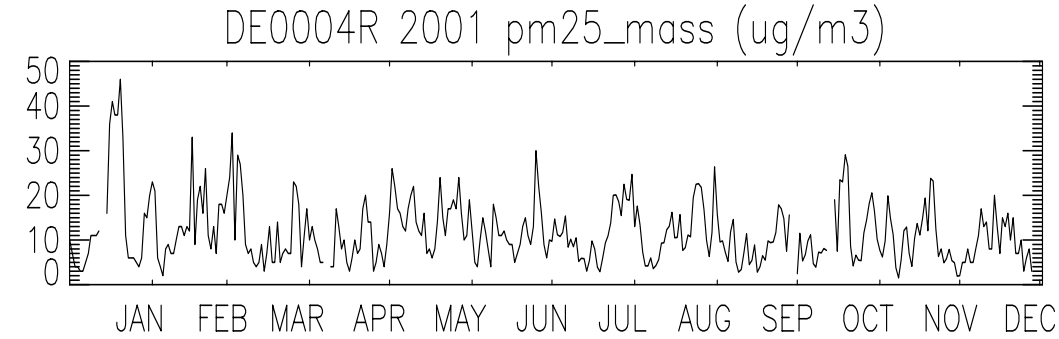
DE0004R 2001 pm25_mass (ug/m3)
50
40
30
20
10
0
JAN FEB MAR APR MAY JUN JUL AUG SEP OCT NOV DEC

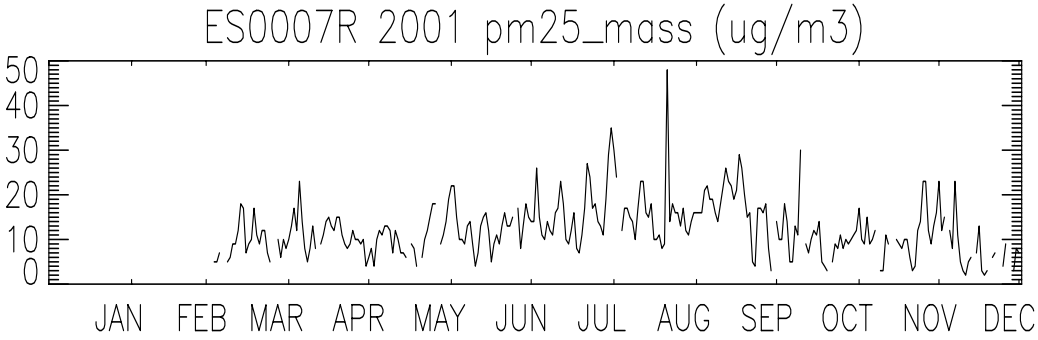
ES0007R 2001 pm25_mass (ug/m3)
50
40
30
20
10
0
JAN FEB MAR APR MAY JUN JUL AUG SEP OCT NOV DEC

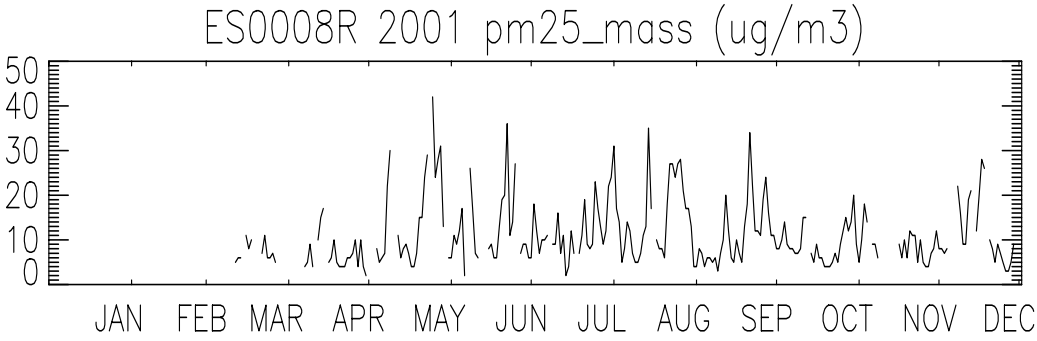
ES0008R 2001 pm25_mass (ug/m3)
50
40
30
20
10
0
JAN FEB MAR APR MAY JUN JUL AUG SEP OCT NOV DEC

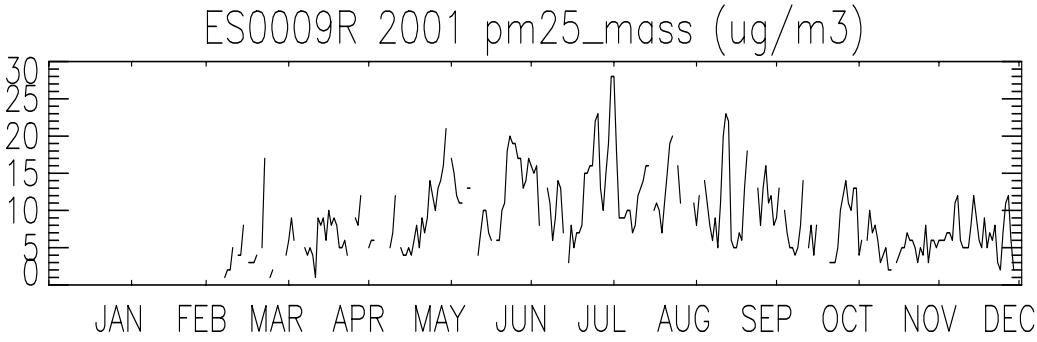
ES0009R 2001 pm25_mass (ug/m3)
30
25
20
15
10
5
0
JAN FEB MAR APR MAY JUN JUL AUG SEP OCT NOV DEC

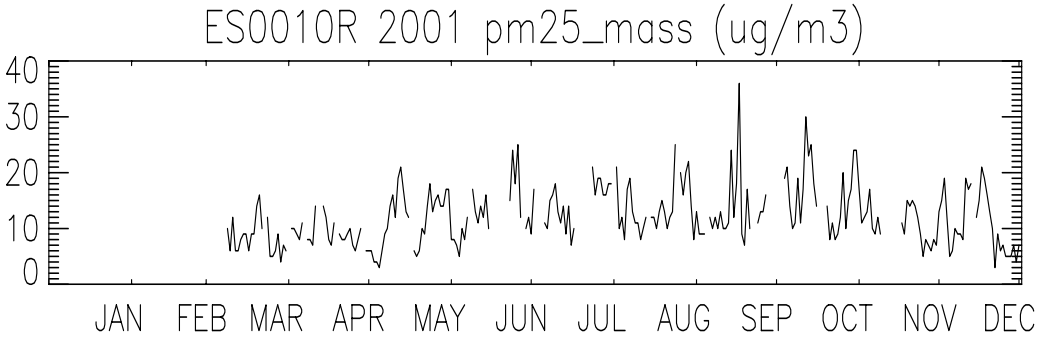
ES0010R 2001 pm25_mass (ug/m3)
40
30
20
10
0
JAN FEB MAR APR MAY JUN JUL AUG SEP OCT NOV DEC

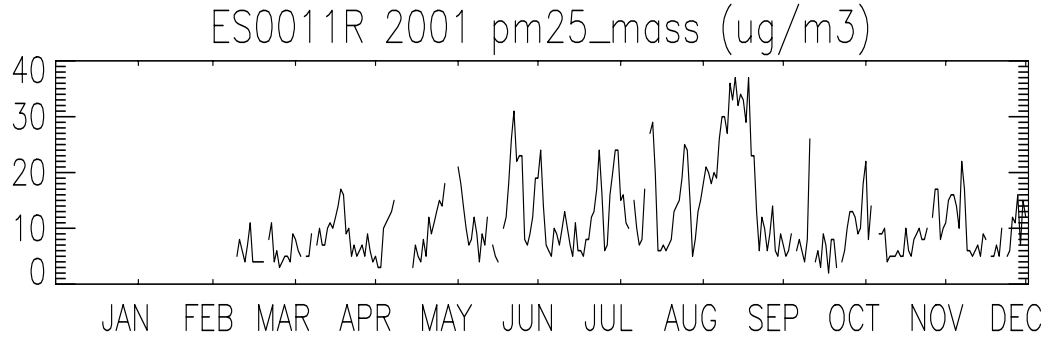
ES0011R 2001 pm25_mass (ug/m3)
40
30
20
10
0
JAN FEB MAR APR MAY JUN JUL AUG SEP OCT NOV DEC

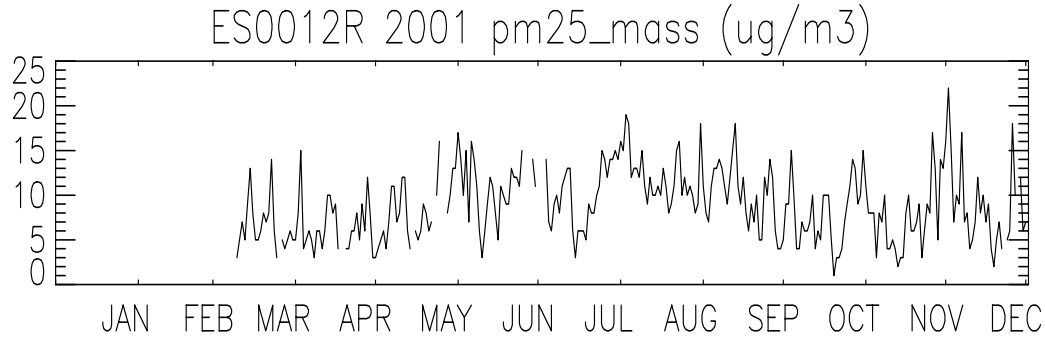
ES0012R 2001 pm25_mass (ug/m3)
25
20
15
10
5
0
JAN FEB MAR APR MAY JUN JUL AUG SEP OCT NOV DEC

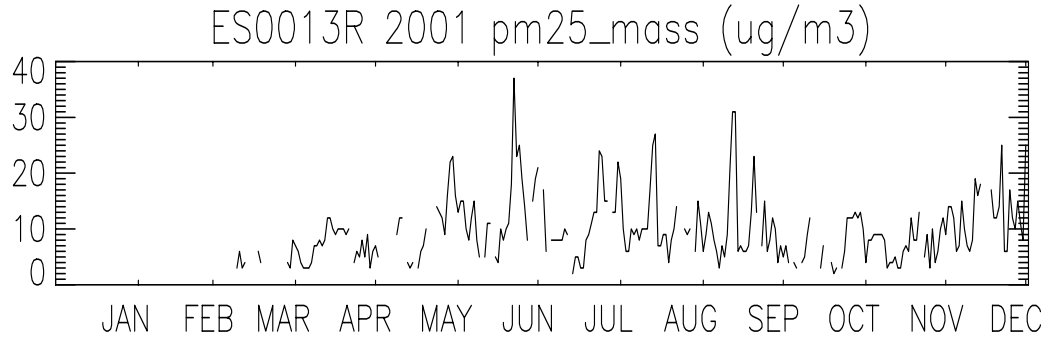
ES0013R 2001 pm25_mass (ug/m3)
40
30
20
10
0
JAN FEB MAR APR MAY JUN JUL AUG SEP OCT NOV DEC

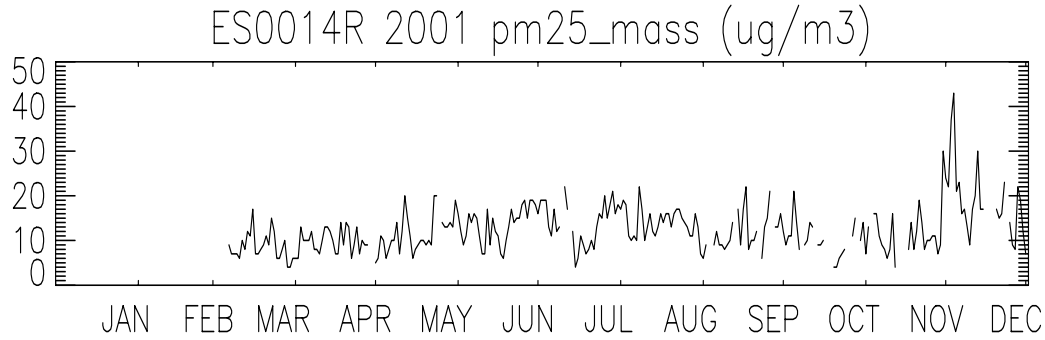
ES0014R 2001 pm25_mass (ug/m3)
50
40
30
20
10
0
JAN FEB MAR APR MAY JUN JUL AUG SEP OCT NOV DEC

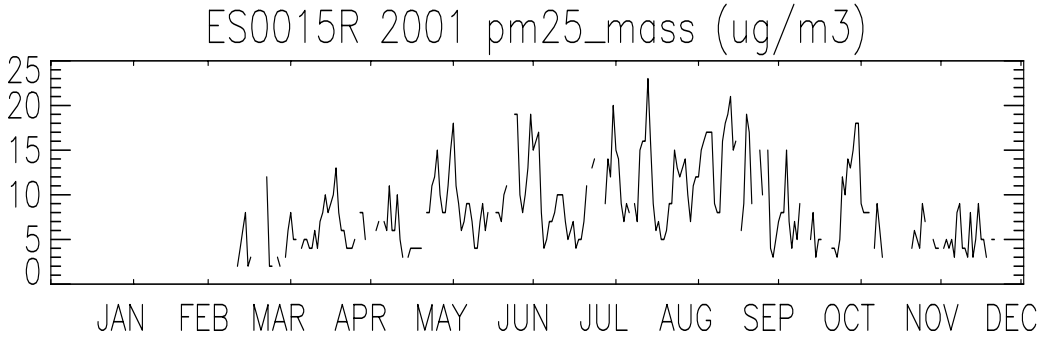
ES0015R 2001 pm25_mass (ug/m3)
25
20
15
10
5
0
JAN FEB MAR APR MAY JUN JUL AUG SEP OCT NOV DEC

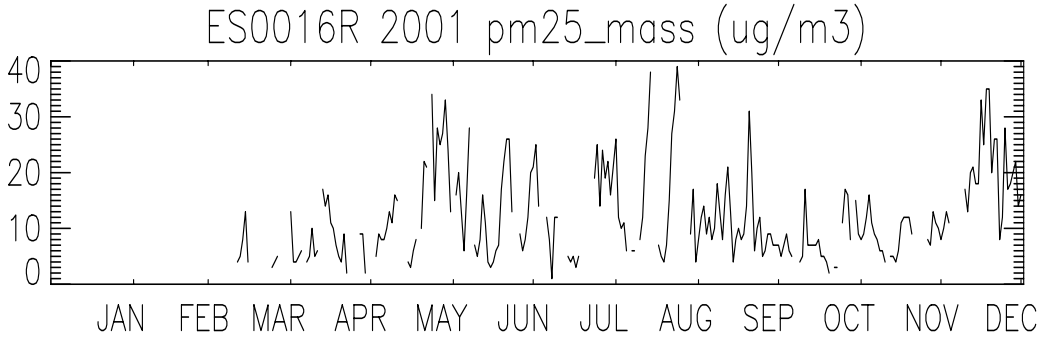
ES0016R 2001 pm25_mass (ug/m3)
40
30
20
10
0
JAN FEB MAR APR MAY JUN JUL AUG SEP OCT NOV DEC

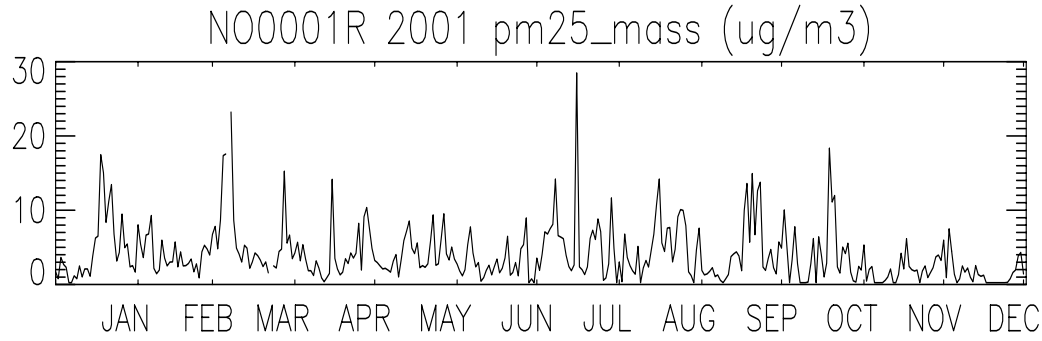
NO0001R 2001 pm25_mass (ug/m3)
30
20
10
0
JAN FEB MAR APR MAY JUN JUL AUG SEP OCT NOV DEC

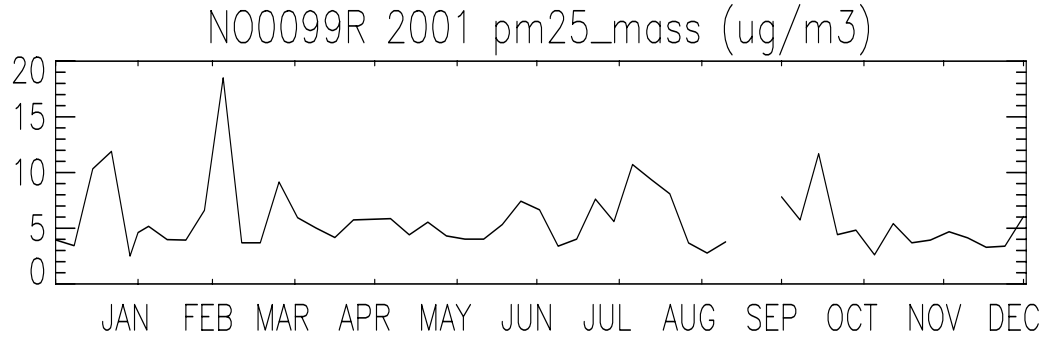
NO0099R 2001 pm25_mass (ug/m3)
20
15
10
5
0
JAN FEB MAR APR MAY JUN JUL AUG SEP OCT NOV DEC

TSP mass concentrations in 2001

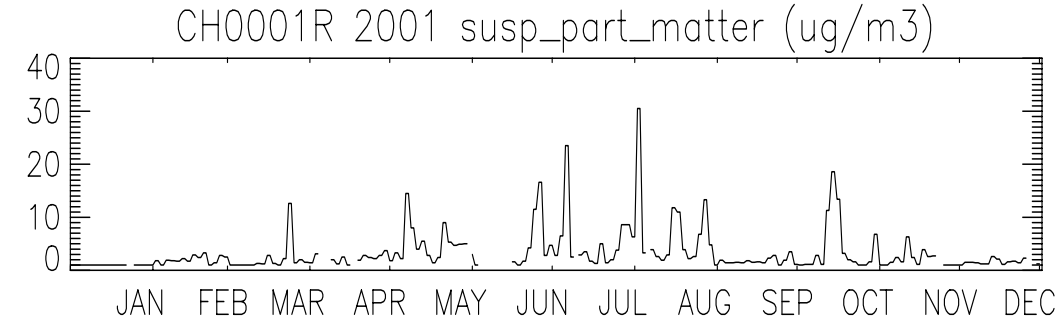

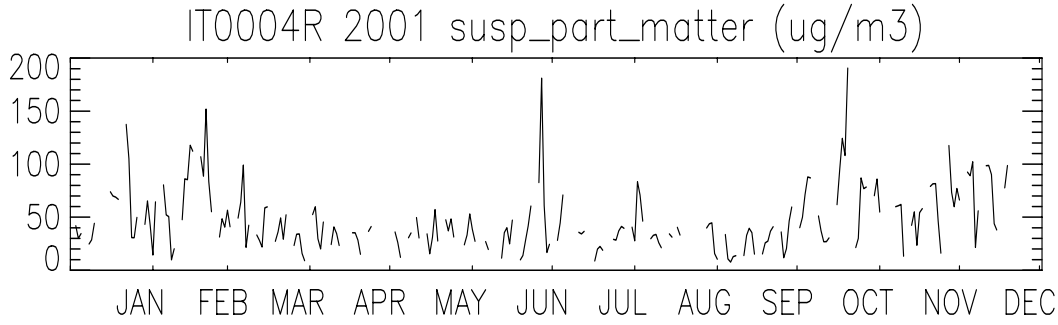

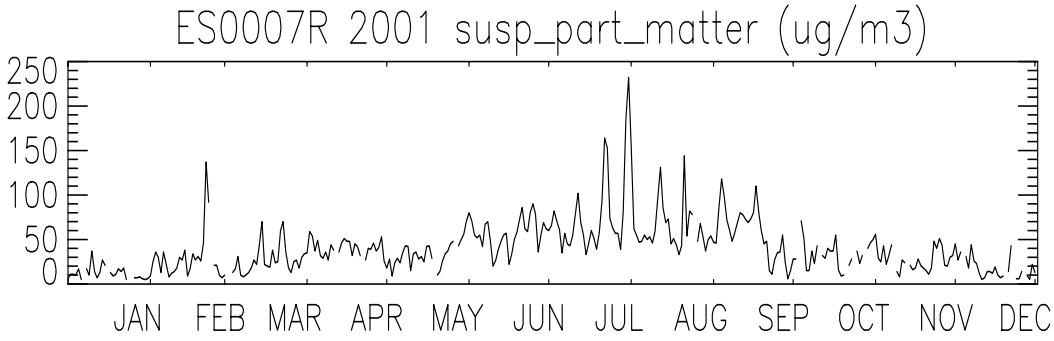
ES0007R 2001 susp_part_matter (ug/m3)
250
200
150
100
50
0
JAN FEB MAR APR MAY JUN JUL AUG SEP OCT NOV DEC

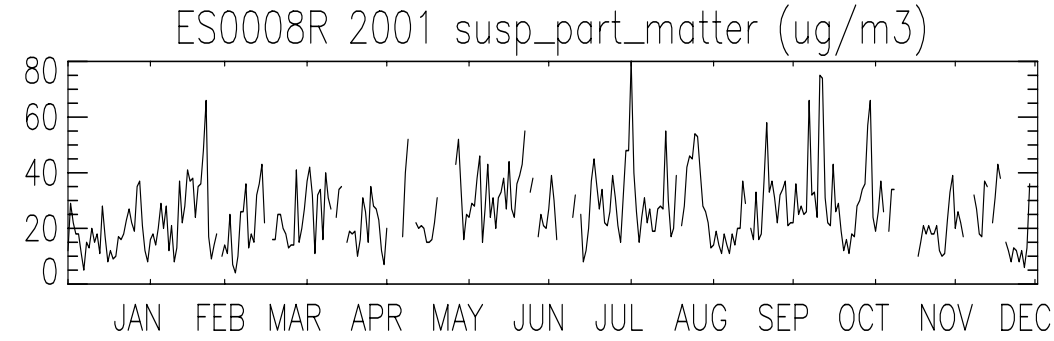
ES0008R 2001 susp_part_matter (ug/m3)
80
60
40
20
0
JAN FEB MAR APR MAY JUN JUL AUG SEP OCT NOV DEC

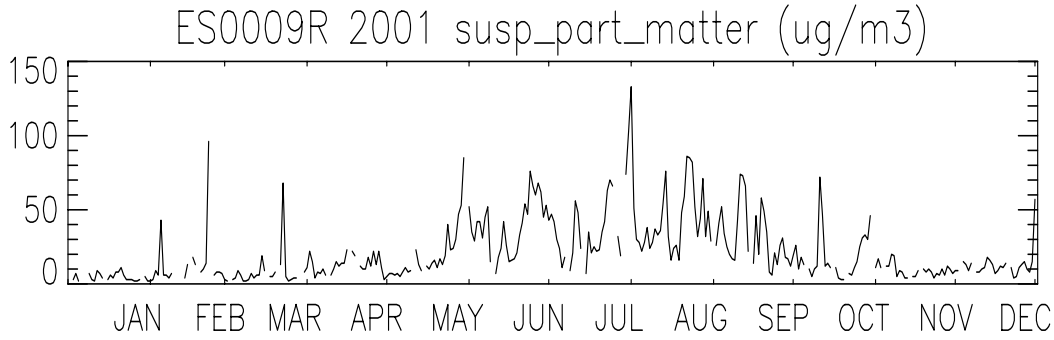
ES0009R 2001 susp_part_matter (ug/m3)
150
100
50
0
JAN FEB MAR APR MAY JUN JUL AUG SEP OCT NOV DEC

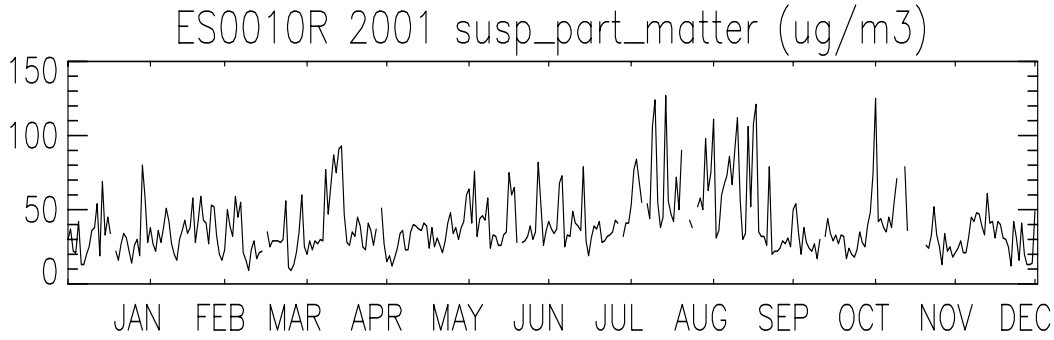
ES0010R 2001 susp_part_matter (ug/m3)
150
100
50
0
JAN FEB MAR APR MAY JUN JUL AUG SEP OCT NOV DEC

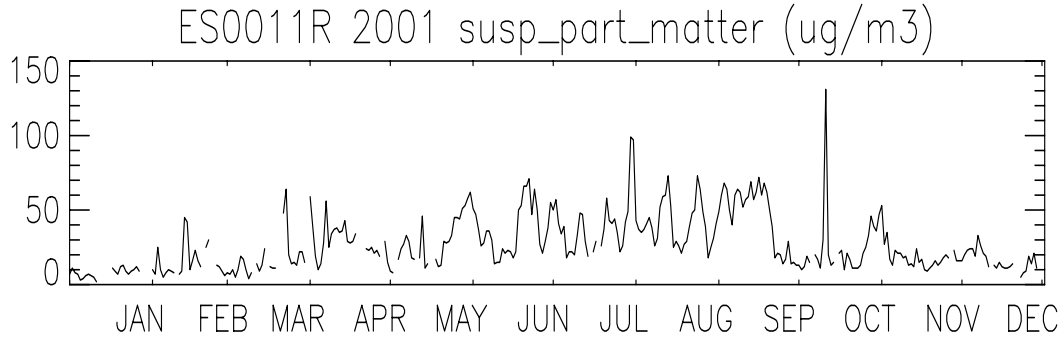
ES0011R 2001 susp_part_matter (ug/m3)
150
100
50
0
JAN FEB MAR APR MAY JUN JUL AUG SEP OCT NOV DEC

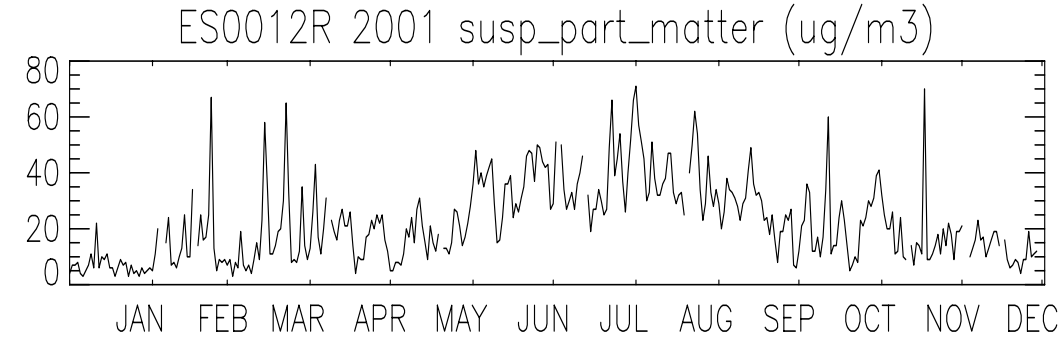
ES0012R 2001 susp_part_matter (ug/m3)
80
60
40
20
0
JAN FEB MAR APR MAY JUN JUL AUG SEP OCT NOV DEC

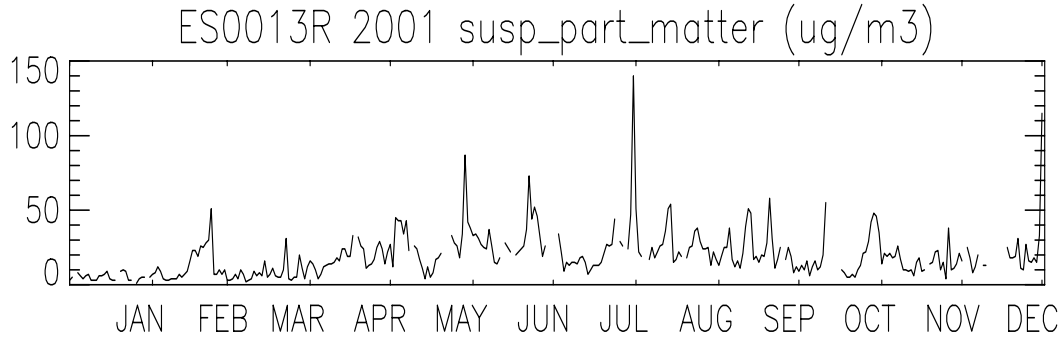
ES0013R 2001 susp_part_matter (ug/m3)
150
100
50
0
JAN FEB MAR APR MAY JUN JUL AUG SEP OCT NOV DEC

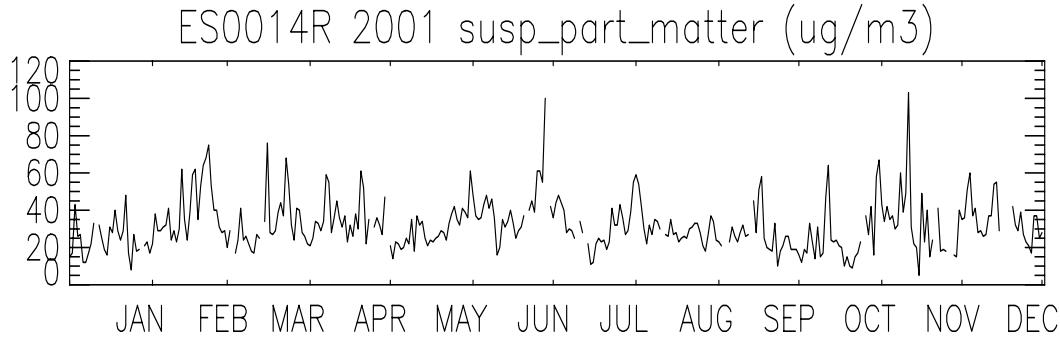
ES0014R 2001 susp_part_matter (ug/m3)
120
100
80
60
40
20
0
JAN FEB MAR APR MAY JUN JUL AUG SEP OCT NOV DEC

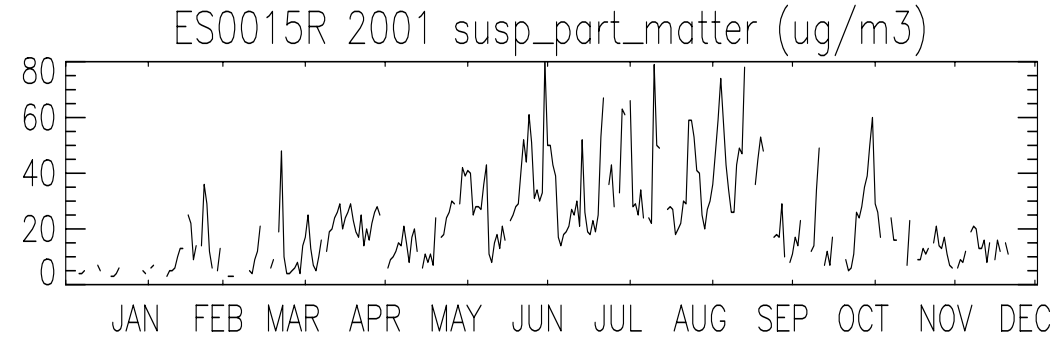
ES0015R 2001 susp_part_matter (ug/m3)
80
60
40
20
0
JAN FEB MAR APR MAY JUN JUL AUG SEP OCT NOV DEC

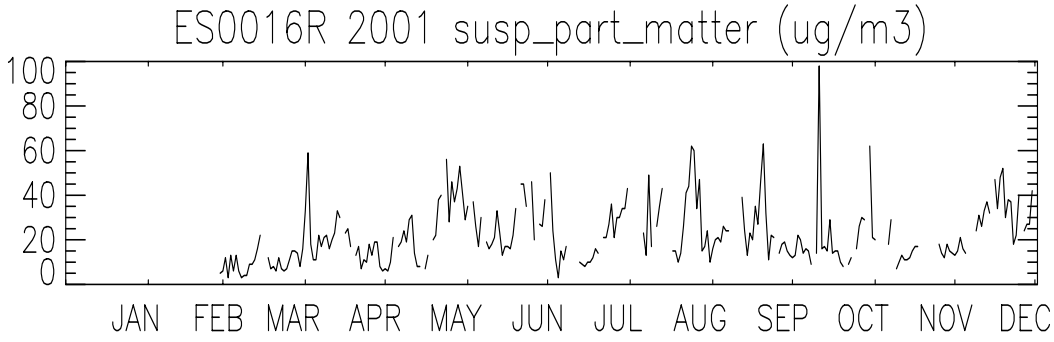
ES0016R 2001 susp_part_matter (ug/m3)
100
80
60
40
20
0
JAN FEB MAR APR MAY JUN JUL AUG SEP OCT NOV DEC